THE CYCLIZATION OF HEXADECANE DICARBOXYLIC ACID TO CYCLOPENTADECANONE ON BASIC HETEROGENEOUS CATALYSTS

Von der Fakultät für Mathematik, Informatik und Naturwissenschaften der RWTH Aachen University zur Erlangung des akademischen Grades eines Doktors der Naturwissenschaften genehmigte Dissertation

vorgelegt von

Diplom-Chemiker Axel Boeke

aus Aachen

Berichter: Universitätsprofessor Dr. Wolfgang F. Hölderich

Universitätsprofessor Dr. Carsten Bolm

Tag der mündlichen Prüfung: 28.10.2010

This work was carried out between January 2006 and May 2008 at the Institute for Fuel Chemistry and Physical - Chemical Process Engineering at the Department of Chemical Technology and Heterogeneous Catalysis of the Technical University RWTH, Aachen, Germany

I would like to thank Professor Dr. rer. nat. Wolfgang F. Hölderich for suggesting this interesting topic, the outstanding working conditions, and his advice and inspiration.

I thank Prof. Dr. Carsten Bolm for accepting to be the second examiner of this work.

This work was carried out as an industrial research project. I am grateful to *Mitsubishi Chemical Corporation* for the funding of this work.

Special thanks go to Dr. rer. nat. M. Valkenberg for helpful discussions, Ms. H. Fickers-Boltz and Ms. M. Nägler for analysing the GC samples, Ms. E. Biener and Ms. H. Bergstein for the ICP-AES analysis and Mr. K. Vaeßen for measuring all the XRD, BET, TPD and TG samples.

I also like to thank Dr. rer. nat. E. Modrogan and Ph. D. A. Charmot with whom I shared the laboratory, for the interesting discussions and their help.

Finally, I thank all those who contributed to the success of this work, especially all the people at the institute who made it a pleasure to work there.

THE CYCLIZATION OF HEXADECANE DICARBOXYLIC ACID TO CYCLOPENTADECANONE ON BASIC HETEROGENEOUS CATALYSTS

Diplom-Chemiker Axel Boeke

To my family.

Contents

Abbreviations

Apart from chemical symbols and SI units the following abbreviations were used in the text.

A	Ampere
Å	Angstrom
AHTN	6-Acetyl-1,1,2,4,4,7-hexamethyltetralin
AIBN	azobisisobutyronitrile
BET	surface area measurement to **B**runauer, **E**mmett und **T**eller
BJT	distribution of desorption volume
c	thermal capacity
°C	degree Celsius
C [%]	conversion in %
cat.	catalyst
cc	cubic centimetre
CN	coordination number
∆G	*Gibbs*-enthalpy
∆H	enthalpy
∆S	entropy
e.g.	exempli gratia (lat.)
EDX	energy-dispersive X-ray spectroscopy
et al.	et alii (lat.)
Fig.	figure
FTIR	*Fourier*-transformed infraredspectroscopy
g	gramme
GC	gas chromatography
h	hour
HDA	hexadecane dicarboxylic acid
HHCB	1,3,4,6,7,8-Hexahydro-4,6,6,7,8,8-hexamethylcyclopenta(g)-2-benzopyran
i.e.	Id est (lat.)
ICP-AES	inductively coupled plasma atomic emission spectroscopy
J	Joule
K	Kelvin
kg	kilogramme
lat.	latin
m	mass
MeOH	methanol
min	minute
ml	millilitre
MS	massspectroscopy
NBS	*N*-bromsuccinimide
p	pressure
p.a.	per annum (lat.)
PID-controller	proportional, integral, differential controller

ppm	parts per million
R	rectus
S	sinister
S [%]	selectivity in %
SEM	scanning electron microscope
T	temperature
T	time
TG	thermo gravimetry
THF	tetrahydrofurane
TOF	turnover frequency
TON	turnover number
TPD	temperature programmed desorption
V	voltage
wg%	weight percent
WHSV	weight hour space velocity
XRD	X-ray diffraction
Y [%]	yield in %

1 Introduction and Aims

1.1 Introduction

A fragrance or perfume is a chemical substance which stimulates the sense of smell. Animals use them for the identification of food, members of the same species and enemies. They play an important function in social behaviour (e.g. identifying the sexual maturity of females) or in orientation and communication (scent marks).

The ability to smell is based on interactions of molecules with cells of the nose lining. Molecules of a fragrance interact with a receptor and are recognized as a stimulus. The combination of stimuli and the intensity of receptors' stimulation is thereby essential. Humans are most sensitive to smells resulting from rotten food. The main metabolic products of bacteria induced decomposition are dimethyl sulfide, methyl mercaptane and ammonia, compounds toxic for human beings.

Humans use fragrances as an expression of individual personality or (like other animals) for sexual advertisement. In addition many products used in our modern daily life are enhanced by fragrances. Among the numerous fragrance classes, macrocyclic ketones play a prominent role.

From among the three different classes of musky fragrances[1-3] – nitroaromatics[4], polycyclic aromates[4], macrocyclic ketones and lactones[4-7] – the last group has been used for the longest time.

Production processes for synthesizing macrocyclic ketones like muscone (**1**), *exaltone* (**2**)[1] or civetone (**3**) are eminently important for the perfume and fragrance industry. While low-molecular aliphatic dicarboxylic acids can successfully be converted to cyclic ketones, this synthetic route is not practicable for the formation of macrocyclic ketones. Their industrial synthesis is still highly labour and cost intensive.

[1] Registered Trade Mark of *Firmenich & Cie, Succrs, de Chuit, Naef & Cie*, Geneva

1.2 Aims

The aim of this project was the use of cheap, easily available dicarboxylic acids (hexadecane dicarboxylic acid (**4**) and octadecane dicarboxylic acid (**5**)) as starting materials for synthesizing macrocyclic ketones like *exaltone* (**2**) (cyclopentadecanone).

To perform this kind of cyclizations, several Na_2O loaded titanium dioxide and zirconium dioxide materials had to be tested. One objective was the preparation of basic and bifunctional (basic-acidic) catalysts supported on very high BET-area materials. In the context of this project catalysts with different basic materials and different amount of loading had been prepared, characterised and tested for their suitability.

An essential goal was the development of an appropriate analytical method. The results in the present case are based on a GC-method without internal standard.

Another important objective was the optimization of reaction conditions, e.g. temperature, type and amount of catalyst, flow rate of carrier gas (and therefore residence time) or catalyst loading. Also, reactor design and configuration was improved in several stages.

2 General Part

The history of perfumery goes back more than 4000 years. In ancient civilizations fragrances served originally as sacrificial offerings for gods. However, people used them as well for body and hair care.[8] Perfumes (lat.: per = via und lat. fumum = fume) as we know today, have been developed towards the end of 19th century and the beginning of 20th century by Parisian perfumers. From the last quarter of the 19th century on, the range of products has been expanded with a continually rising number of synthetic fragrances. After the development of cumarin (1868), vanillin (1874), ionone and synthetic musk followed. The main advantage of synthetic fragrances is their constant quality.[9]

The production costs in the so called functional perfumery (soaps, detergents and house wares) are kept as low as possible. Fragrance components consist mainly of synthetic materials in a price range from 10 to 100 US$/kg. Only 10 percent of them cost between 100 and 250 US$/kg and just a few are beyond that range. Natural raw materials are usually more expensive.[9] Because of the high production costs for macrocyclics, their share in the world market of musky fragrances was less than 25 % in 1998.[3] The share of polycyclic musk fragrances and nitroaromatics will increase until 2008 up to 60-65 %.

2.1 Scents of animal origin

Raw materials of animal origin, such as musk (from the male musk deer) civet (from civet cat) or ambra (from pot whale) and castoreum (from beaver,) etc., are used to be essential ingredients for perfume production (Fig. 2-1). Today, due to ecological and economical constraints, basic notes of modern fragrances have to be products of the chemical synthesis.

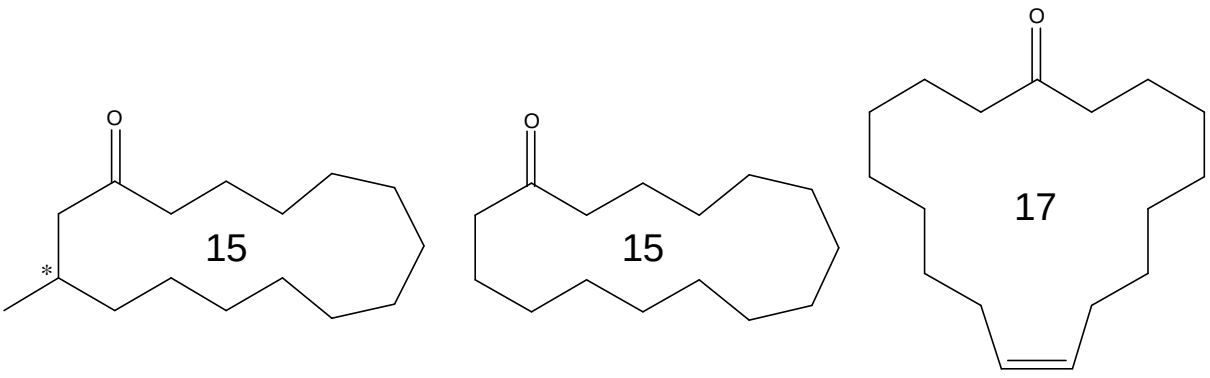

muscone (**1**) *exaltone* (**2**) civetone (**3**)

Fig. 2-1: Cyclic ketones – natural fragrances.

2.1.1 Natural musk odorous substances

Musk is the substance obtained from the odour gland of the male musk deer, an animal living in the Himalayan highlands (*Moschus moschiferus*) (Fig. 2-2). Its extremely strong smelling secretion acts as a marker of territory especially in the rutting season and as a long range attractant of the female deer. The “breathtaking stinking smell” of the pure secretion becomes a very pleasing odour at proper dilution. Hunting, which could not yet be completely prevented, has drastically reduced the population. In 1978 the gland was worth the triple of its weight in gold: it costs 20 US$/g, i.e. a hunter earned more than 500 US$ for shooting one animal.[10] Today Asia is the only market for the natural product because it still believed to be an aphrodisiac. Desperate customers are willing to pay (almost) every price.

In 1906 the German chemist *H. Wahlbaum* isolated the main component (0,5 to 2,0 %) of the fragrance in the form of white crystals[11] and named this compound muscone (**1**). Later it was found that this material was the R(-)-sterioisomer (**1a**).[12] The (*R*)-isomer (**1a**) has a diffuse musk odour (threshold value: 3 ppm) whereas the (*S*)-isomer (**1b**) has a poor and weak musk odour (threshold value: 10 ppm). The (*R*)-isomer (**1a**) has an odour three times stronger than that of the (*S*)-isomer (**1b**). Beside muscone (**1**), cholesterol, androstenone, dehydro epiandrostenone and other macrocyclics were identified as odoriferous components.[13] Nowadays synthetic R(-)-muscone (**1a**) identical with the natural product, as well as the optically active

(S)-form (**1b**) and the racemic form (**1**) are marketed. Their synthesis and application in cosmetics are referred to in patents[14] and literature[15-38].

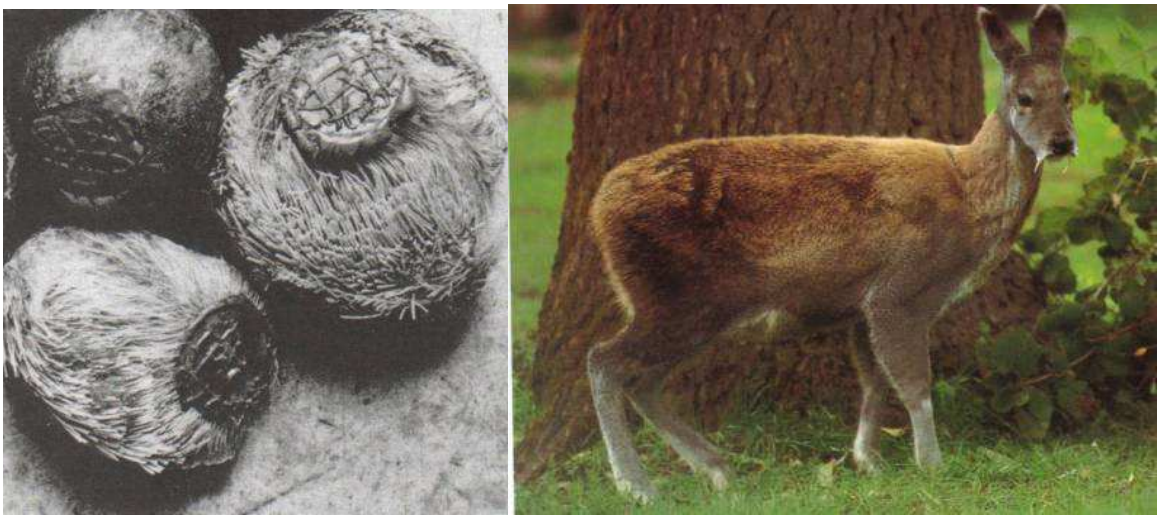

Fig. 2-2: Musk gland und *Moschus moschiferus*.[39, 40]

Some plants also produce lactones which exhibit a musky odour. The roots of *Angelica archangelica*, a plant growing in Central Europe, or the seed pods of the tropical plant *Hibiscus abelmoschus* are cultivated for fragrance production.[41]

2.1.2 Synthetic musk fragrances

Due to the great demand and the huge price of muscone (**1**), synthetic musk odorous substances have been produced early on (Fig. 2-3). Three main classes can be distinguished: polycyclics, macrocyclics and nitroaromatics. Polycyclics are nitro-free compounds of mainly natural origin. The molecular structure of muscone (**1**) was first established by *L. Ružička*[42, 43] (*ETH Zürich*, Nobel Prize 1939) in 1926.[44] He demonstrated the macrocyclic structure of this compound by showing that the same dicarboxylic acid HO_2C-$(CH_2)_{15}$-CO_2H was obtained by oxidizing dihydrocivetone and by the oxidation of the unsaturated *Wolff-Kizhner* reaction product of civetone (**3**) with $KMnO_4$ or ozone. *Ružička's* discovery invalidated the theory of *A. Baeyer* who believed in 1885 that rings with more than eight carbons were not stabile.[45] *Ružička* suggested that the macrocyclic ketones might be formed *in vivo* from α,ω-dicarboxylic acids by *Claisen*-type condensation which is followed by decarboxylation.[44,46]

Seventy years after the exploration of the muscone (**1**) structure there is still no economically feasible synthetic method available. Instead, other compounds which satisfy the demand have been marketed. In 1888 *A. Baur* synthesised the first musk-like synthetic compound, the tert-butyl-derivative of 2,4,6-trinitrotoluene (TNT). He has patented his discovery as *Musk Baur*. [47] The inventor of nylon, *W.H. Carothers*[48] later found out that some polyesters decompose by heating to a colourless oil which smells of muscone (**1**). This synthetic muskoil is still in use today and is significantly cheaper than the original.

Macrocyclics like ketones, lactones, dilactones and carbonates are of particular interest. Their smell is less intensive than the synthetic nitro-, polycyclic indan- or tetralin-like musk odours.

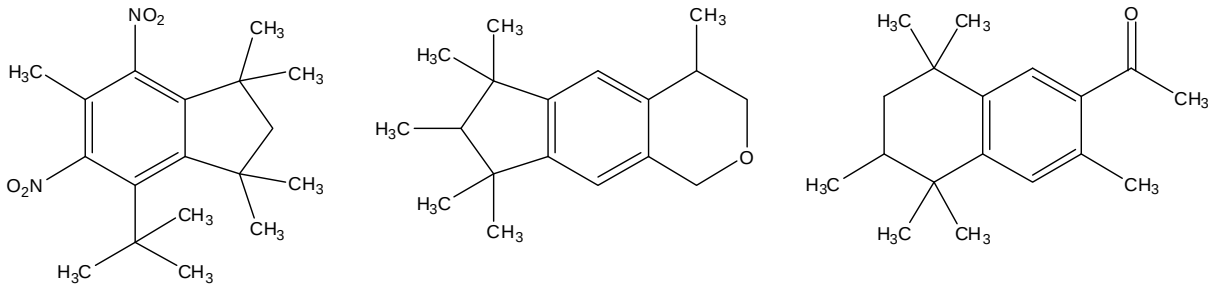

Fig. 2-3: Synthetic musk odorous substances

Macrocyclic ketones have been characterised by *K.A. Bauer*.[49] In the first forty years the common strategy used for synthesizing the macrocyclic scents muscone (**1**), *exaltone* (**2**) and exaltolide was based on the cyclization of aliphatic precursors with functional groups at both ends of their chain. A real breakthrough in *exaltone* (**2**) synthesis was achieved by a method based on acyloin condensation. For the synthesis of exaltolide the depolymerisation method and for muscone (**1**) the cyclization reaction was applied.[9] Large amounts of nitro musk, musk ketone and musk xylene are being used in perfumery even today (see Fig. 2-3). The world production of the two most important representatives of the group, galaxolide (HHCB) and tonalide (AHTN) amounts to over 5000 tons p.a.. For this reason, these substances are now virtually ubiquitous in samples of human tissue and environmental material.[50] They are much easier to synthesise than the macrocyclics.

Because of its photosensitising effect ambrett musk has been taken out of market in all applications involving skin contact. *Versalide* ([1-(3-ethyl-5,6,7,8-tetrahydro-5,5,8,8-tetramethyl-2-naphthalenyl)ethanone]) has also been removed from product lists because nerve discolourations after feeding tests of mice were observed. As other nitroaromatics have poor biodegradability and cause ecotoxicologic problems as well, unobjectionable musk fragrances are increasingly in the focus of academic and industrial research.[51-56]

Nitro musk and other polycyclic musk compounds accumulate in fish, human fat and milk.[52-54] The international umbrella organisation of fragrance industry the "International Fragrance Association" (IFRA) implemented a self-regulation code in 1975, which controls fragrance application in consumption products. Currently there are application recommendations for over 100 fragrances. They go from compliance of purity criteria over application limits to total banning.

Over 10.000 tons of synthetic musk flavours are produced annually. These inexpensive copies of the natural fragrance are marketed under the trade names *Galaxolide*, *Tonalide* and *Traseolide*.

2.2 Heterogeneous catalysts

Chemical reactions carried out by means of catalysts (e.g. the enzymatic fermentation of sugar to alcohol) have been known since antiquity. The Swedish chemist *J. Berzelius* (1779-1848) introduced the term catalysis (Greek *κατάλυσις*) for the first time in 1836.[59] He observed that many chemical reactions take place only in the presence of certain substances which are not consumed in the process. Later on, a deeper understanding of the thermodynamic background of catalytic reactions was achieved. A catalyst is described by *W. Ostwald* as follows:

„A catalyst is a substance which accelerates a chemical reaction, without been spent and without shifting the position of thermodynamic equilibrium of the reaction."[57]

For his work in catalysis *Wilhelm Ostwald* was awarded the Nobel Prize for Chemistry in 1909.
The effect of a catalyst consists in altering the reaction mechanism. The catalysed reaction has a lower activation energy than the uncatalysed one. Thereby the number of molecules posessing the necessary activation energy rises and the reaction rate is increased.[58]

One must differentiate between bio-, homogeneous and heterogeneous catalysis. In the last one (also known as contact or surface catalysis), the catalyst is a solid surface on which reactants are coordinated and activated by chemosorption and physisorption. In homogeneous processes the catalyst has to be separated after reaction from the product for ecological and economical reasons (catalyst recycling). Heterogeneous catalysts have the advantage of simple separation from the reaction mixture.

Today, the fact that more than 90 % of all industrial chemical processes run over catalytic synthesis routes, proves the prominent significance of catalysis.[59] Stringent environmental requirements will increase the demand of energy saving and environmentally friendly catalytic processes in the chemical industry. This trend is further promoted by a change in the raw material base, “away from crude oil based resources, towards synthesis gas chemistry”.[61] The rising demand of special chemicals with defined adjusted characteristics is requested by new applications.

Selectivity, activity and lifetime are important parameters in catalysis. The extent to which a catalyst increases the reaction rate at any given temperature is the activity of the catalyst. A suitable catalytic process requires a high turnover number (TON), defined as number of moles product per mole catalyst, and a high turnover frequency (TOF), defined as TON per second or hour.

The extent to which a catalyst preferentially accelerates just one reaction out of different competitive reactions (the formation of a certain product) is defined as selectivity. One must differentiate between enantiomeric selectivity and group selectivity, respectively.[60] In the present work the performance of the catalyst in cyclization was assessed by the fraction of *exaltone* (**2**) in reaction mixture.

Selectivity is of eminent importance for industrial chemistry because it is the key to low production costs (purity, avoidance of by-products), product- and process safety and the growing importance of environmental compatibility standards.[61]

Catalysts prepared by incipient wetness or impregnation consist of a catalytically active component dispersed on the support material. This support offers a high specific surface to the dispersed, active component. Support materials can be inert but can also be a part of an active surface. The catalytically active component can be present in three different forms:

- The support acts just as substrate, the catalytically active component remains chemically unmodified.
- A mixed phase is formed in which the active component generates a chemical compound.
- A close composition is formed and the active component is dissolved in the support.

2.2.1 Acidic and basic centres

Many chemical reactions can be described as an acid-base interaction between feed material and catalyst. Therefore methods for characterisation of active centres have been developed and published.[62] Many acidic catalysts have been investigated and published in the literature. Prominent among their uses is the catalytic cracking of heavy hydrocarbons in the petrochemical industry.[62] Acidic catalysts are also used in alkylation and isomerization reactions.[63, 76]

Basic catalysts, however, are less common. *Pines* and *Pillai* have been the first who applied ammonia modified aluminium oxide as basic heterogeneous catalyst in the dehydratisation of alcohols in the early sixties of the last century.[64] A further early example of basic catalysis is the use of dispersed sodium metal on alumina acting as an effective catalyst for the double bond isomerization of alkenes, by *Pines* et al..[65] In the early seventies the catalytic activity of basic zeolites was reported.[66] Since then,

heterogeneous basic catalysis was established as field of research in its own right. *Tanabe* classified solid bases according to their strength.[67] Different types of heterogeneous basic catalysts can be specified:

1. Single component metal oxides:
    - Alkaline earth oxides
    - Alkali metal oxides
    - Rare earth oxides
    - ThO_2, ZrO_2, ZnO, TiO_2
2. Zeolites
    - Alkali ion-exchanged zeolites
    - Alkali ion-added zeolites
3. Supported alkali metal ions
    - Alkali metal ions on alumina
    - Alkali metal ions on silica
    - Alkali metal on alkaline earth oxide
    - Alkali metals and alkali metal hydroxides on alumina
4. Clay minerals
    - Hydrotalcite
    - Chrysotile
    - Sepiolite
5. Non-oxide
    - KF supported on alumina
    - Lanthanide imide and nitride on zeolite

Types of catalysts mainly used in industrial processes are ion-exchange resins, phosphates, sulfates, carbonates, immobilized enzymes and sulfonated polysiloxanes. Most of the heterogeneously catalyzed industrial processes require zeolites, oxides, complex oxides, ion-exchange resins and phosphates. Zeolites contribute with about 41 % of all acid-base catalysts applied. Clays, immobilized enzymes, sulfates plus carbonates and sulfonated polysiloxanes are of less importance in industrial processes.[76]

The acidic (or basic) effect of a solid depends on the characteristics on the surface. The HSAB-concept („principle of **h**ard and **s**oft **a**cids and **b**ases“) of *Pearson* assigns

the terms 'hard' or 'soft', and 'acid' or 'base' to chemical species i.e. donor-acceptor-interactions. 'Hard' applies to species which are small, have high charge states (the charge criterion applies mainly to acids, to a lesser extent to bases), and are weakly polarizable. 'Soft' applies to species which are big, have low charge states and are strongly polarizable.[58] The adsorption behaviour of metal cations can be interpreted in terms of this principle. Coordinative unsaturated oxygen anions constitute the basic *Lewis*-centres, while *Brönsted* acidic centres are surface hydroxylic groups which can be deprotonated by basic molecules. Not every hydroxylic group present on the surface can be deprotonated. Acidic and basic sites are never isolated but come forth as acid-base couple. A catalyst is called basic if the number of basic sites prevails over the number of acidic centres. The catalytic activity usually involves both forms of centres together.

The preparation method affects the catalyst characteristics. Water, carbon dioxide, oxygen and nitrogen cover the active sites on the surface at room temperature. By this blocking of active centres the activity of the catalyst is reduced. In order to develop full catalytic activity these compounds have to be desorbed by thermal treatment in form of activation or calcination before reaction. Molecules anchored by weaker surface interactions can desorb even at lower temperatures, since the desorption energy depends on the strength of active centre-molecule bond. Centres occupied by molecules desorbing at higher temperatures are "strong". The nature of basic sites varies with the severity of the pretreatment conditions for most heterogeneous basic catalysts.

Different methods for the characterisation of acidic or basic centres are available. The amount of basic or acidic centres can be measured by adsorption methods like temperature programmed desorption (TPD), titration in the presence of *Hammett*-indicators[68-70] test reactions[15, 71] and spectroscopic methods like IR of pyridine, pyrrole or carbon dioxide, XPS (*x-ray PES*), UV adsorption and luminescence. The theoretical background of two of these methods used in the present work is presented below.

Temperature programmed desorption (TPD)

Adsorption and spectroscopic methods utilize the adsorption interactions between small molecules with acidic (or basic) properties and the basic (or acidic) solid surface. By Temperature Programmed Desorption (TPD), the amount and the strength of active centres can be determined simultaneously. Probe molecules are chemisorbed on the surface before heating with a preset heating rate. Consequently these probe molecules desorb at a defined temperature. For basic samples probe molecules such as pyrrole, CO_2 and H_2 are used, as well as CH-acid compounds like acetylene, benzene or even CH_4, SO_2, H_2S, NO, CO and phenol. For acid samples strong bases like ammonia or pyridine are used. To minimize the effect of adsorbed base on the distribution of acid sites of different strengths, weaker bases are sometimes used as probe molecules.[72] Sometimes it is assumed that the peak temperature, i.e. the temperature of probe molecule desorption, is an indicator of strength of the particular centre. The amount of active sites correlates with the detected peak area. The nature of active centre can not be analysed by TPD alone. Further methods like IR-spectroscopy (see below) are needed for identification. To get an overview of the amount and strength of active centres different compounds have been measured and compared under similar conditions.[62,72] The strength of different earth alkali metal oxides measured by CO_2-TPD increases as follows: MgO < CaO < SrO < BaO. The amount of centres increases in almost reverse order: BaO < SrO < MgO < CaO.[62] The analysis of surfaces by *Aramendía et al.* with 2,6-dimethylpyridine (DMPY), pyridine (PY) etc. at ZrO_2.[71] DMPY showed selective adsorption to *Brønsted*-acid centres. For steric reasons *Lewis*-acid centres were not covered. Pyridine (PY) adsorbs to both *Brønsted*-acid and *Lewis*-acid centres. The direct influence of calcination temperature on the amount of acid centres was subject of *Aramendías* research.

IR-spectroscopy

Additional to TPD-measurements, IR-spectroscopy generates information about adsorbent structure. Also in this case CO_2 is used as probe molecule because its small size has a low steric hindrance. Due to its acidic electrophilic character CO_2 interacts with basic centres of surfaces containing metal oxide. Basic oxygen atoms give rise to different carbonate structures.[73]. These carbonates show different absorption bands in IR-spectra and the basicity of the surface can thus be assessed. Unidentate carbonate is formed on strong basic centres, bidentate carbonate is formed on basic centres of medium strength and bicarbonate is formed on weakly basic ones.[73] Depending on the covering ratio different carbonate forms can result. *Fukuda* and *Tanabe* have shown that bidentate carbonate is formed if low amounts of CO_2 are adsorbed to MgO-surfaces.[74] If the amount of adsorbed CO_2 increases, unidentate carbonate becomes dominant. CaO surfaces exhibit only unidentate carbonate at room temperature. If the adsorption temperature is high, bidentate carbonate is formed.

IR-spectroscopic analysis of basic centres can be carried out with pyrrole and CH-acide compounds such as acetylene, propyne, trichloromethane, etc.[75] The location of the stretch oscillation band (3520 - 3650 cm^{-1}) of acidic OH-groups gives information of their strength. The position of this band is controlled by the bond angle and external factors like temperature etc. *Brønsted*-acid centres can also be assessed with pyridine, CO and N_2. *Brønsted*-acid centres e.g. in zeolites are detected by the ring deformation oscillation at 1632 cm^{-1} or 1540 cm^{-1} using pyridine.[72,75] *Lewis* acid centres can also be identified with NH_3, pyridine, acetonitrile or CO. *Lewis*-acid centres have bands in the range of 1620 cm^{-1} with NH_3 and near 1440 – 1551 cm^{-1} with pyridine. Interactions of CO with acidic hydroxyl groups lead to the formation of H-bonds. The shift of the original oscillation band of the hydroxyl group is a measure of acidity.

The incentive for the development of new catalysts is the optimisation of production processes for manufacturing cheap, safe and ecologically friendly products. The main focus of the present thesis concentrates on the effect of basic catalysts on the

cyclization of dicarboxylic acids. This reaction will be examined in more detail in the next chapters.

2.2.2 Metal oxides in catalysis

Catalytic activity can be exhibited by a wide variety of materials. Metal and metal oxides with semiconducting properties contain free electrons available for chemical bonding and can therefore facilitate redox reactions like dehydrogenations, oxidations or hydrogenations. Other materials with basic or acidic properties catalyse such reactions as esterifications, alkylations or hydrations which occur via an acid-base-mechanism. Bifunctional catalysts like platinum on acidic aluminium oxide show redox- and acid-basis-properties as well.

Among heterogeneous catalysts metal oxides constitute a large group. Since the beginning of the last century, metal oxides have been used in catalytic processes. The catalytic ammonia synthesis developed by *Fritz Haber* in 1909 for reacting H_2 with N_2 on a reduced iron oxide catalyst (Fe_3O_4, magnetite) ranks among the most significant discoveries.[59] Numerous other catalytic applications of metal oxides have been developed since.[76] Many aspects have been clarified by modern analytical techniques, including spectroscopy, so that an in-depth characterisation of properties like surface texture, chemical composition and catalyst structure is now possible.

The strength of catalytically active sites correlates with the coordination number of the metal atoms on the catalyst surface. However, the relationship between coordination sphere and catalytic activity has not yet been completely elucidated. Surface metal atoms having a low coordination number are very reactive and strongly adsorb CO_2 molecules.

A metal oxide consists of a metal cation (M^{n+}) and an oxygen anion (O^{2-}). The metal cation constitutes the *Lewis*-acidic centre and the oxygen anion the basic site. Due to this charge difference the heterolytic chemisorption of organic molecules on metal oxides is possible. Favoured adsorption sites are e.g. the coordinative unsaturated centres on catalytic surfaces of transition metals. These peculiar centres are for instance generated by thermal treatment of metal oxides. Water molecules linked to

the surface or resulting from hydroxylic groups on the surface are desorbed by calcination. By dehydroxylation metal cations lose their direct neighbours and become coordinative unsaturated. They are *Lewis*-acidic centres. The acid strength depends on their size and the oxidation level, hence from the polarisation of the metal cation.

Alkali earth metal oxides

The catalytic properties of alkali earth metal oxides (MgO, CaO, SrO and BaO) have been thoroughly investigated. They possess strong basic centres rising in following order: MgO < BaO < SrO < CaO. Their catalytic activity is influenced by impurities in the vicinity of the reaction centre, as adsorbed CO_2 and H_2O deactivate the surface. Alkali earth metal oxides have a high affinity to proton abstraction in the allyl position. For example they are used in isomerization reactions like 1-butene to 2-butene and the amiation of conjugated dienes.[62]

Rare earth metal oxides

Rare earth metal oxides in oxidation level +1 to +3 have basic centres and are used e.g. for isomerization reactions. Moreover they are relevant in hydrogenation of olefins and the dehydration of alcohols. Oxides with oxidation levels higher than +3, e.g. CeO_2, Tb_4O_7, Pr_6O_{11} have weak basic centres and catalyse the aldol condensation of ketones.[62, 77]

Zirconium oxide

Zirconium oxide shows a bifunctional behaviour. Both acidic and basic centres are located on its surface. These centres are weak and these materials constitute efficient catalysts. Because of the low strength the active centres are not deactivated by CO_2 and H_2O. The detailed structure of these bifunctional centres is still discussed.[78] On industrial scale ZrO_2 is used for dehydratisation of 1-cyclohexanol to vinylcyclohexane and reduction of aromatic carboxylic acids with H_2 to aldehydes.[62,79, 80]

Aluminium oxide

Aluminium oxides exhibit a highly complex surface structure. Like ZrO_2, Al_2O_3 in γ-modification can have both acidic and basic sites. Models of *Peri*[81] and *Knözinger / Ratnasamy*[82] describe the different types of coordinated hydroxyl groups respectively. The complex surface structure of Aluminium oxide has the ability to

catalyse different reactions where various active centres are needed. *Pines* and *Pillai* used ammonia modified Aluminium oxide for the dehydration of alcohols in the early 60´s of last century.[83]

On industrial scale Al_2O_3 is used e.g. by *Mobil* to convert methanol to dimethyl ether.[76] Stabilized γ-Al_2O_3/Pd catalysts are used for crack reactions in refinery processes in huge scale. Amorphous SiO_2-Al_2O_3 and zeolites are used for hydrocracking and Fluid Catalytic Cracking (FCC) of heavy oil distillates.[84].

Solid superbase catalysts, as developed by researches of *Sumitomo Chemicals* are a further industrial application of alumina.[85] These catalysts consist of alkali metal hydroxide/alkali metal on γ-alumina $(MOH)_x/M_y/\gamma$-Al_2O_3, wherein M, x, y are described as M = Li; Na;K; Rb; Cs; x = 5-15 wt:% on γ-Al_2O_3 and y = 3–8 wt:% on γ-Al_2O_3. They have an extremely high basicity, sometimes higher than $H_0 > 37$. Such super bases do not catalyze cracking reactions, do not deactivate due to strong adsorption of compounds containing basic N or O groups and have a long service time. However they are sensitive to moisture and CO_2 and therefore have to be handled carefully. Nevertheless, they are already applied as highly active and effective catalysts for double bond isomerization and side-chain alkylation of alkylbenzenes such as the *Sumitomo*-process for the production of 5-ethylidene-bicyclo[2.2.1]hepta-2-ene from 5-vinyl-bicyclco[2.2.1]hepta-2-ene via isomerization over the superbase Na/NaOH/γ-Al_2O_3 and the *Sumitomo*-process for the production of *t*-amyl-benzene by side-chain alkylation of cumene with ethylene over K/KOH/γ-Al_2O_3.[76, 86] The superbase catalyst NaOH/Na/γ-Al_2O_3 can also successfully be employed for the isomerization of safrol (1-allyl-3,4-(methylene-dioxy)-benzene) to iso-safrol (3,4-(methylenedioxy-1-propenyl)-benzene) as well as for the isomerization of 2,3-dimethylbutene-1 to 2,3-dimethyl-butene-2, a valuable intermediate for the production of pyrethroids.[87] Recently such super base catalysts can be used for transesterification of dimethylterephthalates with ethylene glycol to form bis-hydroxyethylthrephthalate (BHET).[88], [86]

2.3 The manufacture of cyclic ketones

Due to the ever increasing ecological awareness and also for safety reasons, considerable efforts have been directed toward the development of fragrances identical or similar to the natural substances. Unlike many other synthetic musk compounds, macrocyclic ketones, esters and lactones identical or similar to the corresponding natural products are ecologically harmless and constitute the object of industrial research.[89] Over the years various synthetic processes found industrial application. To date, the huge number of reaction steps, poor yields and high production costs pose considerable problems. Furthermore, in the case of substituted chiral macrocyclics a pure optical isomer has to be available as precursor (e.g. (+)- or (-)-3-methyl-glutaric acid for muscone (**1**).). Along ring-enlargement reactions, ring-closing reactions are the key steps in the synthesis of macrocyclic musk.[90, 91] Most of these reactions are carried out without any catalyst.

2.3.1 Ring enlargement reactions

Since cyclododecanone (**6**) is easily available, this compound is predestinated as feedstock for ring enlarging reactions.[92] The synthesis proceeds over the trimerisation of 1,3-butadiene, followed by hydrogenation and oxidation. This component is enlarged over bicyclic intermediates by three carbon atoms (Fig. 2-4).

Stobbe condensation[93] of cyclododecanone (**6**) with diethyl succinate forms β-carbethoxβ-cyclododecylidenepropionic acid with is cycled to a bicyclic vinylogous β-keto ester by zinc chloride[94] in acetic acid or preferably which polyphosphoric acid.[46] Followed by an acid hydrolysis bicyclo[10.3.0]-$\Delta^{1(12)}$-pentadecene-13-one (**7**) can be smoothly obtained. The hydrogenation of the bicyclic ketone (**7**) to the homologue alcohole requires the presence of *Raney*-nickel and 1 wg.% NaOH. A subsequent dehydratisation of the alcohol by benzene sulfonic acid in boiling toluene, generates bicyclo[10.3.0]-$\Delta^{1(12)}$-pentadecene (**8**). This compound reacts by ozonisation and following catalytically hydrogenation to the diketone 5-oxocyclopentadecanone (**9**). The process ends with the quantitative partial catalytic hydrogenation of the olefinic double bond of **10** in the presence of *Raney*-nickel to cyclopentadecanone (**11**).[95]

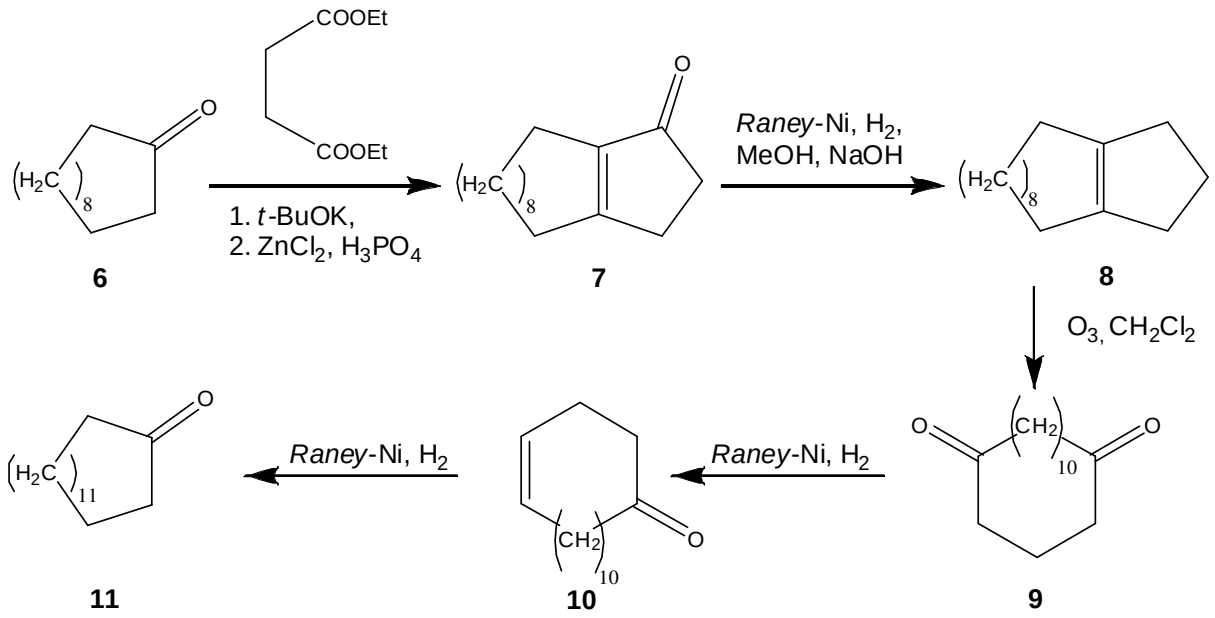

Fig. 2-4: Ring enlargement of cyclododecanone over bicyclic intermediates to Ohloff.[95]

Another synthetic route involves the epoxidation of the α,β-unsaturated carbonyl compound (**7**) (Fig. 2-5). The ring enlargement step implies the fragmentation of the α,β-epoxyketone (**12**) and the corresponding *p*-tosylhydrazone (**13**) to the respective alkinone (**14**). The stumbling block in this sequence is the low yield of the epoxidation. The consecutive catalytic hydration over Pd/charcoal or a *Lindlar*-catalyst results in the cyclopentadecanone (**11**) or the cyclopentadec4-en-1-one (**10**), respectively.[96]

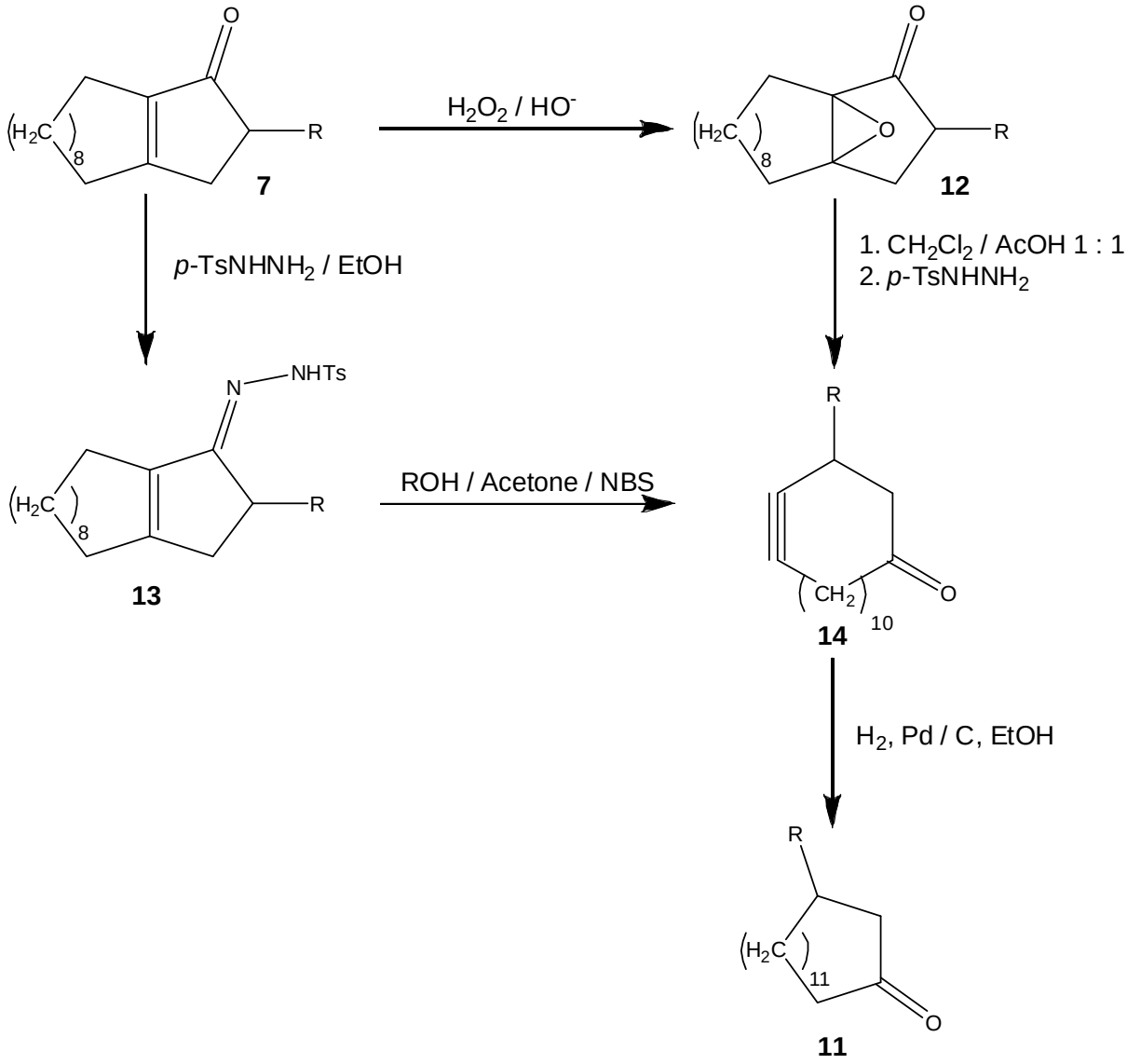

Fig. 2-5: Ring enlargement by fragmentation of a bicyclic compound.[96]

Later this tosylhydrazone route was complemented by structural variants[97] such as the fragmentation of α,β-epoxyketonoximes with hydroxylamine-O-sulfonacid in alkaline solution[98] as well as the fragmentation of hydrazones from

α,β-epoxyketones (**13a**) and substituted *N*-aminoaziridines initiated just by heating (**Fig. 2-6**).[99]

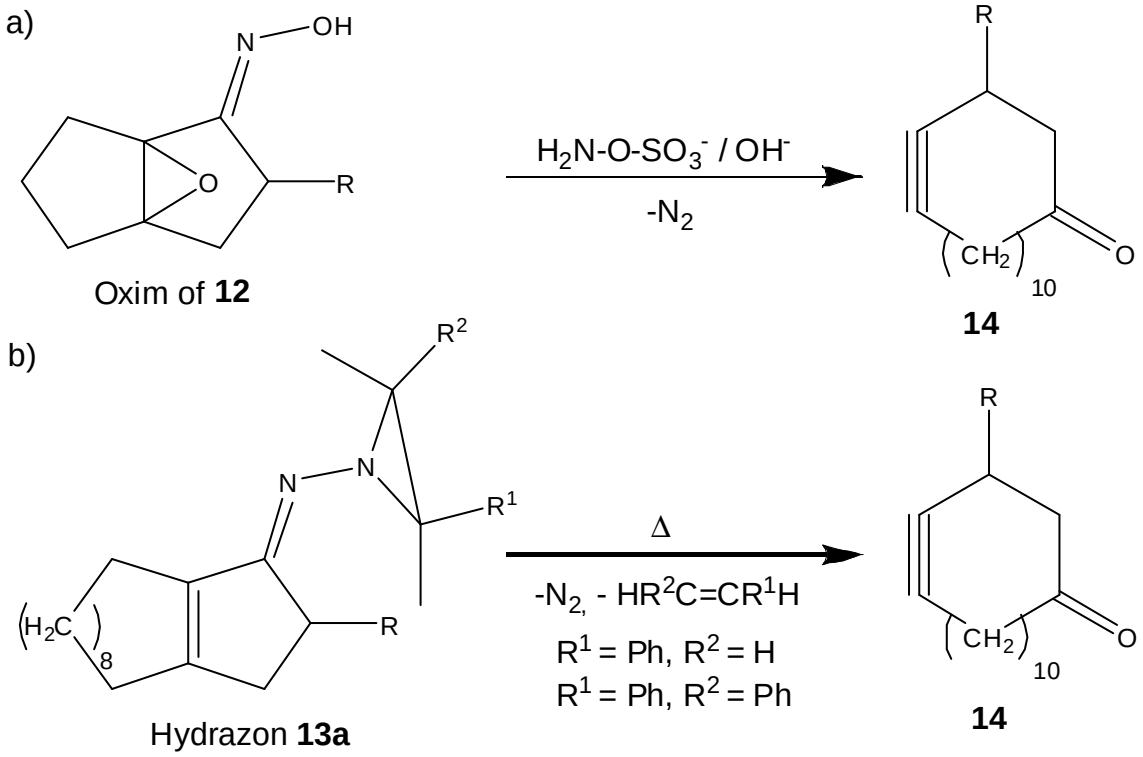

Fig. 2-6: structural variants of tosylhydrazone route.

The Oxy-*Cope* rearrangement involves allyl vinyl carbinols. Yet, many catalytic processes are also known.[100] Chlorination of **6** with sulfuryl chloride yields α-chlorketone (**15**) which is treated with vinylmagmesium. In a one-step divinylation a cis/trans-mixture of 1,2-divinylcyclodecan-1-ol (**16**) is formed. After a first vinylation the rearrangement (1,2-migration of the vinyl group) takes place at a temperature higher than 50 °C. The intermediate reacts further in situ with vinylmagnesium chloride producing **16**. Like the *Claisen* rearrangement, the *Cope* rearrangement is in most cases initiated by temperature. After the unstable enol derivative of ketone (**6**) is obtained in the first stage, **16** immediately readily undergoes rearrangement and gives the corresponding carbonyl compound **18**. The Oxy-*Cope* rearrangement was commercialized on industrial scale in the synthesis of Ambretone® (Toray Ind.) (**18**) and its methyl analog from cyclododecanone (**6**) (Fig. 2-7).[101-103]

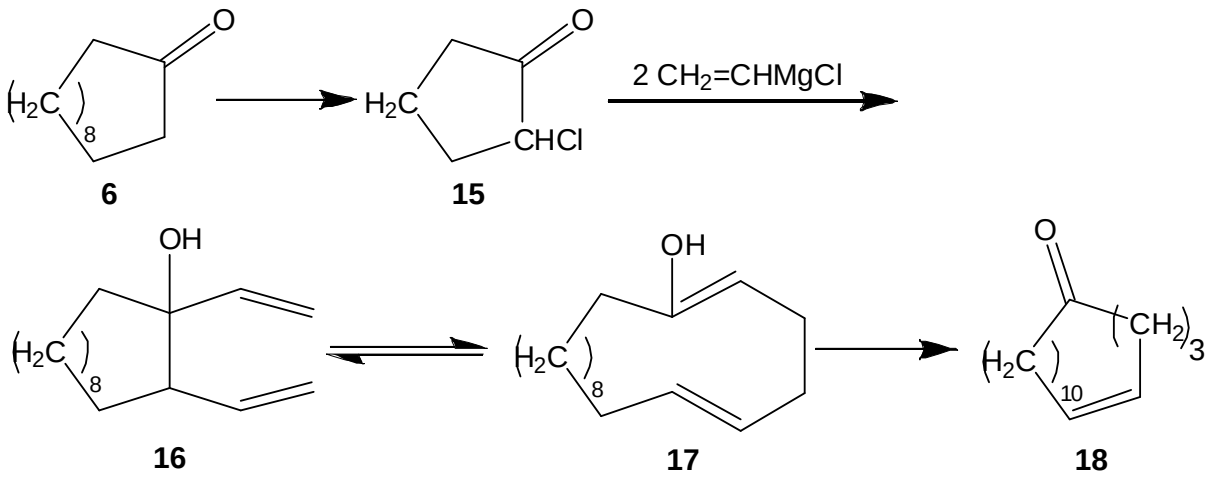

Fig. 2-7: Industrially applied synthesis of cyclohexadec-5-en-1-one (18) from cyclododecanone (6).[89]

A ring expansion via a photochemical cleavage of a bicyclic ketone yielding *exaltone* (**2**) has already been reported in 1967.[104] Another C_3 ring enlargement strategy depends on a radical-initiated addition of HBr and subsequent regeioselective *Baeyer-Villiger* reaction of substituted cyclododecanone (**19**) to bromo lactone (**20**) by a peroxy acid (Fig. 2-8). The reaction of **20** (containing 1,2-dibromoethane as initiator) with Mg or Li in THF creates an organometallic species (**21**). Through this intermolecular *Grignard* or lithium-supported reaction yields over 75 % have been attained. An intramolecular nucleophilic attack on the carboxylic group by **21** or by a stabilised carbanion (**23**) generates a C_{15}-macrocycle (**25**) via a six-membered cyclic transition state (**22**).[105] The formation of the pyran-like intermediate (**22**) and the preparation in extreme dilution prevent a nucleophilic attack on the carboxylic group of the hydroxyketone. Similarly successful are the cyclizations of the anion (**23)** derived from sulfone and the subsequent removal of the sulfonyl group.[106-108] By a radical-initiated addition of thiophenol to 2-allylcyclododecanone (**19**) a thioether is formed. Without any purification the oxidation to the sulfone is caused by an excess of peracetic acid. In the presence of BF_3-etherate at 50 °C for several days a regeioselective *Baeyer-Villiger* reaction affords a sulfonyl lactone (**23´**). The ring is closed under basic conditions generating the sulfonyl ketone (**24**) which is selectively reduced to the hydroxyl ketone (**25**) by Al(Hg).

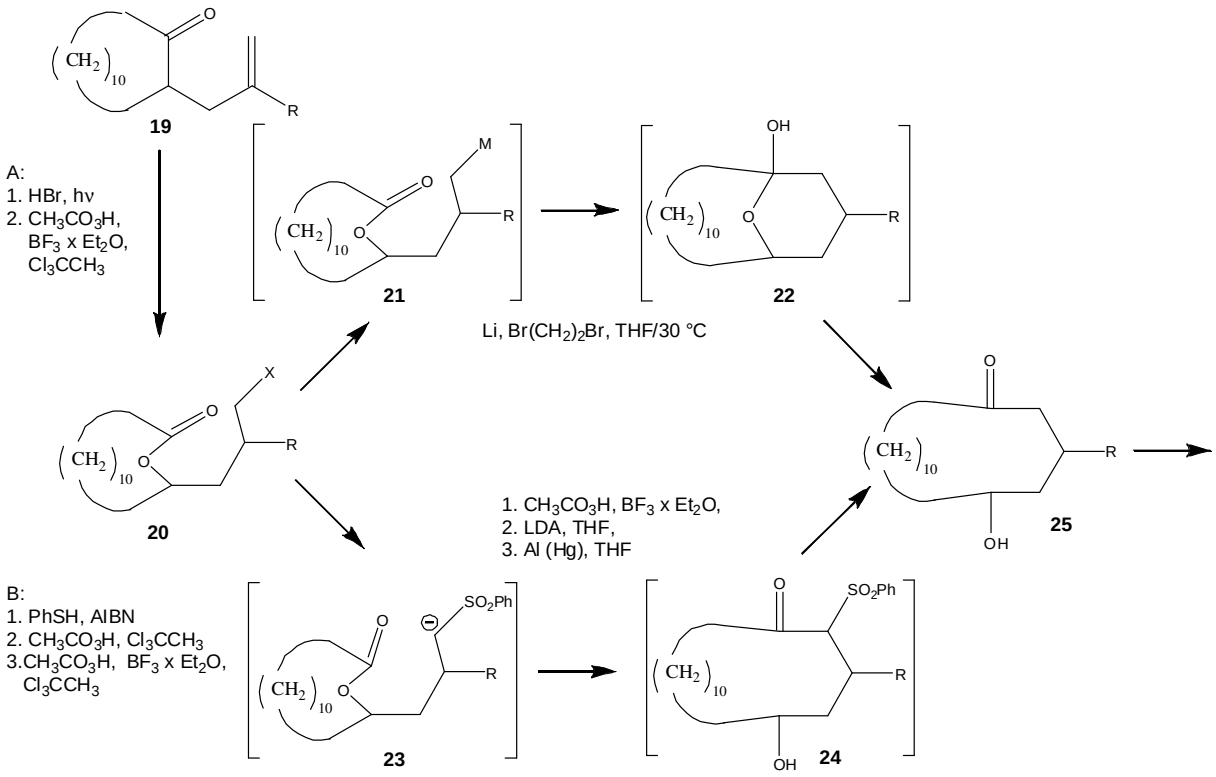

Fig. 2-8: Ring enlargement by intramolecular *Grignard*- et.al. nucleophilic reactions.[105]

Another example of a ring enlargement is presented by *Sugimone et. al.*.[109] Cyclic ketones are transformed into bicyclic alcohols by a three carbon annelation followed by a regioselective radical cleavage of their fused bond. Key step is the transformation of an iodide into a single bicycle[10.3.0]pentadecan-1-ol by a *Grignard* reagent or butyl lithium in THF.

Another pathway developed by *Firmenich* for producing racemic muscone (**1**) passes two key steps: 1.) the intramolecular En-reaction catalyzed by *Lewis*-acid (**26**→**27**) and 2.) the β-cleavage of bicyclic alkoxides (**27**) to macrocyclic Enone (**28**) (Fig. 2-9).[110]

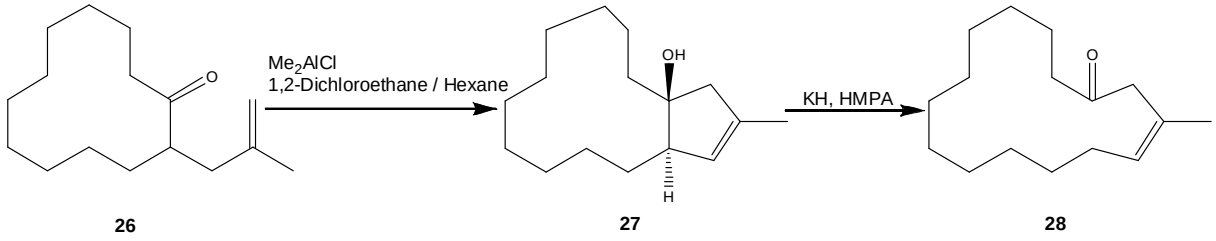

Fig. 2-9: Ring enlargement by an intramolecular En-reaction.[110]

An additional procedure of macrocyclic ketone formation is the two-carbon ring expansion by thermo-isomerization. In two repetitive cycles *exaltone* (**2**) can be prepared from cycloundecanone.[111]

2.3.2 Ring-closing reactions

The first synthesis of a macrocyclic musk compound was published by *Ružička* in 1926 (Fig. 2-10).[44] He successfully generated *exaltone* (**2**) in yield of 2 % by pyrolysis of thorium salts of hexadecane dicarboxylic acid (**4**).

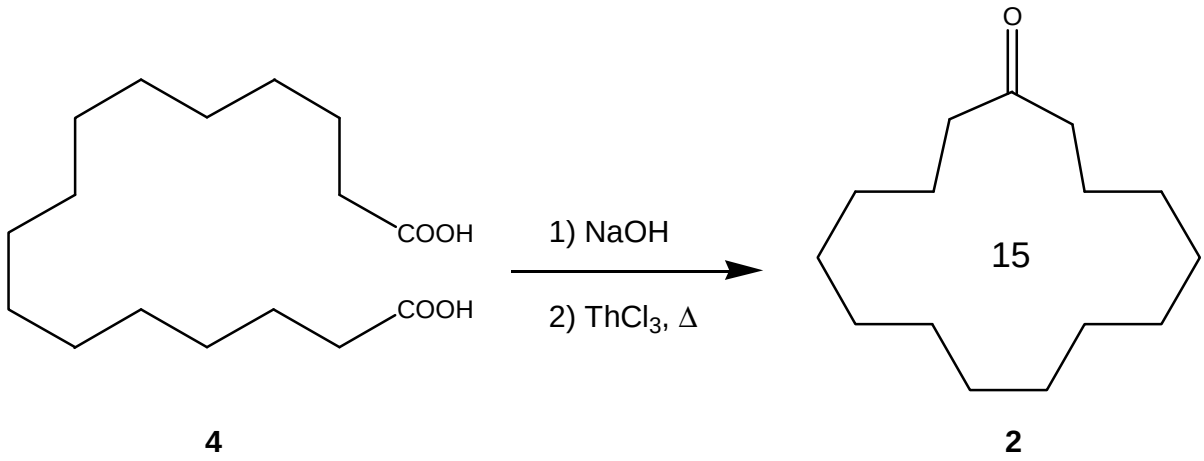

4 **2**

Fig. 2-10: The first *exaltone* (2) synthesis by *Ružička.*

Even though this preparation was optimised up to yields of 60-70 %, this method was not used for industrial production because of the high dilutions necessary to favour the intramolecular reaction over oligomerisation and polymerisation. Other high dilution macrocyclizations relying on *Ziegler´*s work were reported: *Hunsdiecker*[112, 113] proposed an intramolecular condensation and *Blomquist*[114] a ketene dimerization approach.

To avoid this problem *V. Prelog* and *M. Stoll* independently developed a method based on the acyloin condensation to muscone (**1**).[115; 116] Since the reductive coupling occurs on the sodium surface high dilutions were no longer necessary and very practical conditions of around 1 M solutions are possible (*Rüggli-Ziegler* dilution principle).

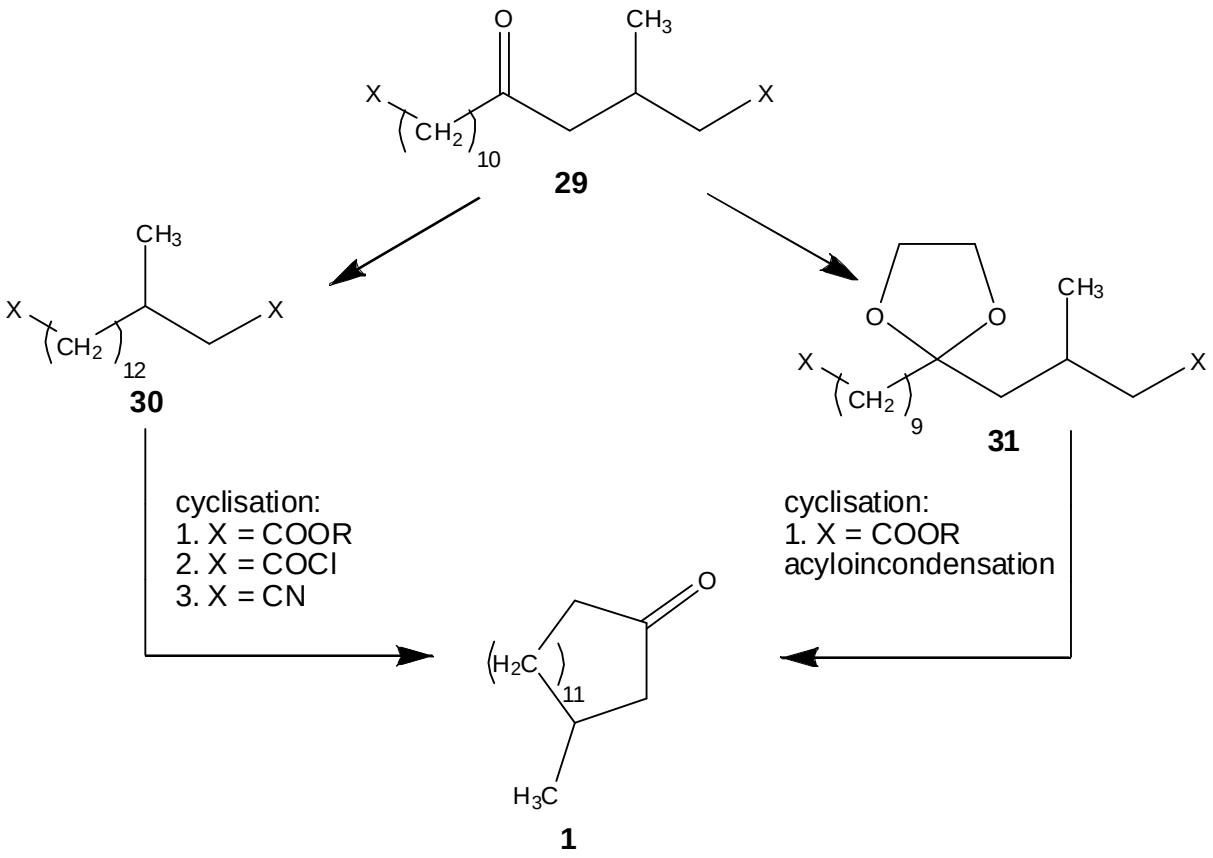

Fig. 2-11: Alternate routes to *rac*-moscone (1) from derivatives of 3-methyl-hexadecanediacid (29).[117]

From an industrial point of view, high dilution reactions are not economical, as the reactor volume is taken up by solvent rather than the value added product. The first industrial synthesis was developed using an intramolecular acyloin condensation[118] (Fig. 2-11). According to the method of *M. Stoll* and *A. Commarmont,* muscone (**1**) and the isomeric 4-methyl-cyclopentadecanone can be obtained by ester condensation of the diethyl ester (**30**) of 3-methyl-5-oxo-hexadecane-α,ω-diacid (**29**).[119-121] The reduction of the methyl-substituted keto diester (**29**) is followed by ester condensation while making use of the dilution principle, and subsequent removal of the carbethoxy group to afford **1**.

Applying the same method the ketal-protected ketone of the diester can be cyclized, deoxidised to the ketal diol (**31**) which is converted to the unsaturated ketone. This ketone is hydrogenated and deprotected to give muscone (**1**).[15] The hydroxylic group of the acyloin in α-position can either be dehydrated over alumina to the α,β-unsaturated ketone or reduced with zinc dust in acid media to provide muscone (**1**) [122] An alternative reduction with HI is also possible.

In addition to acyloin condensation ring-closing reactions can also be carried out by intramolecular ester condensation of the e.g. alkyl substituted diester (*Dieckmann*-condensation).[123] followed by cleavage of the ethoxy carbonyl group, obtaining the cycloalkanone.[124] The *Dieckmann*-condensation is actually an intramolecular *Claisen*-condensation (in which esters having α-hydrogen are condensed in the presence of a strong base to form a α,β-ketoester). In the *Dieckmann*-condensation the two esters groups involved in the reaction are present in the same molecule and an α-alkoxycarbonylated macrocyclic ketone is formed. The α-alkoxycarbonylated macrocyclic ketone can be converted into the macrocyclic ketone by hydrolysis and decarboxylation according to the known method.[125] In general, *Dieckmann*-condensation is advantageous for the formation of 5-, 6-, or 7-membered rings. Also civetone (**3**) has been produced by this intramolecular condensation in the presence of titanium tetrachloride or zirconium tetrachloride and a trialkylamine.[126] By ring-closing reactions of the diester, the diacid chloride[127] or the diacid nitrile[128], [129] of 3-methyl-5-oxo-hexadecan-α,ω-diacid (**29**), racemic *D*,*L*-muskone (**1**) can be generated.

The first synthesis of optically pure stereoisomers of muscone (**1**) was successfully performed by *S. Ställberg-Stenhagen* in 1951.[130] It involved the cyclisation of the dichloride of (+)- or (-)-3-methyl-hexadecane diacid. (+)- or (-)-3-methyl-glutaric acid were used as enantiomerically pure intermediates for the preparation of the dicarboxylic acid. Afterwards, the necessary optically active esters of ketodicarboxylic acids were made by homogeneous asymmetric hydrogenation of the unsaturated ketodiester or ketals.[131, 132]

Further approaches based on intramolecular *Wittig* reaction[133] and intramolecular acylation[17] of ω-trimethylsilylethynylalkanoyl chlorides on $AlCl_3$ have been reported. Even superior and without dilution conditions is the intramolecular alkylation of a cabanion generated from protected cyanohydrins by sodium hexamethyl-disilazane.[134] Furthermore an intramolecular aldol condensation reaction[116] is suitable to form cyclic structures. So 3-methyl-2-cyclopentadecen-1-one can be generated from 1,15-hexadecandione via the Mg[115], Al, Ti[135] and Zn enolates. After preparing the cyclic enone according to the *Tsuij*[136,137] method by organoaluminium,

the (E)- and (Z)-isomeres were separated and applied to a p-tolyl-BINAP-Ru catalysed asymmetric hydrogenation by *T. Yamamoto*.[138]

Along *Diekmann*- acyloin- and aldol condensation the intramolecular metathesis[139, 140] is another possibility to build rings (Fig. 2-12). By this method e.g. civetone (**3**) (*cis*-9-cycloheptadecene-1-one) was prepared in a three step synthesis from methyl-*cis*-9-octadecanoate (**32**) via intramolecular metathesis under high dilution on a heterogeneous $Re_2O_7/SiO_2{\times}Al_2O_3$ catalyst.[141, 142] Metathesis is best described as a reaction between two alkenes in which an intercharge of alkylidene groups takes place. The yield of 12 % lies in same range as the in preparation of civetone (**3**) via *Diekmann* condensation.[143]

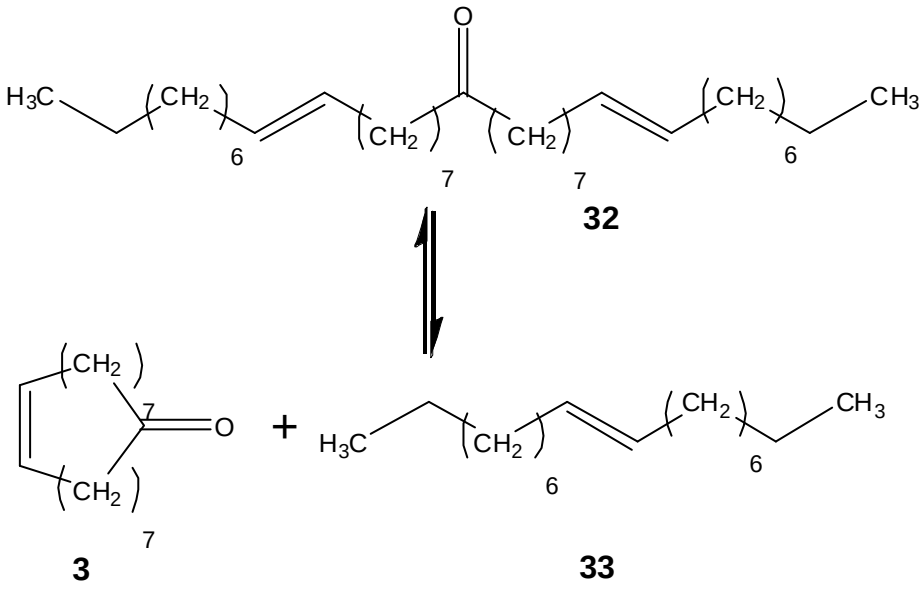

Fig. 2-12: Ring closing via intramolecular metathesis.[142]

A. Fürstner[144] reported stereoselective homogeneously catalysed alkine metathesis affording civetone (**3**). The cyclizations were carried out by using catalytic amounts of a *Schrock*-alkine complex $(t\text{-BuO})_3W{\equiv}CCMe_3$ or via an in situ generated catalyst consisting of $Mo(CO)_6$ and *p*-trifluoromethyl phenol.[145,146]

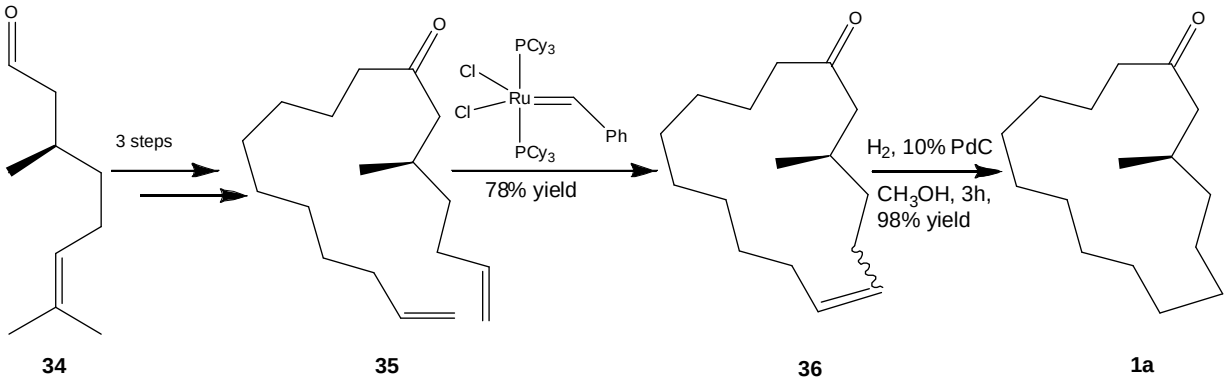

Fig. 2-13: Synthesis of (R)-(-)-muscone (1a) from (+)-citronellal (34) by ring-closing metathesis

In the same year the synthesis of (*R*)-(-)-muscone (**1a**) by a macrocyclization based on ring-closing olefin metathesis (RCM) as the key step was published. Commercially available (*R*)-(+)-citronellal (**34**) was employed as a precursor in preparing the acyclic diolefinic substrate (**35**), which in turn was contacted with bis(tricyclohexyl-phosphine)benzylidene ruthenium dichloride catalyst (*Grubbs* I)[147] to afford the cyclic RCM reaction product in 78% yield. Catalytic hydrogenation of (**36**) gave enantiomerically pure (R)-(-)-muscone (**1a**).[148,149,150] Further syntheses using a metathesis reaction step to generate this product are mentioned in literature.[151-153]

Shorter aliphatic acids have successfully been converted by intramolecular decarboxylation-dehydratisation reactions to suitable cyclic ketones. In these commercialyzed processes the aliphatic acids react in liquid phase at 250 °C in presence of certain metals or their compounds (B, Al, Ga, In, Th, Sn, Sb, Bi, Mo, Rb, Cr, or V) to the ketone.[154] Also well known is the preparation of small cyclic ketones from aliphatic acids on TiO_2 catalysts impregnated with Na_2O and K_2O as filed in the patent of W. Hölderich et al..[155] Over such a catalyst methyl isopropyl ketone was prepared from mixtures of acetic and isobutyric acid. Other catalysts such as ZrO_2 or ThO_2 on Al_2O_3 were less successful.[156] The best results were achieved by Na_2O- and K_2O-impregnated anatase supports.[157; 158, 155] A similar method could be applied for the intramolecular decarboxylation/dehydratisation reaction.

Recently *BASF AG*[159] published the possibility of synthesizing macrocyclic ketones like *exaltone* (**2**) from the diesters of the corresponding acids by using the same TiO_2 catalyst impregnated with Na_2O and K_2O.[160] These findings constitute the starting point of this thesis.

2.4 Support materials

2.4.1 Production processes for TiO_2-support materials

The main industrial methods used in the production of titanium dioxide for pigments are the chloride and the sulfate process.

The sulfate process for titanium dioxide production was developed in Norway by *F. Farup* and *G. Jebsen* in 1915 and industrially applied since 1919 (Fig. 2-14). This process still retained its prominent position. The chemical digestion of the finely ground and enriched titania ore ilmenite is carried out with sulfuric acid. The iron oxide in the ore reacts to iron sulfate and the titanium oxide to titanium sulfate. The large amounts of sulfur dioxide generated in this process are neutralised by sodium hydroxide solution so that just small amounts of sulfur dioxide are emitted in the environment today. Titanium sulfate settles and the iron sulfate solution is separated and then crystallised to green iron(II)-sulfate heptahydrate. Titanium sulfate is easily hydrolised with boiling water to titanium oxide hydrate which is then calcinated at 800 to 1000 °C in a rotating oven to pure white titanium dioxide after an extensive washing process.[161]

Titanium dioxide production by the chloride process starts from enriched ilmenite or rutile. The ore is mixed with coke and reacted with chlorine gas in fluidized bed at approximately 1000 °C in special chlorine resistant reactors to gaseous titanium tetrachloride and carbon dioxide. Low-volatile impurities resulting after chlorination, e.g. $FeCl_2$, are separated, then dissolved in water and crystallised. Chlorine gas also reacts with the residual wetness in the slag forming hydrochloric acid which is washed out and sold as a by-product. Afterwards the gaseous titanium tetrachloride is condensed and purified by distillation. Pure titanium dioxide is generated by burning the titanium chloride in oxygen; titanium chloride is oxidised to titanium dioxide and pure chlorine gas is released and recycled to the reaction process.

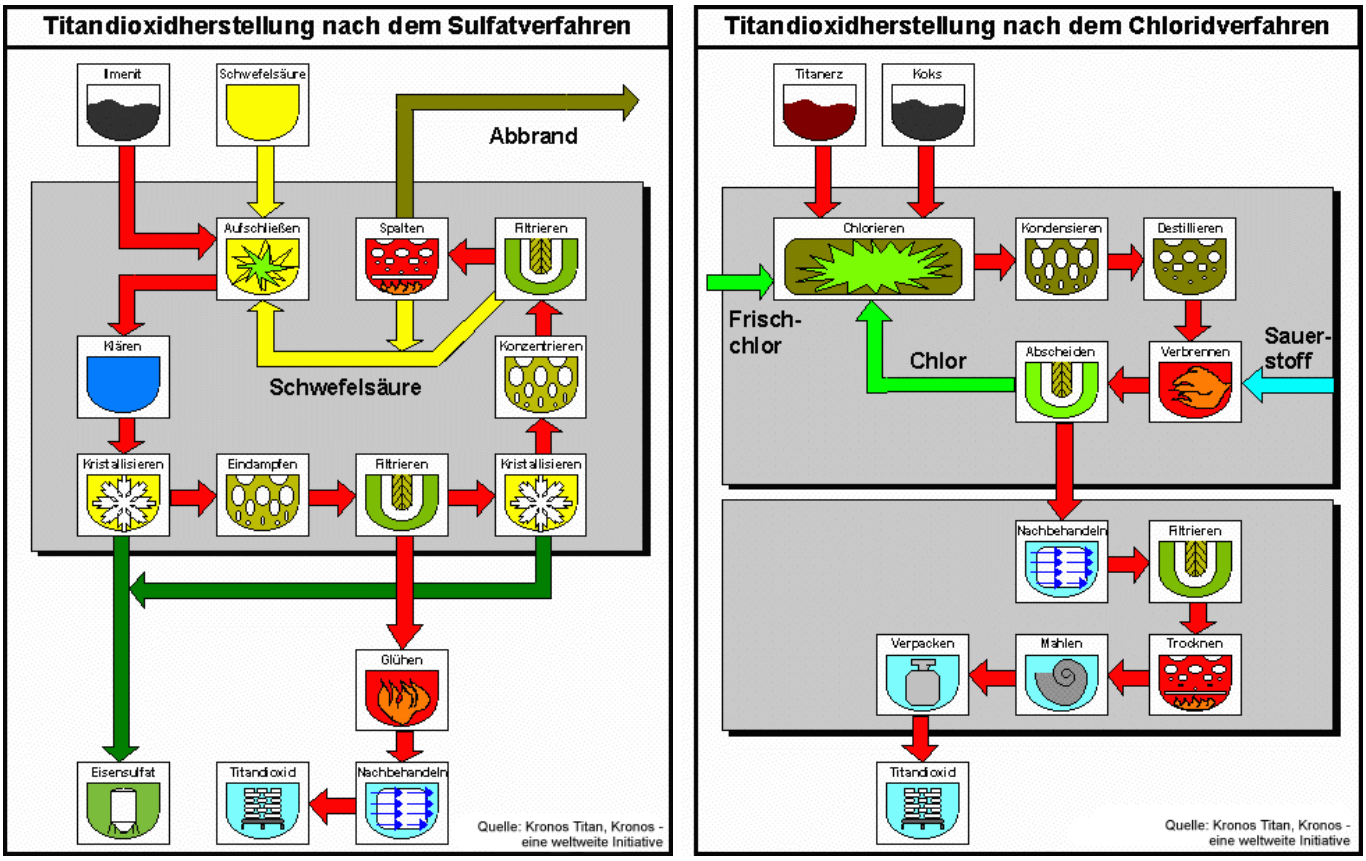

Fig. 2-14: Production process of TiO_2-support materials [162]

Materials resulting from both processes show essential differences in catalytic application. Higher specific surfaces can be obtained by the sulfate method but the material includes small amounts of sulfate.[163, 164] This fact has an important effect on application in catalysts because sulfate-containing materials possess increased *Brönsted*-acidity.

The 3rd *Pauling* rule, *"The sharing of edges and particularly faces by anion polyhedra decreases the stability of an ionic structure",* directly applies to the different modifications of polymorphous TiO_2: the rutile modification (combination over two common edges of a TiO_6-coordination polyhedron) is more stable than brookite (three common edges), and this again is stabler than anatase (four common edges).

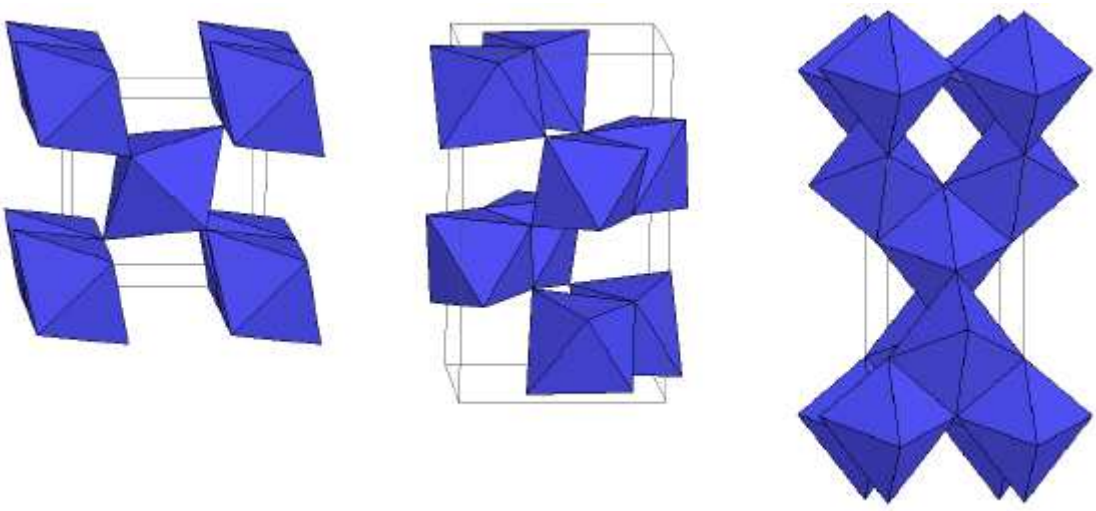

Fig. 2-15: Spatial arrangement of TiO_6-coordination polyhedrons: rutile, brookite and anatase.[165]

2.4.2 Production process of ZrO_2-support materials

The starting point of zirconium oxide production is zirconium silicate $ZrSiO_4$. This silicate sand is separated from impurities by washing, cleaning and calcination processes and transformed into zirconium oxide. Zirconium oxide occurs in three modifications: it is monoclinic at room temperature with a CN of 6 (baddeleyite), above 1170 °C it is tetragonal with a CN of 8 and above 2370 °C it is cubic with a CN

of 8 (fluorite-type). The structures are commonly described as cubic centred lattice of O^{2-} ions with filled gaps.

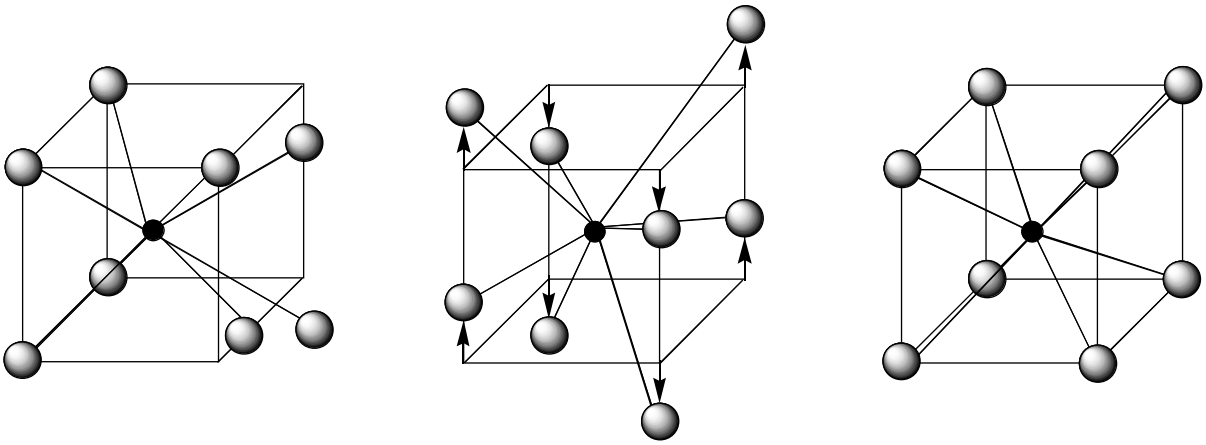

Fig. 2-16: Three modifications of ZrO_2: monocline, tetragonal und cubic.

2.4.3 Alternatives of immobilisation

Catalytic active components can be immobilised on different ways. Some examples of the most important immobilisation methods are summarily presented below.[166, 167]

- Impregnation. The active component is added as a solution. The excess solvent is decanted or concentrated in vacuum. By drying the active substance remains deposited on the support.

- Incipient Wetness. Only as much of a solution of catalytic active substance is added as the support can absorb. The wet powder is then dried.

- Adsorption. Unlike Incipient Wetness this technique does not necessitate any solvent since the active substance itself is a liquid. The support material is treated with just the amount of liquid active component to keep the catalyst in powder form.

2.5 Previously realized reaction studies

The present reaction has already been investigated in part by *Dr. D. Das* within the framework of his post-doctoral work at the *TCHK*-institute in Aachen (Fig. 2-17).

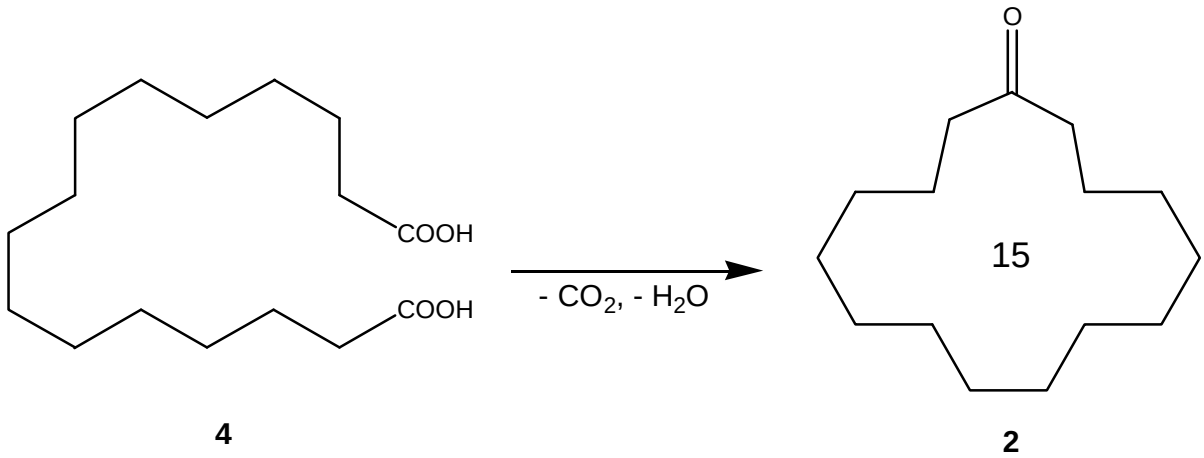

Fig. 2-17: Cyclization of hexadecane dicarboxylic acid (4) to *exaltone* (2).

He firstly carried out the decarboxylation-dehydation reaction of hexadecane dicarboxylic acid (**4**) in liquid phase. The catalyst support was titanium dioxide P25 form *Degussa AG*[168] and zirconium dioxide by *Sigma-Aldrich Co.*[169] loaded with 2 wt% alkali metal oxide (Na_2O and K_2O). Ethanol and tetrahydofuran were used as solvents. Typically 250 mg of dried catalyst were added to a mixture of 155 mg HDA (**4**) and 20 g solvent. This mixture was heated under reflux (60 °C for THF and 80 °C for ethanol) during 6-8 hours before filtering out the catalyst. The liquid phase has been analysed by gas chromatography. Additionally some experiments have been carried out in the melt. In both cases no product was detected.

In a next step the ring-closing reaction was carried out in gas phase (experimental set-up I - gas phase continuous flow reactor with external saturator). Experiments in which the substrate vapour from a vaporizer was passed along with a carrier gas (substrate-saturated nitrogen stream) through the catalyst fixed bed were also unsuccessful. Due to the low volatility of the substrate, even at a temperature of 350 °C only low amounts of substrate were transported. The addition of different solvents into the vaporizer had no positive effect at all.

Another approach for solving the substrate feeding problem was to build a gas phase continuous flow reactor (experimental set-up II) fed with a substrate/THF solution (WHSV = 0,9 g HDA × h^{-1}/g ml catalyst fill). Nitrogen was used as carrier gas (Fig. 2-18). The product mixture was analysed by HPLC or, after esterification of the residual dicarboxylic acid, by GC. By esterification the boiling point drops, ensuring thus the mobility in the GC column. By feeding the reactor with 3 wt% of substrate selectivities of 97 % and conversions of 3 -12 % have been achieved. The amount of product leaving the reactor was, however, small. Since the esterification process does not achieve total conversion, product work up was later on changed to silylation.

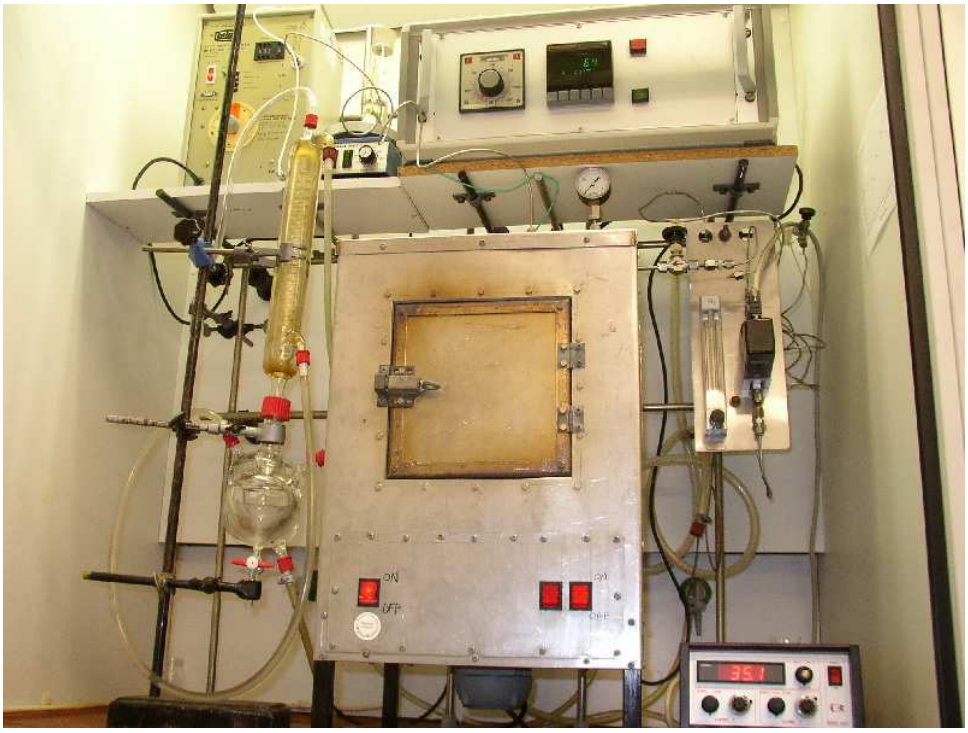

Fig. 2-18: Set-up II; liquid feed gas phase continuous flow reactor.

Based on this initial success, further catalysts have been produced and tested. *D. Das* reported that with the catalyst ZR-5 (zirconium dioxide from *Degussa AG*[168] with 1,7 wt.% Na_2O) a conversion of 18 % and with the catalyst T-5 (titanium dioxide from (*Sigma-Aldrich Co.*[169] 4,2 wt.% K_2O) a conversion of 12 % at selectivities of 95 % were achieved.[170] These experiments have been carried out at a higher substrate feed of 5 wt.%. A larger catalyst amount of 6 g, based on supports from *Sachtleben GmbH*[171] with high BET-surface areas of 110 or. 333 m^2/g respectively, leads to conversions of 5 to 11 %.[172] A perennial problem in all of the experiments was the plugging of the reactor by (non analysed) reaction products.

The starting point of the present thesis was to check these promising results using anatase materials with high BET-surface areas and the zirconium dioxide form *Degussa AG*. In order to check the reproducibility and to get a constant quality, larger amounts of catalyst were manufatured by extrusion. The implementation of these catalysts in the existent liquid feed gas phase continuous flow reactor (set-up II) presents the same problems. Reproducibility was hardly achieved. Because just small amounts of reaction material left the reactor and were detected low conversions and high selectivities were obtained. The transport of lower boiling *exaltone* (**2**) is easier than that of other reactants. Accordingly, the results showed a high selectivity. Deposits of non-converted hexadecane dicarboxylic acid (**4**) have been identified on used catalysts by TG analysis. The low desorption from the surfaces of tubes and catalyst was recognised as a major problem. The solution was the injection of steam into the reaction system. In set-up IV (Fig. 2-18) a yield of 5 % and a selectivity of 99 % was achieved.

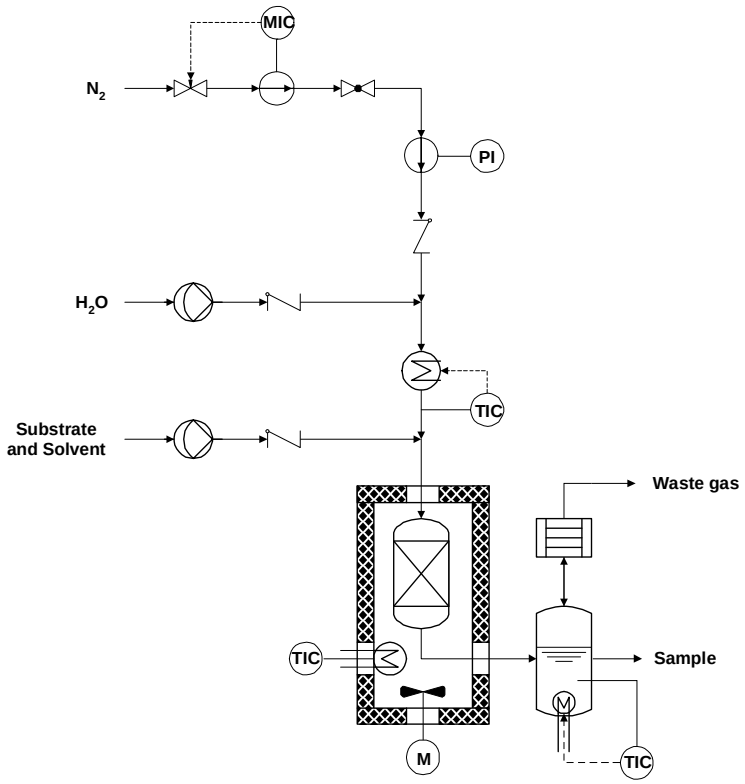

Fig. 2-19: Flow chart for liquid feed gas phase continuous flow reactor set-up IV

However, higher boiling reactants remained inside the reactor and were not detected. The variation of loading amount had no clear effect on the result. Increasing the amount of catalyst and operating the reactor at higher temperatures (450 °C) had, as expected, a positive effect on yield. The aim of the work presented in this thesis was to further improve the catalyst, find the best reaction conditions and optimise the experimental set-up.

3 Results and Discussion

3.1 Support materials

For the catalytic gas phase reaction of HDA (**4**) to *exaltone* (**2**) various support materials have been tested. Mainly titanium dioxide materials like Hombikat Typ II, Hombikat K 03, Hombikat UV 100 from *Sachtleben-Chemie GmbH*[171] and P25 from *Degussa AG*[168] have been used. Some additional experiments were carried out with zirconium dioxide support VP ZrO_2 from *Degussa AG* and with materials prepared in our laboratory.

The characteristics of these materials are presented in Table 3-1:

Table 3-1: Titanium dioxide materials

Type	A_{BET} [m^2/g]	Sulfate content [%] (producer data)
Hombikat UV 100	>300	n/a
Hombikat K 03	>100	1,5
P25	>50	0
Hombifine N	>300	0,5 - 1,5
Hombikat Typ II	>100	0,5 - 1,5

The titania materials of *Sachtleben-Chemie GmbH* show a high specific surface area and a relatively low sulfate content. Because of the chloride production process the titania material P25 from *Degussa AG,* produced by the chloride method, has a lower specific surface area and lacks sulfate.

According to the manufacturer, the VP ZrO_2 from *Degussa AG* has low acid sites and a BET-surface area of 39,9 m^2 / g.

3.2 Catalyst preparation

The used catalysts consisting out of the support material and the active component like Na_2O and K_2O have been generated by the incipient wetness method. In chapter 5.2.2 this method is explained in more detail. In a first step the support particles have been produced. Titanium dioxide and other support materials were mixed intensively with low amount of water and some oxalic acid in an electric blender. The oxalic acid functions like a binder in the following step of extrusion. The extruder presses the ductile mass with a load of 60 tons through a nozzle of 2 mm diameter. The pressed material was dried overnight, calcinated and sieved to 1,0-2,0 mm sized particles. The oxalic acid is burned residue-free in the calcinations process. When smaller amounts were needed pellets were pressed manually without binder at 10 t / cm^2 and then crushed. For impregnation a small amount of these particles was treated with a solution of e.g. sodium hydroxide and one drop dimethyl amine to achieve the desired metal oxide loading. Dimethylamine lowers the surface tension of the alkaline solution, allowing a complete coating of the support surface, including in the pores. After drying at reduced pressure in a rotary evaporator and in an air oven the pellets were finally calcinated. The catalysts listed in Table 3-2 have been generated by this standardised method. Variations of the preparation method are explained in chapter 5.2.2.

Table 3-2: BET-surface areas and loading of prepared catalysts and support materias.

Material	Doped material	Doping $_{ICP}$	A_{BET} [m^2 / g]	A_{BJH} [m^2 / g]	V_{BJH} [m^2 / g]	$V_{Mikropore}$ [cm^3 / g]	Pore diameter [Å]
Hombikat UV 100[1)]	/	/	320	205	0,306	0,018	59,6
T-8	Na_2O	3,22	54	59	0,326	0,003	220,6
Hombikat K 03[1)]	/	/	101	110	0,365	0,002	131,9
T-9	Na_2O	2,30	61	73	0,271	0,004	147,6
ZrO2 (VP)[2)]	/	/	39	32	0,123	0,0002	152,2
ZR-5	Na_2O	2,02	30	38	0,152	0,002	157,6
SG-Zirconia[3)]		/	152	147	0,259	0,003	51,1

Material	Doped material	Doping $_{ICP}$	A_{BET} [m^2 / g]	A_{BJH} [m^2 / g]	V_{BJH} [m^2 / g]	$V_{Mikropore}$ [cm^3 / g]	Pore diameter [Å]
ZR-6	Na_2O	0,41	144	139	0,253	0,003	52,3
Hombifine N[1)]	/	/	315	301	0,354	0,027	56,0
T-10	Na_2O	2,71	62	61	0,314	0,003	186,0
T-10B	Na_2O	6,58	49	51	0,282	0,002	221,0
T-16	K_2O	2*	72	71	0,303	0,003	156,1
T-17	Li_2O	0,54	33	32	0,217	0,001	249,0
T-18	Cs_2O	2*	68	66	0,279	0,002	153,0
T-20	CaO	2*	146	143	0,616	0,004	152,1
T-21	Na_2O	0,74	69	68	0,317	0,001	142,5
T-21.2	Na_2O	0,56	65	64	0,303	0,001	146,1
T-21.3	Na_2O	0,51	80	78	0,341	0,002	132,9
T-21.4	Na_2O	0,58	76	78	0,291	0,002	134,4
T-21.5	Na_2O	0,40	100	118	0,297	0,001	100,5
T-21.6	Na_2O	0,51	73	83	0,266	0,002	127,7
T-21.7	Na_2O	0,66	96	112	0,287	0,001	102,1
T-22	K_2O	0,5*	86	84	0,329	0,001	117,9
T-22.2	K_2O	0,5*	84	82	0,336	0,002	124,0
T-23	Cs_2O	0,5*	85	83	0,308	0,0003	109,5
T-27	BaO	n.n.	89	99	0,302	0,0002	121,5
Degussa P25[4)]	/	/	55	46	0,183	0,0003	156,9
T-11	Na_2O	3,10	31	35	0,249	0,002	277,9
T-11B	Na_2O	6,58	22	23	0,196	0,0005	337,4
Hombikat Typ II[1)]	/	/	107	104	0,361	0,001	126,8
T-12	Na_2O	2,95	55	67	0,282	0,004	167,4
T-12B	Na_2O	6,56	42	204	0,235	0,002	204,6
T-13	K_2O	2*	69	68	0,297	0,004	145,2
T-14	Li_2O	0,44	42	41	0,243	0,002	182,1
T-15	Cs_2O	2*	66	65	0,281	0,003	140,7
T-19	CaO	2*	84	82	0,362	0,003	153,3
T-24	Na_2O	0,27	78	76	0,315	0,003	124,3
T-25	K_2O	0,5*	78	76	0,308	0,003	125,5
T-26	Cs_2O	0,5*	76	74	0,298	0,002	124,5

Material	Doped material	Doping $_{ICP}$	A_{BET} [m^2 / g]	A_{BJH} [m^2 / g]	V_{BJH} [m^2 / g]	$V_{Mikropore}$ [cm^3 / g]	Pore diameter [Å]
SiO_2[5)]	/	/	47	31	0,132	0,003	169,2
Si-1	Na_2O	0,67	48	40	0,354	0,003	352,0
Al_2O_3[6)]	/	/	112	84	0,302	0,004	144,8
Al-1	Na_2O	0,46	110	130	0,396	0,001	121,8

1) Hombifine and Hombikat from *Sachtleben*; 2) VP from *Degussa*; 3) SG-Zirconia from *Saint-Gobain; 4)* P25 from *Degussa 5)*. Kieselgel 350, 0592 from Degussa; 6) C-Typ from Degussa

The ICP-method is not sensitive enough for the quantitative measurements of the elements K and Cs.

3.3 Catalyst characterisation

Some of the physical properties of the supports and catalysts obtained were determined.

3.3.1 Acidity

The pure anatase materials Hombikat UV 100, Hombikat K 03, Hombikat Typ II and Hombifine N from *Sachtleben* have been analysed by NH_3-temperature programmed desorption (TPD) (Fig. 3-1). The principle of this method consists in the adsorption of a gas (NH_3) on the catalyst surface by *Van-der-Waals*-forces (physisorption) or chemical bonding (chemisorption). The amount of desorbed ammonia is recorded by a thermal conductivity detector and plotted against temperature. The TPD-plot of undoped anatas materials shows two maxima. These are located at around 280 °C and 460 °C in case of Hombikat UV 100, Hombikat K 03. Hombifine N shows a stronger acidic site at around 440 °C. Especially in Hombifine N these stronger groups are dominant. Weaker attached physisorbed NH_3 is desorbed at much lower temperatures and is not detectable in this case. The maxima at higher temperatures

correspond to a higher bonding energy of the adsorbate on the surface. Since the maxima are separated by a temperature difference of approx. 180 °C the existence of differently strong attached monolayers on the surface is not plausible. Probably two different types of acidic sites do exist. Because of the higher specific surface area Hombikat-UV 100 shows more acidic centres than Hombikat K 03. Hombifine N is even more acidic.

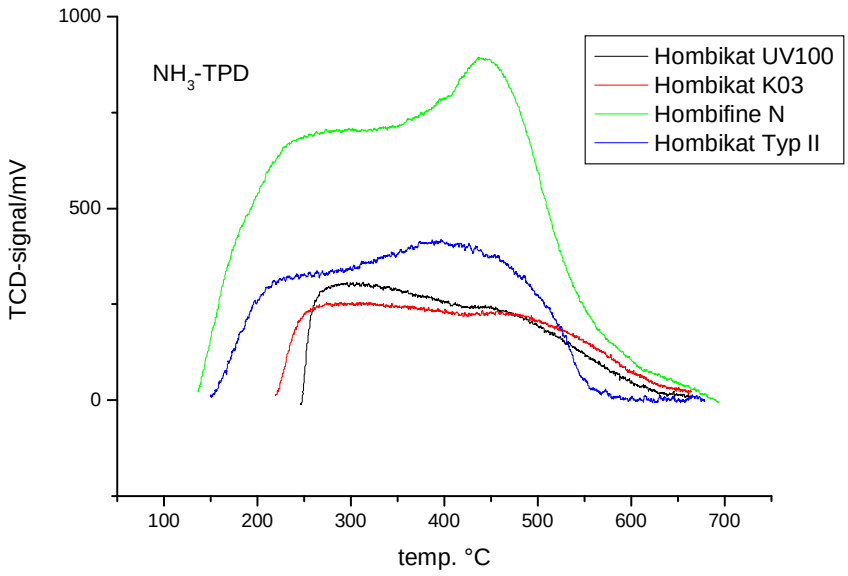

Fig. 3-1: NH_3-TPD of TiO_2-support materials

In order to evaluate the basicity of the materials additional CO_2-temperature programmed desorption (TPD) measurements have been carried out. According to the same principle, acidic CO_2 adsorbs on basic centres and desorbs in the course of the rising temperature profile.

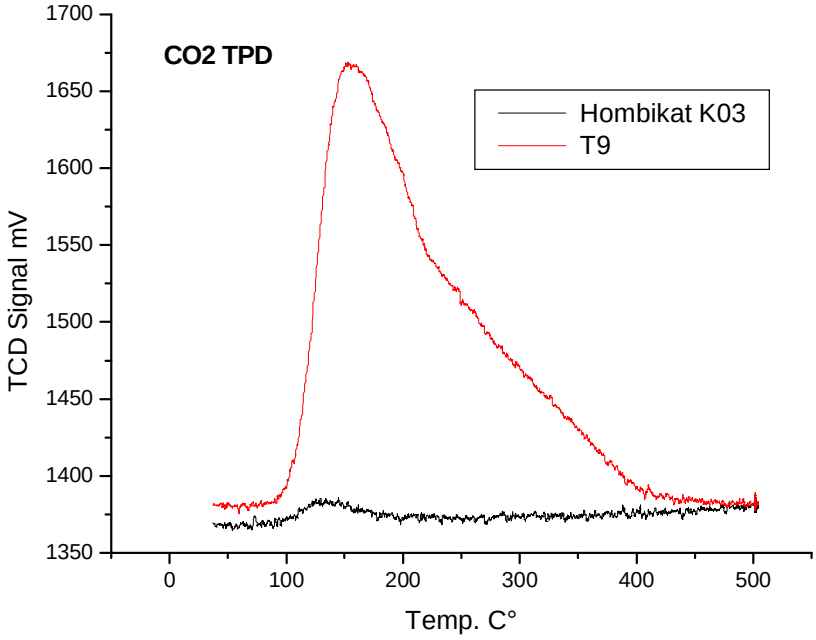

Fig. 3-2: CO_2-TPD of T-9 and the support Hombikat K03.

The support Hombikat K03 features no basicity as expected; just physisorbed CO_2 is identifiable. By doping with Na_2O a basic catalyst is obtained. The desorption gradient of the TPD-plot in Fig. 3-2 shows a maximum at 150 °C. The shoulder at 250 °C indicates a strong basicity. Signals of other measurements are presented below in

Table 3-3. If the TCD-signal is plotted verses time and the signals are fitted to a *Gaussian* function the signal areas can be generated. With a calibration factor of 5,65406154981346E-07 mmol/mV * s the amount of basic sites can be calculated. These results are fraught with a certain error and are to be used with caution.

Table 3-3: Results from CO_2-TPD measurements.

* calculated data, can not be quantified by ICP

Material	Doped Material $_{ICP}$	T_{Max} [°C]	TCD-Signal [mV]	Signal Area [mV * s]	Signal area x Factor [mmol/g]
Hombifine N					
T-17	0,54 % Li_2O	152	357	1,57E+05	8,88E-02
T-20	2 %* CaO	151, 407	322, 37	1,87E+05	1,06E-01
T-21	0,74 % Na_2O	139	119	4,65E+04	2,63E-02
T-21.2	0,56 % Na_2O	141	125	5,33E+04	3,01E-02
T-21.3	0,51 % Na_2O	142	151	6,65E+04	3,76E-02
T-21.4	0,58 % Na_2O	138	149	6,20E+04	3,51E-02
T-21.7	0,66 % Na_2O	139	92	3,75E+04	2,12E-02
T-22	0,5 %* K_2O	134	115	4,39E+04	2,48E-02
T-22.2	0,5 %* K_2O	134	111	4,58E+04	2,59E-02
T-23	0,5 %* Cs_2O	133	70	2,62E+04	1,48E-02
T-27	BaO	142	256	1,18E+05	6,68E-02
Hombikat Typ II					
T-14	0,44 % Li_2O	147, 235	225, 81	1,03E+05	5,85E-02
T-15	2 %* Cs_2O	128	21	7,97E+03	4,51E-03
T-19	2 %* CaO	156, 420	305, 101	2,37E+05	1,34E-01
T-24	0,27 % Na_2O	135, 451	52, 11	2,76E+04	1,56E-02
T-25	0,5 %* K_2O	127, 439	33, 6	1,66E+04	9,37E-03
T-26	0,5 %* Cs_2O	129, 425	25, 4	1,64E+04	9,27E-03

Other analytical methods to describe the amount of basic and acidic centres like the titration in presence of *Hammett*-indicators have not been applied. [173, 78]

In FT-IR-spectroscopy almost the entire radiation energy of the infrared source permeates the sample, thus a high signal to noise ratio is obtained. With the pyridine adsorption method (an IR-spectroscopic analysis of adsorbed pyridine) one can distinguish between the two types of acidic sites (*Lewis*- or *Brönsted* acidity) and their relative strength.[68] The peaks in the IR spectrum of pyridine adsorbed on the surface of the sample can be assigned either to *Brönsted*-protonated pyridinium ions or *Lewis*-adsorbed pyridine. With increasing substitution of *Brönsted*-acid protons by *Lewis*-acid metal cations the ratio of *Lewis*-centres to *Brönsted*-centres increases,

which can be detected by the larger area of *Lewis*-selective peaks compared to those of *Brönsted*-selective peaks in the infrared spectra. Thus an evaluation of the degree of substitution becomes possible. The shift in the IR spectra with respect to the support can be assigned to the *Lewis*-acid centres.

To illustrate this method, the unimpregnated support Hombikat K03 and the catalyst T-9 have been analysed (Fig. 3-3, Fig. 3-4). The necessary pellet of Hombikat K03 could only be obtained after a calcination process (500 °C, heating rate: 1 °C / min). As Hombikat K03 is manufactured by the sulfate process, the presence of acidic sited was expected. This is confirmed by several peaks in the IR spectrum. The bond at 1604 cm^{-1} can be assigned to the adsorption of pyridine to semi-strong *Lewis*-centres and the peak at 1575 cm^{-1} to weak ones. The bond at 1604 cm^{-1}, which is well-defined up to temperatures of 400 °C, correlates with the strength of *Lewis*-acids. The smaller bond at around 1491 cm^{-1} and the stronger one near 1445 cm^{-1} can also be regarded as characteristic for *Lewis* acids (Fig. 3-3). [78, 174 - 176]

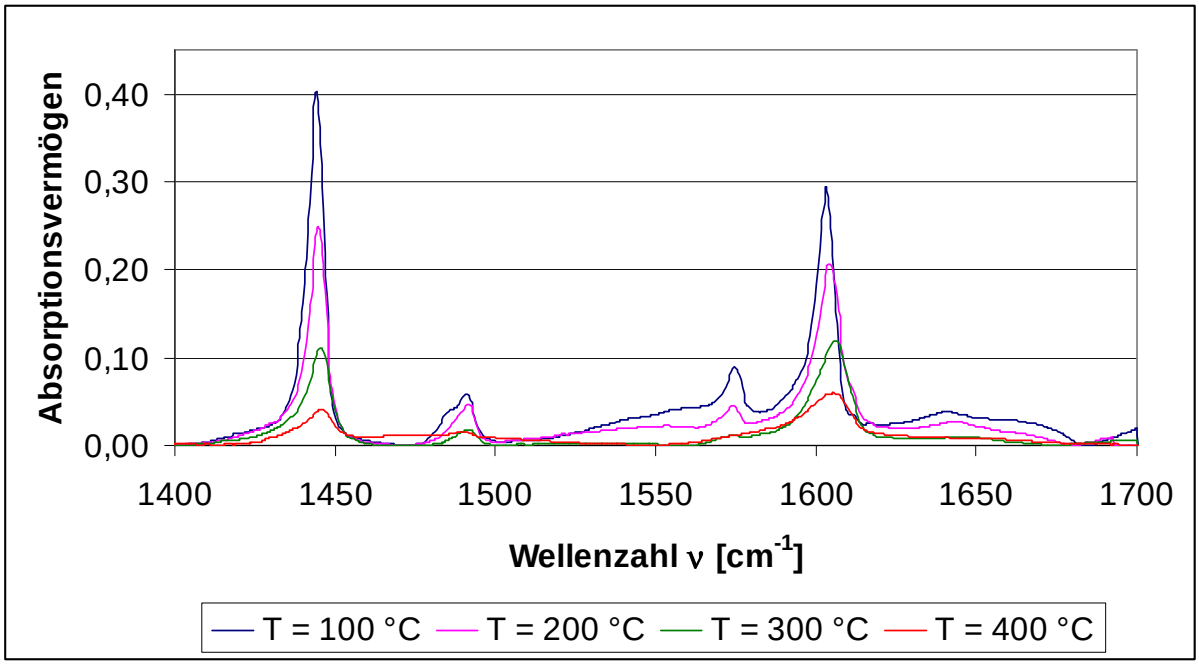

Fig. 3-3: FTIR-pyridine-adsorption spectroscopy of the acidic support Hombikat K03.

The catalyst T-9 features two distinctive bond ranges. The bond at 1604 cm^{-1} can be assigned to semi-strong *Lewis*-acidic centres as mentioned before, its intensity is, however, far lower than that of the undoped support. At a temperature of 200 °C the bonds can no longer be identified. Physisorbed pyridine can be identified at 100 °C at

1592 cm^{-1} (Fig. 3-4). The bond at 1540 cm^{-1} which is arises from adsorption of pyridine to *Brönsted*-acid centres is non-existent in both materials.

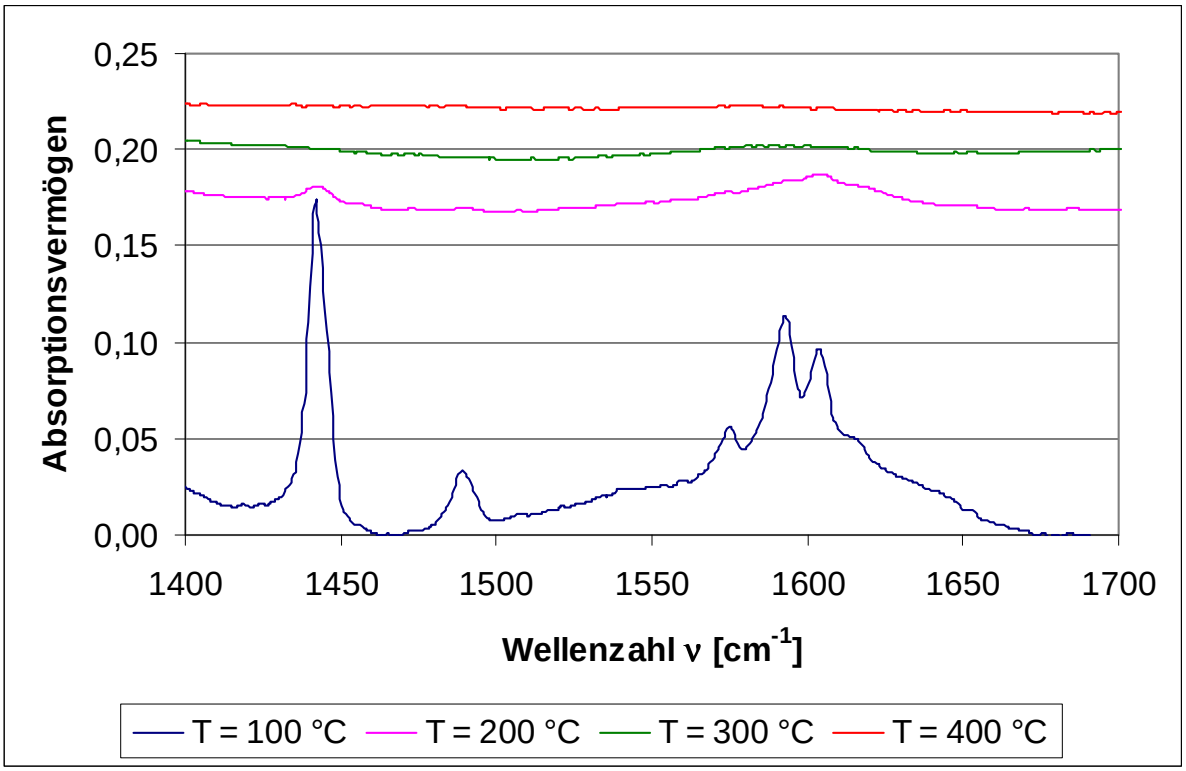

Fig. 3-4: FTIR-pyridine-adsorption spectra of the basic cat. T-9.

The amount of the sites can also correlate with peak intensity at a temperature of 200 °C. Just a few *Lewis*-acidic centres can be detected in the doped materials. A similar behaviour is expected in case of the other titanium dioxide-based catalytic materials employed.

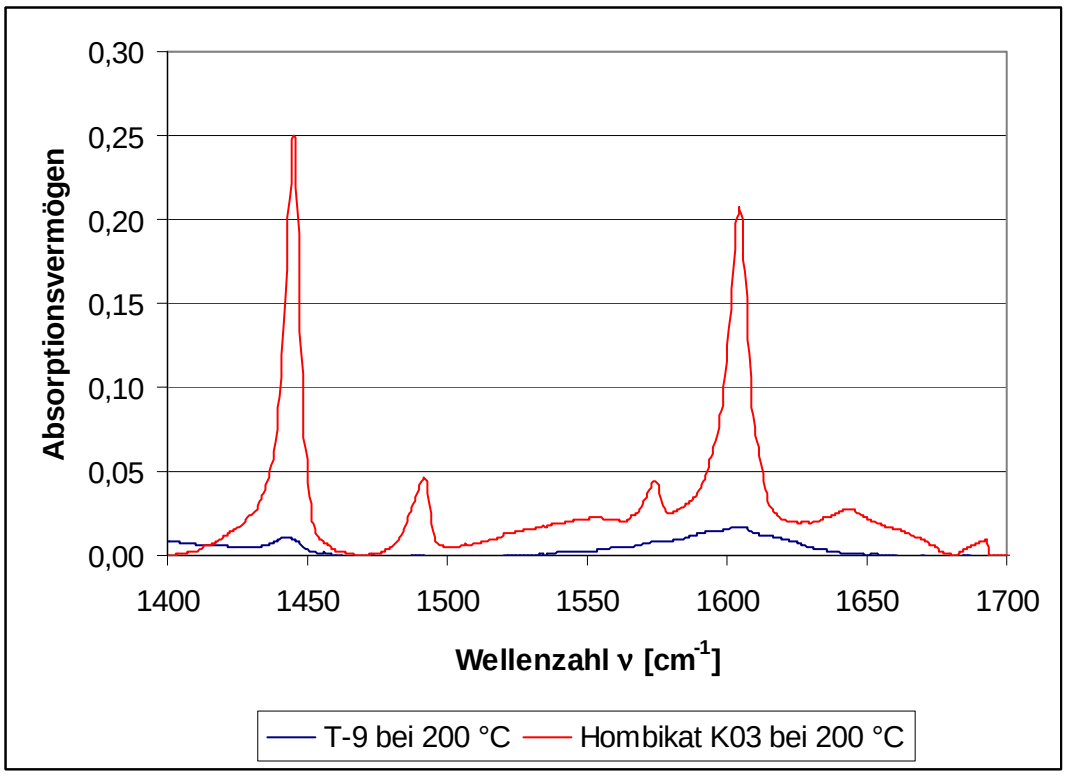

Fig. 3-5: Comparison of acidity of cat. T-9 and Hombikat K03.

An amount of 2 wt% Na_2O suffices to affect the predominant number of *Lewis*-acid centres. Since one can assume that the alkali completely covers the outer surface, the acidic sites inside the micropores are probably not accessible to pyridine.

3.3.2 Crystallinity

Further investigation of the support materials by X-ray powder diffraction (XRD) showed the existence of pure anatase in case of Hombikat-UV 100, Hombikat-K 03, Hombikat Typ II and Hombifine N (see examples in Fig. 3-6 and Fig. 3-7). No rutile modification was detected. Extraneous reflexes have not been detected. Differences in intensity and breadth of the reflexes indicate slight differences of crystallinity. Because the scans have been recorded in series this phenomenon is not an aging effect of the X-ray source. The X-ray scans allow a qualitative evaluation of crystallite size.[59] This information can be derived from peak breadth.

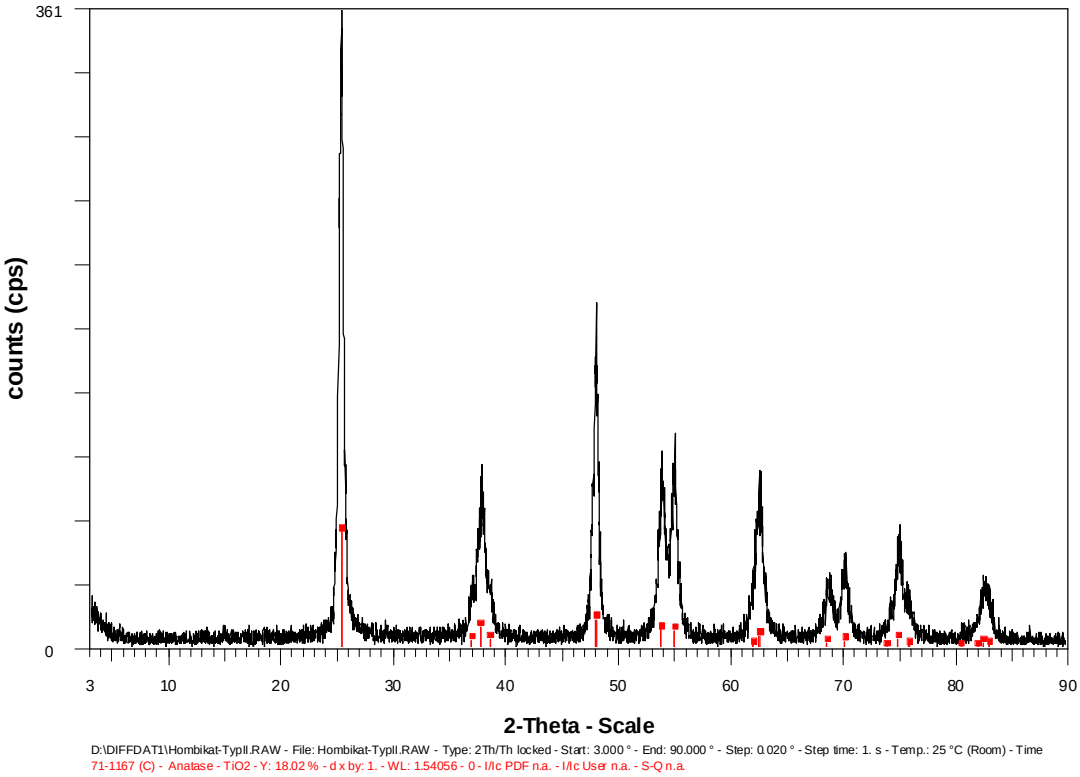

Fig. 3-6: XRD-scan of Hombikat-Typ II from *Sachtleben*.

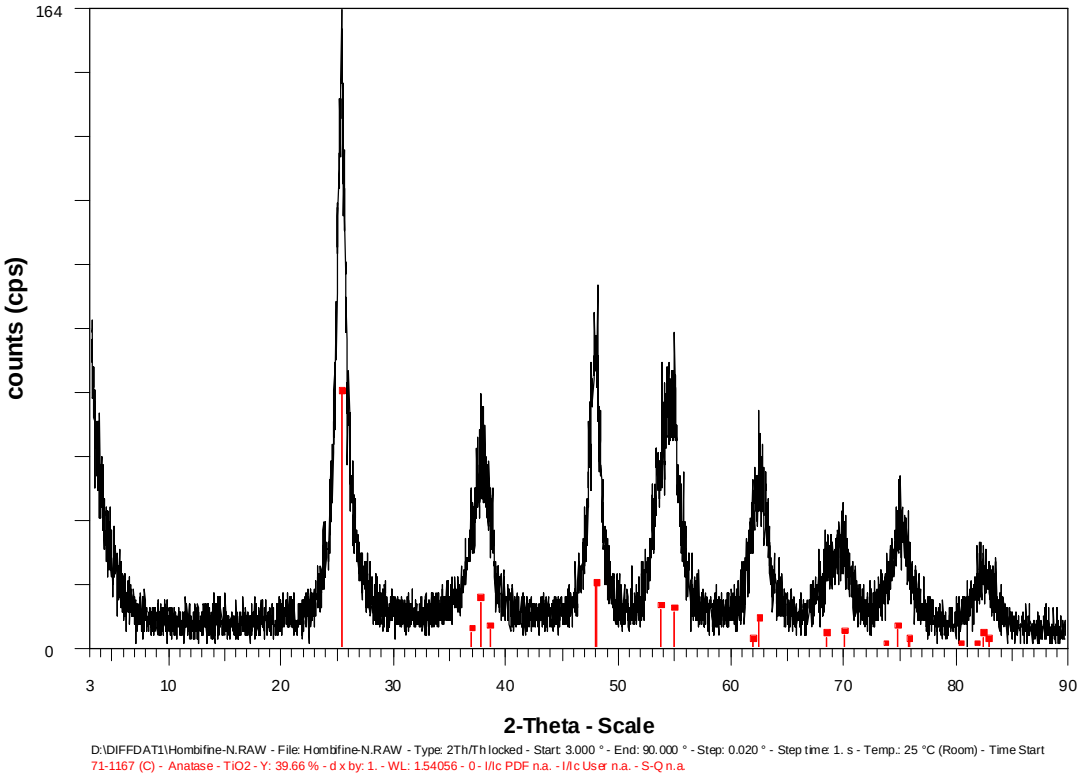

Fig. 3-7: XRD-scan of Hombifine-N from *Sachtleben*.

The diffractogram of Hombikat-K 03 shows narrower reflexes, indicating larger crystallites, while Hombifine N has smaller crystallites, as evidenced by the wider reflexes in the X-ray scan (Fig. 3-7). Because of the low concentrations reflexes of doping materials are not detected.

As expected the VP-ZrO_2 material from *Degussa* shows a monocline structure (Fig. 3-8).

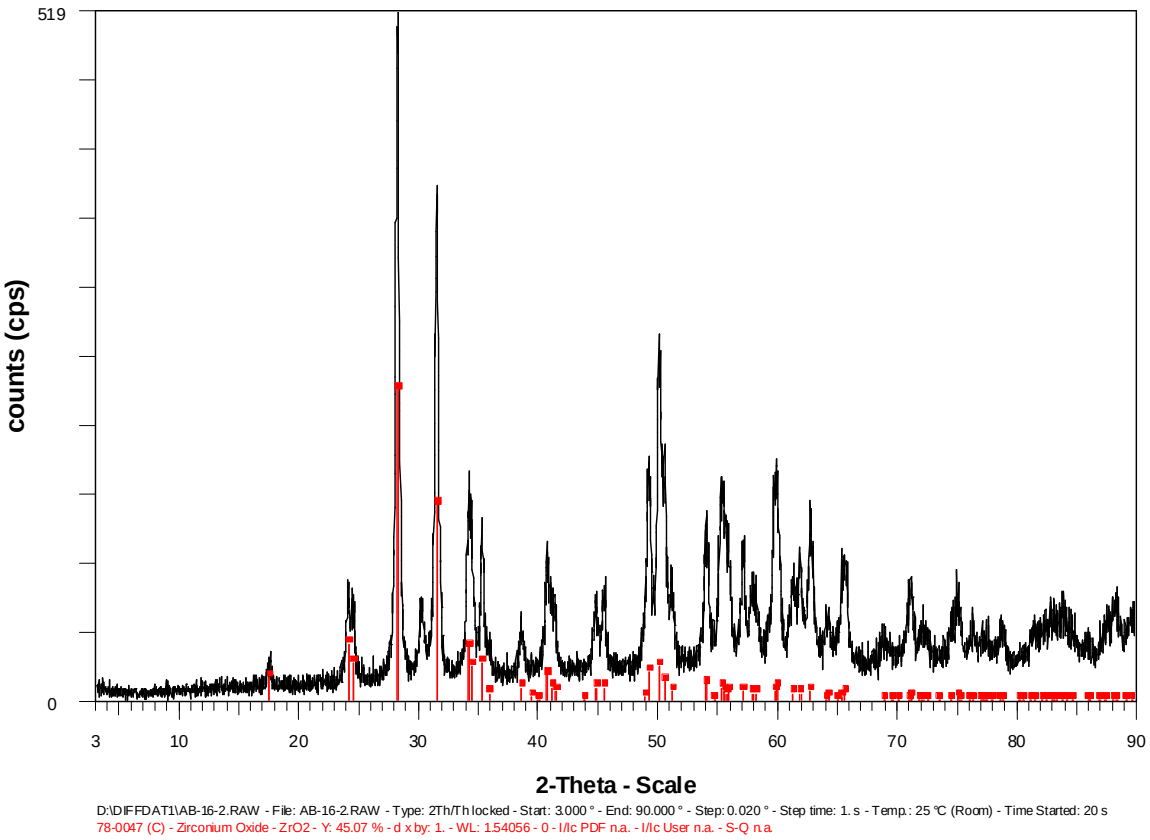

Fig. 3-8: XRD-scan of the ZrO_2 material (VP) from *Degussa*.

3.3.3 Surface properties

In order to characterise the texture of a heterogeneous catalyst the specific surface area, pore size and the average pore volume have to be determined. Support materials and prepared catalysts have been analysed by measuring nitrogen-

adsorption isotherms according to *S. **B**runauer*, *P.H. **E**mmet* and *E. **T**eller* (BET). Using the BET equation for multilayer adsorption the specific surface area can be calculated from the adsorption isotherm.[173, 177] This equation contains some approximations and the measurement of the monomolecular layer is rather uncertain, hence the method does not deliver absolute data of specific surface area but is, however, suitable for the purpose of comparing various catalysts.[177]

Additionally, the substrate molecule is considerably larger than that of the nitrogen used as adsorbant. Hence just a fraction of the measured surface area is available for the reaction. For illustration, the adsorption isotherm of T-21 is presented here (Fig. 3-9), others are shown in the annex. The properties of the prepared materials have been presented above in Table 3-2.

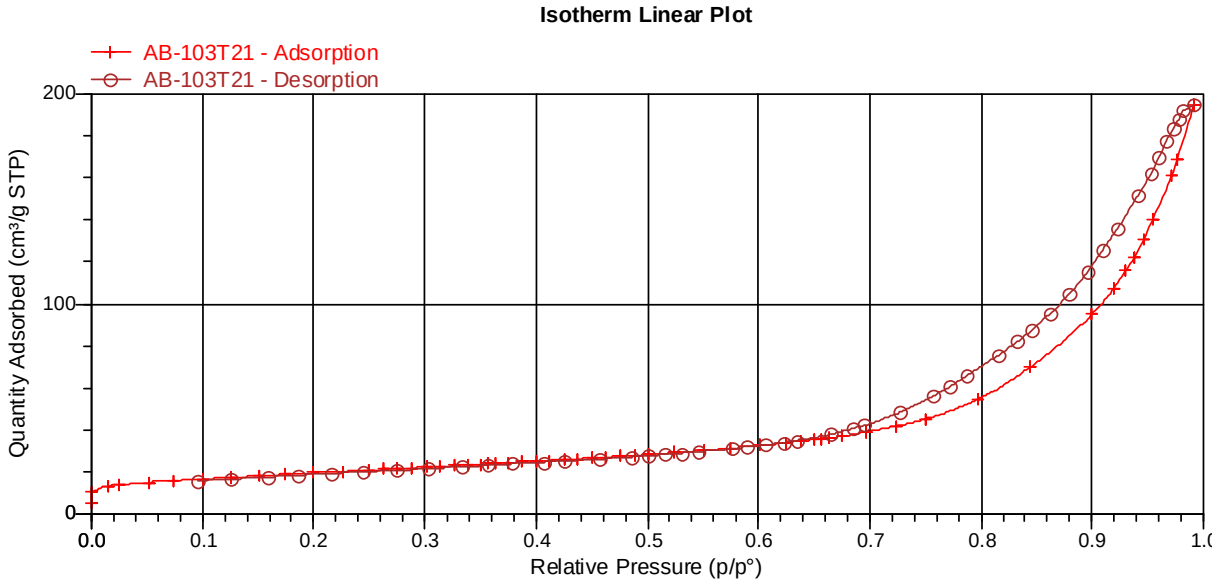

Fig. 3-9: Typical BET-isotherm of catalyst T-21.

During catalyst preparation a loss of surface area is observable. During the preparation process of catalyst T-8 the BET-area of the UV 100 material (321 m^2 / g) decreased after impregnation to 252 m^2 / g and after calcination to just 54,9 m^2 / g. A less dramatic loss of surface is recorded when preparing catalyst T-9 from the support material K 03 with larger pores and consequently lower BET-surface. The surface area decreases from 101 m^2 / g to 93,6 m^2 / g after impregnation and 61,7 m^2 / g after calcination. This loss of area is also observed at catalysts based on Hombifine N (315 m^2 / g) - e.g. catalyst T-21.6 (73 m^2 / g) - or catalysts based on Hombikat Typ II (107 m^2 / g) and the corresponding catalysts. This effect is

mentioned in Table 3-2. The low crystallinity of Hombifine N mentioned in chapter 3.3.2 leads to the highest BET-surface area of all used support materials. Alternatively, a blockage of pores by alkali is responsible for lower BET areas. An important support of this assumption is the decreasing BET-area of differently doped catalysts T-10/T-10-B, T-11/T-11B and T-12/T-12B.

The BET-surface of the zirconium dioxide material (VP) from *Degussa* decreases from 39,9 m^2 / g to 30,5 m^2 / g. A possible explanation is that the surface and porous structure of the materials collapses by sintering during calcination, although a very low heating rate had been chosen. Also supposable is a plugging of pores by alkali.

In the context of characterisation of doped supports, a number of SEM investigations have been carried out. Conceivably, the catalytic active species is not evenly distributed on the support material and agglomeration prevents a better performance. This notion is supported by Fig. 3-10 and Fig. 3-11. Additionally, the difference in surface characteristics of the UV 100 material used for T-8 and the K 03 material used for T-9, respectively, becomes visible. The UV 100 material has got a porous cleft surface while K 03 is smooth and scaly. This explains the differences in BET-areas.

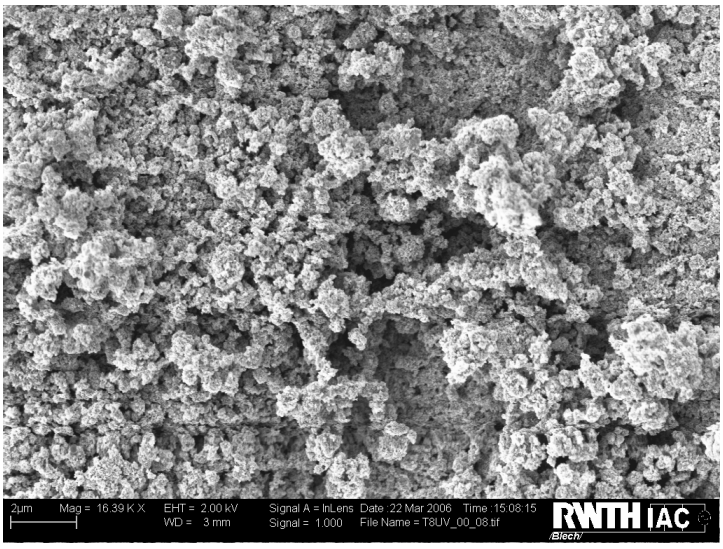

Fig. 3-10: SEM of catalyst T-8 with sodium oxide particles.

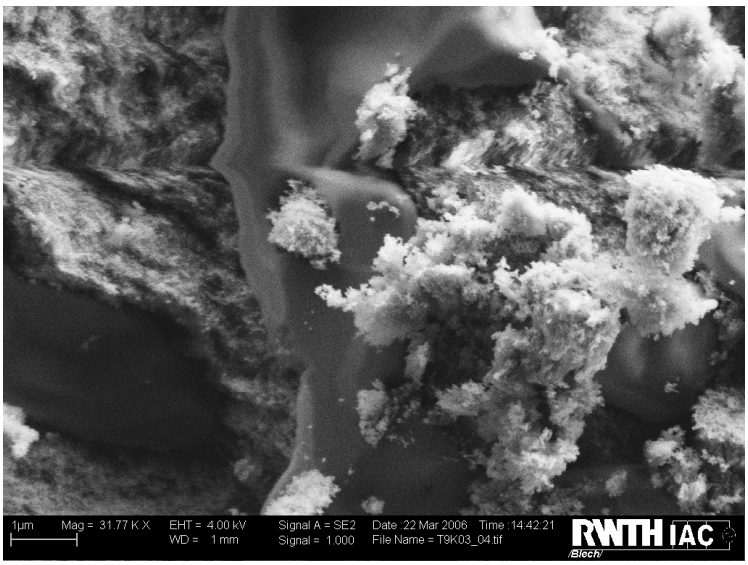

Fig. 3-11: SEM of catalyst T-9 with sodium oxide particles.

The pattern of sodium distribution is not homogeneous (see the blue line below, Fig. 3-12.) Because the catalysts are calcinated in air, carbonates may have formed. The red plot could be an indication along this line. This small concentration of carbonate can not be detected by XRD.

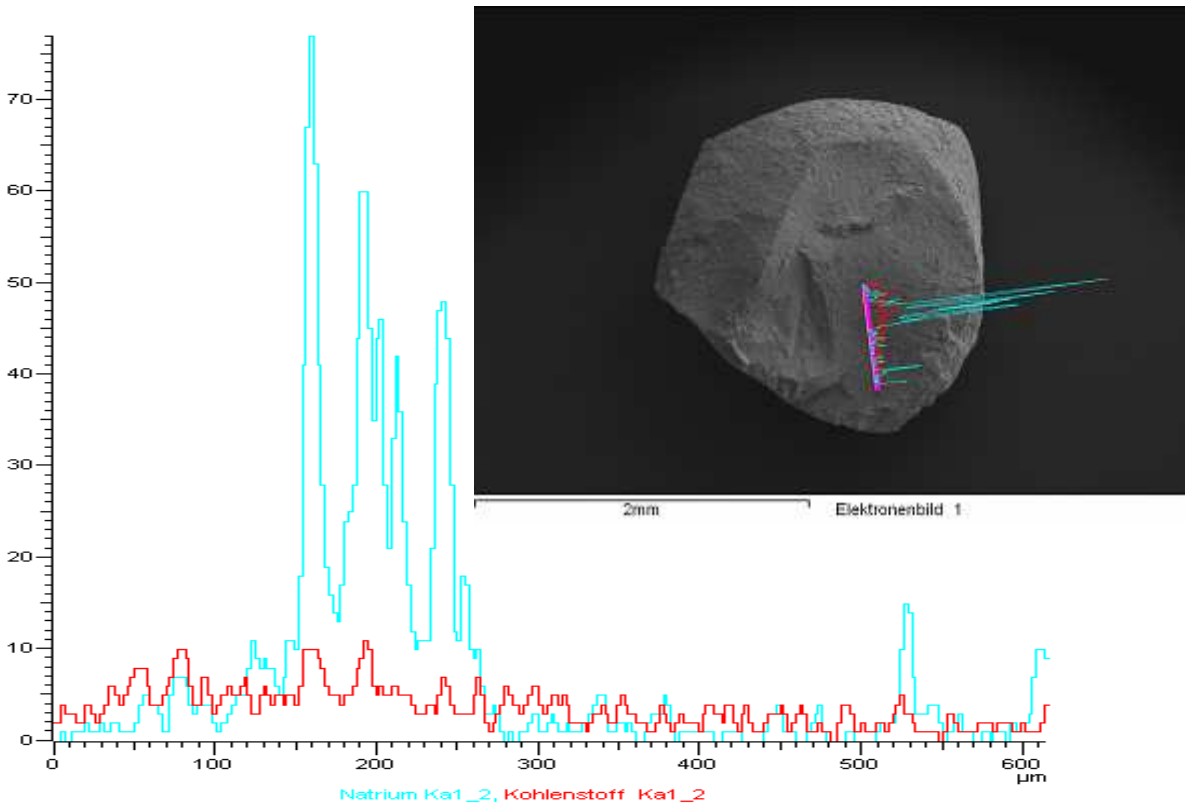

Fig. 3-12: SEM and EDX of catalyst T-12B, no homogeneous distribution of sodium.

3.4 Reaction thermodynamics

In a chemical reaction a rearrangement of atoms takes place, along with an energy conversion. The equilibrium position of a chemical reaction depends on reaction enthalpy ΔH and reaction entropy ΔS. In a chemical reaction at temperature T these state variables combine to the state variable ΔG (free enthalpy or *Gibbs*-enthalpy). The *Gibbs-Helmholz* equation is:

$$\Delta G = \Delta H - T \times \Delta S \quad \text{(A)}$$

The substrate can follow different reaction paths. Two of these are the inter- and (the desired) intramolecular oxidative dehydration, respectively (Fig. 3-13). Additionally, two hexadecane dicarboxylic acid (**4**) molecules could react, yielding the macrocyclic diketone. The reactions have different entropy values ΔS. The position of the chemical equilibrium can be influenced by temperature T:

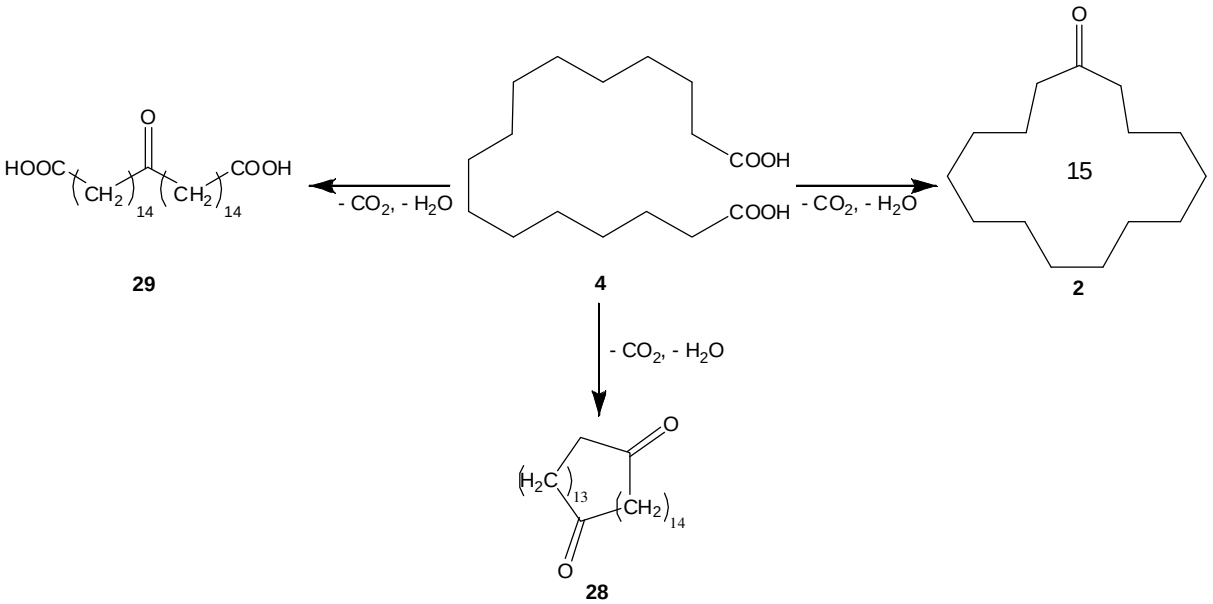

Fig. 3-13: The competing inter- und intramolecular reactions.

For these alternative reactions a thermodynamic estimation was performed, since no detailed thermodynamic data are available for this system. For calculations a computer model based on the density-functional theory (DFT) was used. The underlying idea of DFT is that the density-function of a system of N electrons is a

function of just three Cartesian coordinates x,y,z while the wave function depends on the 3N Cartesian coordinates of the electrons. *Hohenberg* and *Kohn* were able to show that the energy of a system is defined by the density function. The exact correlation between density-function and energy is not yet known in detail. This correlation is mathematically described by a so-called functional. A series of such approximation functionals does exist. The functional applied in this case is known as B3LYP and is due to *Lee, Yang* and *Parr*.[178]

For calculations the split value basic set 6-31G (D) was used. These basic sets are a combination by different functions. Firstly, the *Slater*-type-orbitals (STOs), which give good results both in the vicinity of nucleus and at long range. The mathematical handling of these orbitals is however difficult and requires considerable computing power. Secondly, the *Gauss*-type orbitals which can be handled easier but are less exact in the vicinity of the nucleus, while giving results similar to the STOs at long range.

Split-valence basic sets differ for valence shell and inner shells. The orbitals of the valence shell are approximated by two or more contractions of the *Gauss* function. An exact description of the valence shell is thus obtainable. These contracted *Gauss*-functions have different space dimensions. Uncontracted *Gauss* functions with small orbital exponents are sometime used in conjunction with contracted ones. 3-21G is an example for a split-valence basic set. Atomic orbitals of shells close to the nucleus are approximated by three primitive *Gauss* functions. The basic functions of the valence shell are contracted *Gauss* functions combining two primitive *Gauss*-functions with a broad, uncontracted *Gauss*-function consisting of just one primitive function.

To calculate the thermodynamics an optimization of the geometry has to be performed first. Subsequently the thermochemistry of the different compounds and reactions can be calculated. In Fig. 3-14 the geometry optimized target *exaltone* (**2**) is presented.

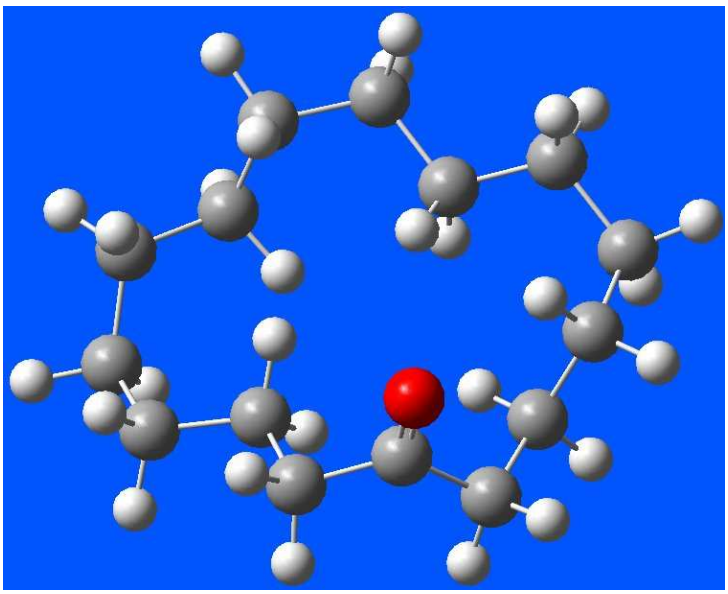

Fig. 3-14: Optimized geometry of the target *exaltone* (2).

Both geometry optimization and thermochemistry were calculated with the same method and basic set B3LYP/6-31G(d). For calculations the programme *Gaussian* available at the RWTH data centre was used.[179]

Three selected possible reaction alternatives of the present reaction system have been calculated by this method: the inter- and intra molecular reaction and the formation of the macro cyclic diketone (**37**). Data for the following molecules have been computed:

Table 3-4: *Gibbs* enthalpy of the reaction participants in atomic units.

molecule	25 °C	350 °C	400 °C	450 °C
	G / a.u.	G / a.u.	G / a.u.	G / a.u.
Educt HDA (**4**)	-928,326111	-928,434662	-928,455387	-928,477118
Exaltone (**2**)	-663,328585	-663,41791	-663,435037	-663,453022
Diketone (**37**)	-1326,67268	-1326,84032	-1326,87299	-1326,90741
Diacid (**38**)	-1591,67403	-1591,87288	-1591,91103	-1591,95108
Water	-76,404157	-76,429213	-76,433313	-76,437465
CO_2	-188,590066	-188,618656	-188,623367	-188,628147

Table 3-5: *Gibbs* enthalpy differences of alternative reactions at different temperatures

reaction	25 °C	350 °C	400 °C	450 °C
	Δ G / kJ/mol	Δ G / kJ/mol	Δ G / kJ/mol	Δ G / kJ/mol
Reaction to *Exaltone* (**2**)	8,670375	-81,682125	-95,36625	-108,9795
Reaction to Diacid (**38**)	-42,084	-134,99325	-149,4675	-163,94175
Reaction to Dicetone (**37**)	-23,37825	-175,168875	-198,3975	-221,542125

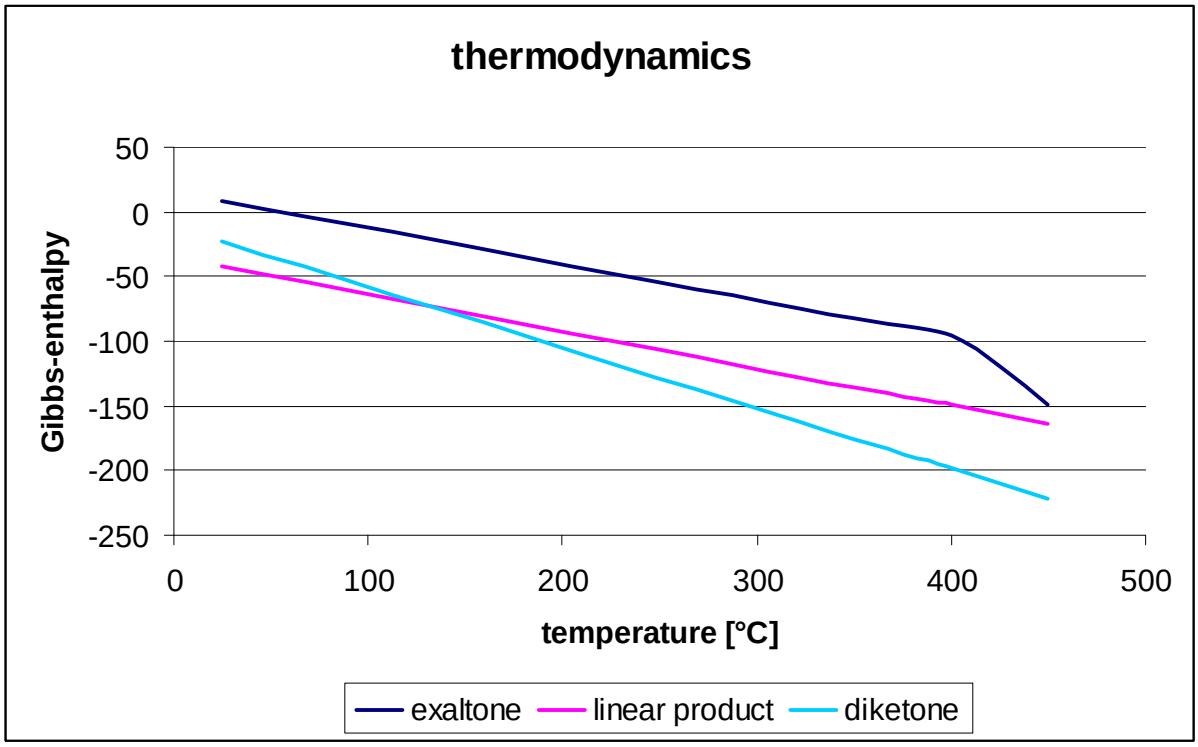

Fig. 3-15: The *Gibbs* enthalpy of competing reactions at different temperatures

The formation of *exaltone* (**2**) is thermodynamically disadvantaged compared to the other products. This emphasizes the need for a rigorous kinetic control during the reaction. Since the *Gibbs*-enthalpy is positive even at room temperature, high reaction temperatures are necessary. In this work the effect of temperature- and residence time were examined in detail. Temperatures above 400 °C have been chosen because Δ G drops faster in this range.

3.5 Catalytic experiments

In order to improve on the results formerly obtained, a liquid feed gas phase continuous flow reactor operated under reduced pressure (set-up V) was built. This set-up is described in detail in the experimental part, chapter 5.2.3. The experiments have been carried out in continuous gas phase inside a coiled tubing reactor viz. inside an integral packed bed. The catalyst was utilized in form of sieve fraction $1{,}0 < d_p > 2{,}0$ mm in size. By intensive shaking and the application of compressed air after filling the reactor the formation of unwanted voids could be prevented.

First of all the experiments have been carried out in set-up V. Two units were used (Fig. 5-2). Catalysts T-8, T-9, T-10, T-10B, T-11, T-11B, T-12, T-12B, T-13, T-14, T-15, T-16, T-10 have been applied. The amount of catalyst charged varied between 6 g and 4 g. The resulting Weight Hourly Space Velocity (WHSV) is mentioned in the tables below and ranges from 0,225 g HDA × h^{-1}/ g to 0,15 g HDA × h^{-1}/ g. The substrate HDA (**4**) was fed as a 5 wt% solution in THF. Nitrogen was used as carrier gas at a rate of 20 mL / min. The range of the temperature was between 300 °C and 500 °C at atmospheric or reduced pressure. To assist the desorption of products from the catalytic surface, steam was injected into the reaction system. Additionally steam is used as a heat carrier and ensures a uniform temperature profile inside the reactor, facilitating thus the transport of the HDA (**4**). The reaction products were collected in the cooling trap for 120 min or 300 min (TOS) and worked up before the gas chromatographic analysis. The boiling point of non-converted HDA (**4**) is too high for direct GC-analysis, therefore a derivatization to the homologous silyl ester was necessary. N,O-bis(trimethyl silyl) trifluoro acetamide (BASTFA), one of the most powerful silylation agents known was used for this purpose. The material remaining inside the detachable coil reactor was accounted for in the mass balance later on. A difficulty in performing the experiments was the impossibility of analysing non-condensable reactants or those deposited inside the apparatus. Because of reactor fouling the pressure inside the set-up varied occasionally. Furthermore, the output of the feeding pumps varied with the pressure inside the reactor, so the amount of used material was measured gravimetrically. In some cases fouling plugged the pipes and the experiment had to be repeated. After the ending of the experiment, the pipes

were flushed with pure solvent, the weight of reaction products and reactor was determined and the used catalyst was analysed by TG. Details are explained in chapter 5.2.3.

The high enthalpy of evaporation of the substrate (**4**) of 78,65±6,0 kJ / mol e.g. a boiling point of 457,5±18,0 °C outline the transport problem. The formed *exaltone* (**2**) with a enthalpy of evaporation of 58,16±3,0 kJ / mol and a boiling point of 338,3±0,0 °C is more mobile. The cyclic ketone (**2**) shows less polarity and a smaller molecule. Possibly the acid (**4**) is too strongly adsorbed onto the basic catalyst. The increase of the reactor weight during the experiment and the formation of graphite black or dark brown coloured deposits on the used catalyst indicate that substrate (**4**), product (**2**) or eventually formed oligomers and other side products remain inside the reactor and on the catalyst. Since not all of these reactants can be analysed, the mass balance may appear to indicate high selectivities of up to 50 %. TG-experiments showed that smaller amounts of HDA (**4**) have been deposited on the catalyst (see chapter 3.7).

A radical, homolytic cleavage (cracking) is improbable at the reactor operation temperature. However, cracking reactions catalysed by the acidic groups present on titanium dioxide may occur.

Before optimising the reaction conditions in detail a suitable catalyst had to be found. Therefore catalysts doped with various alkali metals were used.

Table 3-6: Results of decarboxylation-dehydratisation reactions on T-8 and T-9 catalysts in gas phase at 280 mbar, 120 min TOS.

Catalyst/ exp. No.	Doping Na_2O $[\%]_{ICP}$	Catalyst amount [g]	N_2-flow [cc/min]	T [°C]	WHSV [g HDA×h^{-1} / x ml Kat.]	Conversion [%]	Selectivity [%]	Yield [%]	TG weight loss [%]	Mass balance [%]
T-8/AB37	3,22	4,0	40	300	0,225	19,4	38,5	7,5	11,48	/
T-8/AB35	3,22	4,0	40	350	0,225	25,2	6,5	1,6	9,22	/
T-8/AB36	3,22	4,0	40	350	0,225	14,8	30,3	4,5	14,57	/
T-9/AB38	2,30	4,0	40	350	0,225	13,0	12,7	1,7	13,0	/
T-9/AB41	2,30	4,0	40	400	0,225	22,1	38,5	8,5	22,1	/
T-9/AB42	2,30	4,0	20	400	0,225	17,3	48,7	8,4	8,38	/
T-9/AB43	2,30	**6,0**	20	400	0,150	44,5	28,6	12,7	8,17	/

Using catalyst T-8 on Hombikat UV100 support and T-9 on Hombikat K 03, increasing temperature and amount of catalyst had a positive effect. As expected, conversion increases over 20 % at 400 °C but selectivity declines. Temperatures higher than 400 °C are thus usually needed to carry out this reaction. Particular variations of lower conversion were observed in runs AB-36 (14,8) and AB-42 (17,3). The problem of obtaining reproducible results is obvious. The reasons could be measuring faults, unsteady pressure conditions as well as small variations in fixed bed charge, reactor geometry, output of the pump and work-up. By scaling up the experimental set-up dimension blockades and inhomogenities can be reduced probably. In some cases in which the experiments were carried out with a higher amount of catalyst (and, accordingly, a lower WHSV) the yield increased. This made me pay particular attention to the effect of residence time. The high amount of catalyst charged in the reactor (6 g) caused a considerable flow resistance. Even with a WHSV of 0,150 g HDA × h^{-1}/ g in exp. AB-43 conversion cannot exceed 44,5 %.

Table 3-7: Results of decarboxylation-dehydration reactions on T-10 and T-10B catalysts in gas phase at 280 mbar.

Catalyst/ exp. No.	Doping Na_2O $[\%]_{ICP}$	Catalyst amount [g]	N_2-flow [cc/min]	T [°C]	WHSV [g HDA×h^{-1} / x ml Kat.]	Conversion [%]	Selectivity [%]	Yield [%]	TG weight loss [%]	Mass balance [%]
T-10/AB44	2,71	4,0	20	400	0,225	20,5	43,9	9,0	/	/
T-10/AB47	2,71	4,0	20	450	0,225	100	50,0	50,0	3,45	/
T-10*/AB77	2,71	**5,0**	20	450	0,18	67,1	37,4	25,1	0,78	41
T-10/AB53	2,71	4,0	20	500	0,225	100	27,5	27,5	6,65	/
T-10B/AB70	6,58	4,0	20	400	0,225	99,4	32,9	32,7	/	/
T-10B/AB61	6,58	4,0	20	450	0,225	58,7	5,6	3,3	3,77	/
T-10B*/AB81	6,58	**5,0**	20	450	0,18	94,5	17,7	16,7	2,34	27
T-10B*/AB82	6,58	**5,0**	20	450	0,18	99,6	17,3	17,3	7,99	61
T-10B/AB75	6,58	4,0	20	500	0,225	100	22,2	22,2	3,61	/

***5 h reaction time**

The effect of the amount of catalytic active material was investigated with catalysts T-10 and T-10B on Hombifine N support, catalysts T-11 and T-11B on P 25 support and catalysts T-12 and T-12B on Hombikat Typ II. With catalysts T-10 and T-10B no clear effect of catalyst loading was noticeable. As shown in Table 3-7 conversions of 100 % and selectivities up to 50 % are possible. With a stabler mass balance these results could probably be improved and become more reproducible. Developing the process the mass balance has not bee measured in the early experiments. The verified mass lies in the range of 40 to 90% (see Table 3-8). Although runs AB-81 and AB-82 vary in the assessed mass balance, the results of conversion, selectivity and yield are on a comparable level. The positive influence of a higher amount of catalyst is shown again in runs AB-61 and AB-81 but also challenged in Exp. AB-47 and AB-77. The inscrutable results in experiment AB 47 and AB77 are the result of unsteady pressure conditions as well as small variations in fixed bed charge, reactor geometry, output of the pump and work-up. By scaling up the experimental Set-up dimension blockades and

inhomogenities can be reduced probably. The results of TG-experiments usually show a better desorption of higher boiling point organic compounds from the catalytic surface at higher temperatures. There are several examples in Table 3-6 to Table 3-9 showing higher weight loss at lower temperatures of 300 °C and 400 °C than at higher temperatures (450 °C or 500 °C). The lowest conversion of 20,5 % was found at a temperature of just 400 °C (Exp. AB44). As observed before, a temperature of 500 °C results at a conversion of 100 %. In the course of this work the experiments were carried out at least twice in order to check the results later on. The maximum of selectivity of 50 % was measured at a temperature of 450 °C (Exp. AB47). No influence of the Na_2O loading was noticed here or in the following results presented in Table 3-8 and Table 3-9. Furthermore, higher doped materials show a lower BET-surface because of blockage of pores by alkali and agglomeration of doping material.

Table 3-8: Results of decarboxylation-dehydratisation reactions on T-11 and T-11B catalysts in gas phase at 280 mbar.

Catalyst/ exp. No.	Doping Na_2O	Catalyst amount [g]	N_2-flow [cc/min]	T [°C]	WHSV [g HDA×h^{-1} / x ml Kat.]	Conversion [%]	Selectivity [%]	Yield [%]	TG weight loss [%]	Mass balance [%]
T-11/AB46	3,10	4,0	20	400	0,225	68,8	19,8	13,6	15,63	/
T-11/AB49	3,10	4,0	20	450	0,225	99,8	48,7	48,6	2,21	/
T-11/AB58	3,10	4,0	20	450	0,225	94,9	12,8	12,1	4,17	/
T-11/AB66	3,10	4,0	20	450	0,225	100	15,6	15,6	2,51	72
T-11/AB55	3,10	4,0	20	500	0,225	100	21,4	21,4	2,84	/
T-11B/AB71	6,61	4,0	20	400	0,225	69,0	14,8	10,2	8,17	91
T-11B/AB62	6,61	4,0	20	450	0,225	100	9,1	9,1	6,15	/
T-11B*/AB80	6,61	**5,0**	20	450	0,18	99,9	9,2	9,2	5,50	81
T-11B/AB72	6,61	4,0	20	500	0,225	100	17,3	17,3	1,49	56

***5 h reaction time**

With the P25-based catalyst T-11 and the higher doped T-11B high conversions of nearly 70 % can be attained even at 400 °C (Exp. AB46, Exp. AB71). However, no clear selectivity trend was observed as a function of temperature. AB-49 shows a selectivity of 48,7 % at 450 °C. In case of runs AB-62 and AB-80 a higher amount of catalyst had no noticeable influence on yield. With 5 g of catalyst the selectivity was quite low (just 9,2 %). The time on steam (TOS) was increased to 5 hours to have a lower relative error in the mass balance calculation. Run AB-49 does not fit in AB-58 and AB-66. This result consists of one measure point within 30 min during the running experiment. Later on samples after the experimental run have been collected as reported before. The effect of different amounts of material is not remarkable in tests with catalysts T-11 and T-11B.

Table 3-9: Results of decarboxylation-dehydration reactions on T-12 and T-12B catalysts in gas phase at 280 mbar.

catalyst/ exp. No.	doping Na_2O $[\%]_{ICP}$	catalyst amount [g]	N_2-flow [cc/min]	T [°C]	WHSV [g HDA×h^{-1} / x ml Kat.]	conversion [%]	selectivity [%]	yield [%]	m loss to TG [%]	mass balance [%]
T-12/AB67	2,95	4,0	20	400	0,225	8,6	31,1	2,7	/	89
T-12/AB69	2,95	4,0	20	400	0,225	48,6	18,6	9,1	2,35	63
T-12/AB48	2,95	4,0	20	450	0,225	97,5	50,1	48,9	3,48	/
T-12/AB57	2,95	4,0	20	450	0,225	22,6	11,7	2,6	4,78	/
T-12*/AB78	2,95	**5,0**	20	450	0,18	23,5	10,8	2,5	4,16	64
T-12/AB54	2,95	4,0	20	500	0,225	100	29,6	29,6	/	/
T-12B/AB73	6,56	4,0	20	400	0,225	90,0	7,9	7,1	11,34	/
T-12B/AB63	6,56	4,0	20	450	0,225	78,5	10,0	7,9	3,35	/
T-12B*/AB79	6,56	**5,0**	20	450	0,18	32,4	9,8	3,2	/	79
T-12B/AB76	6,56	4,0	20	500	0,225	100	15,1	15,1	/	40

***5 h reaction time**

The lowest conversion of 8,6 % was observed at a temperature of just 400 °C (AB-67). As mentioned in several cases reproduction of the experiment is difficult. As expected, the highest conversion of 100 % is obtained at a temperature of 500 °C. In Exp. AB-57 and AB-78 the effect of different amount of catalyst T-12 is not significant. The conversion rises little from 22,6 % to 23,5 % and the selectivity stays at around 11 %. In case of the higher loaded catalyst T-12B this trend can not be confirmed. Unsteady pressure conditions small variations in fixed bed charge, reactor geometry, output of the pump and work-up in Exp. AB-79 could be the reason for unusual trend compared to Exp. AB-63. When a higher catalyst amount of 5 g is used, conversion and selectivity fall. The outcome of taking measure points in intervals of 30 min. instead of one at the end of the experimental time of 120 min is a gap in rerun Exp. AB-48 and AB-57 as mentioned before in another case.

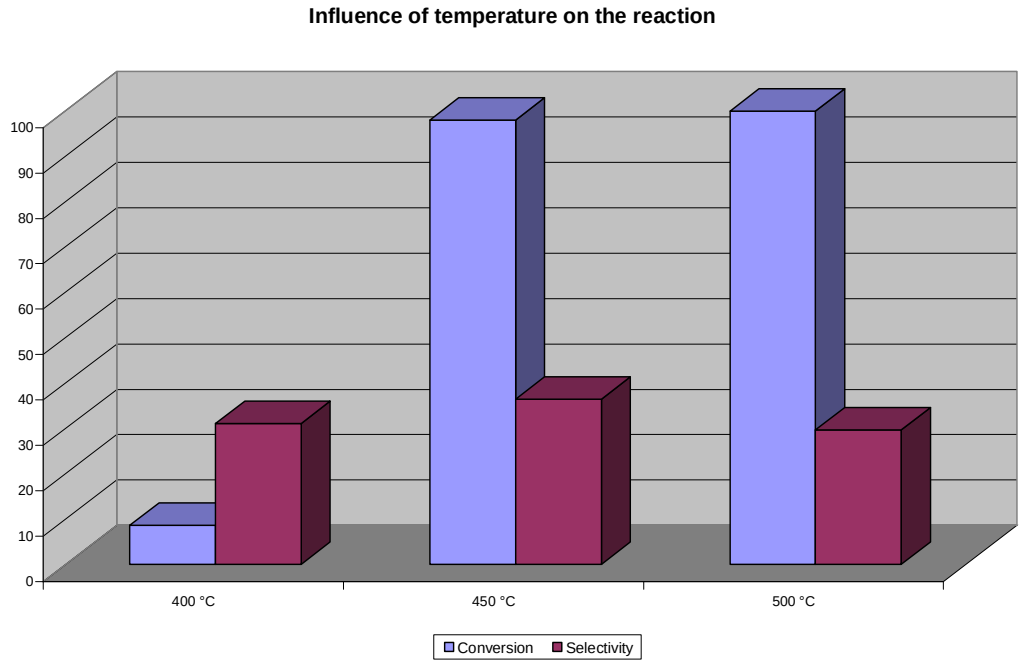

Fig. 3-16: The effect of temperature on conversion and selectivity using 4,0 g catalyst T-12, 120 min TOS.

Table 3-10: Results of decarboxylation-dehydration reactions on different catalysts in gas phase at 280 mbar.

Catalyst/ exp. No.	Metal doping [%]	Catalyst amount [g]	N_2-flow [cc/min]	T [°C]	WHSV [g HDA×h^{-1} / 5 ml Kat.]	Conversion [%]	Selectivity [%]	Yield [%]	TG weight loss [%]	Mass balance [%]
Blank/89	/	**5,0**	20	450	0,18	19,2	6,9	1,3	/	66
Blank/90	/	**5,0**	20	450	0,18	15,8	11,0	1,7	/	75
T-13*/AB85	K_2O 2,0	**5,0**	20	450	0,18	6,4	16,1	1,0	7,84	75
T-14*/AB86	Li_2O 0,44 $_{ICP}$	**5,0**	20	450	0,18	12,5	10,8	1,3	6,23	78
T-15*/AB87	Cs_2O 2,0	**5,0**	20	450	0,18	7,9	31,5	2,5	4,36	87
T-16*/AB88	K_2O 2,0	**5,0**	20	450	0,18	23,6	48,5	11,5	3,46	54
T-19*/AB92	$Ca(OH)_2$	**5,0**	20	450	0,18	83,9	11,2	9,4		/
T-20*/AB91	$Ca(OH)_2$	**5,0**	20	450	0,18	59,3	10,9	6,5	0,16	29
HX-C10/AB50	Cs_2O	4,0	20	450	0,225	100	0,0	0,0	/	/

***5 h reaction time**

When glass pearls are used instead of catalyst (Runs AB-89 and AB-90) a low conversion is measured at 450 °C. Some contamination of catalytic material from previous experiments could account for this pyrolysis. Other basic oxides like Li_2O, K_2O, Cs_2O and CaO have shown catalytic activity in this reaction as well. A trend towards a higher selectivity can be noticed from potassium to caesium (AB-85 to AB-87). The comparatively high BET-surface of 72 m^2/g at T-16 is doubtless a positive factor to the conversion of 23,6%. Catalysts T-13, T-14 and T-15 based on Hombikat Typ II lead to a lower conversion (6,4 % to 12,5 %) than catalytic materials like T-16 based on Hombifine N. Thus, the K_2O-loaded T-16 shows a conversion of 23,6 % and the CaO-loaded T-20 a conversion of 59,3% at 450 °C. T-19 based on Hombikat Typ II and the Hombifine N-supported T-20 show the most intensive TCD-signals in CO_2-TPD measuring. They have more basic centres than any other prepared catalyst.

Both calcium doped catalyst have two differently strong basic centres. The maximum of the first basic-centre signal lies in both cases above 150 °C. Furthermore these two catalysts possess a higher BET-surfaces than the rest of the presented materials, resulting from the different preparation method (see chapter 5.2.2). Sodium doped catalyst show the best conversion as seen in the tables before. The CsO_2 loaded catalyst HX-C10 in AB-50 based on a zeolite support (CsH-β) is not suitable for this reaction.

All experiments presented below here have been carried out in set-up VI. As in set-up V, steam addition and reduced pressure have been applied to facilitate desorption of the product and other high boiling compounds from the surface of the catalysts. The technical modification of set-up VI is a heated reactor outlet (Fig. 5-4). Instead of a cooled separating funnel with reflux condenser a heated reactor outlet is connected to a glass cooling trap integrated in a Dewar flask. Thus less product accumulates inside the apparatus and can be detected. Two of those units were operated. To compare the results Set-up VI-A and set-up VI-B have been tested under same conditions. The catalyst T-21.3 was tested at a reaction temperature of 450^{o}C. Carrier gas feed rate was adjusted to 20 cc per min.. A 5 wt% solution of the diacid in THF was fed into the reactor on 5 g of the catalysts within 5 hours.

Table 3-11: Comparing of Set-up VI-A and Set-up VI-B, 5,g cat, 20cc/min N2, approx 18g H20.

Catalyst/ exp. No.	Doping Na_2O $[\%]_{ICP}$	T [°C]	WHSV [g HDA×h^{-1} / x ml Kat.]	Conversion [%]	Selectivity [%]	Yield [%]	TG weight loss [%]	Mass balance [%]
T-21.3/AB116.1A	0,51	450	0,180	100	54,3	54,3		99,9
T-21.3/AB116.5A	0,51	450	0,180	100	52,2	52,2	13,00	99,9
T-21.3/AB116.6A	0,51	450	0,180	77,9	34,0	26,5	14,61	93,0
T-21.3/AB116.4B	0,51	450	0,180	100	42,4	42,4	10,97	99,9
T-21.3/AB116.5B	0,51	450	0,180	25,6	44,7	11,4	11,59	78,6
T-21.3/AB116.6B	0,51	450	0,180	100	49,0	49,0	11,23	42,3

Comparing the two available set-ups in Table 3-11 conversions of 100% are measured using Hombifine N-based catalyst T 21.3 (BET-area 80 m2/g). High conversions are attained by using sufficient catalyst material. Although set-up VI A and VI B are identical in construction, only in set-up VI A selectivities over 50% have been achieved. The different results of varying selectivities of the set ups appear because of pressure variations, temporary fouling and non-constant feed flow rates. The obtained data indicate a better performance of set-up VI-A. The variational results in experiment AB 116.5A/116.6A and AB116.4B/116.5B are the result of unsteady pressure conditions as well as small variations in fixed bed charge, reactor geometry, output of the pump and work-up. By scaling up the experimental set up dimension blockades and inhomogenities can be reduced probably.

Before optimising the reaction conditions in detail only one suitable catalyst had to be chosen. Therefore catalysts doped with various alkali and earth alkali metals and different support materials have been tested. T-21, T-22, T-23 and T-27 are catalysts based on Hombifine N and T-24, T-25 and T-25 are based on Hombikat Typ II. Zr-6 is based on a zirconia support material. Their basicity and effect on catalytic activity are different. The results are presented in Table 3-12. Using the potassium Hombifine N material T-22 an overall conversion of 100 % is possible (Run AB109) compared to just 20 % conversion using the Hombikat Typ II material T-25 (Run AB-112). The selectivity however is better in case of T-25, with two measurements over 53%. According to CO_2-TPD measurements T-22 shows more basic centres than T-25. The T-22 catalyst is additionally favoured by a larger BET-surface of 86 m^2/g. The same trend of reactivity is observed using sodium-impregnated Hombifine N materials T-21 (exp. AB-104) and T-24 (exp. AB-111). T-21 has got more basic centres than T-24. This is comprehensible because of the different Na_2O amounts measured by ICP. Even a lower BET-surface of 69 m^2/g has no negative effect in this correlation.

A similar situation is encountered with caesium impregnated Hombifine N anatas catalysts T-23 (with more than 70 % conversion, exp. AB-110) and Hombikat Typ II material T-26 (with less than 18 % conversion, exp. AB-113). Additionally the comparison of the selectivities is in favour of T-23 with 48% and 50%. Hombikat Typ II materials T-25 and T-26 show relative low amounts of basic centres in CO_2-TPD measurements. Usually just Hombikat Typ II materials show an additional small amount of strong basic centres in CO_2-TPD. This could be one reason of their lower reactivity. Generally, Hombifine N titanium dioxide material is a better support for this reaction.

The catalyst screening was extended by including the barium oxide impregnated catalyst T-27. As mentioned before, barium oxide is successfully employed to synthesize smaller cyclic ketones. Although the results lie within an extremely broad range (conversion 52%-87 %, selectivity 42%-55 %) it is shown that T-27 is also an active catalyst (exp. AB122.1, AB122.2). One reason of these relatively good results is the high BET-surface of 89 m^2/g.

Furthermore, this catalyst shows a comparatively high amount of basic centres at 142 °C in CO_2-TPD measurements. The impregnated silica stabilized zirconia from *Saint-Gobain* shows a BET-surface of 139 m^2. As shown in Run AB114 this material is probably less active.

These experiments do not show a clear indication of a catalyst combining high conversion and selectivity as well. Therefore reaction conditions were optimised mostly using T-21 in further experiments. Using optimal reaction conditions the unequal activity of different materials could get more obvious.

Table 3-12: Tests with catalysts doped with various alkali and earth alkali metals and different support materials

Catalyst/ exp. No.	Doping $Alkali_2O$ $[\%]_{ICP}$	Catalyst amount [g]	N_2-flow [cc/min]	T [°C]	WHSV [g HDA×h^{-1} / x ml Kat.]	Conversion [%]	Selectivity [%]	Yield [%]	TG weight loss [%]	Mass balance [%]
T-21/AB104.4	0,74 Na_2O	5,0	20	450	0,180	91,4	31,5	28,8		64,8
T-21/AB104.5	0,74 Na_2O	5,0	20	450	0,180	100	26,5	26,5		99,9
T-21/AB104.6	0,74 Na_2O	5,0	20	450	0,180	100	29,9	29,9	11,86	99,9
T-22/AB109.1	0,5* K_2O	5,0	20	450	0,180	98,6	26,8	26,5	13,28	99,9
T-22/AB109.2	0,5* K_2O	5,0	20	450	0,180	98,2	32,2	31,7		99,9
T-22/AB109.3	0,5* K_2O	5,0	20	450	0,180	98,7	25,7	25,4		99,9
T-23/AB110.1	0,5* Cs_2O	5,0	20	450	0,180	74,9	47,6	35,6	14,67	99,9
T-23/AB110.2	0,5* Cs_2O	5,0	20	450	0,180	72,1	50,0	36,0		99,9
T-23/AB110.3	0,5* Cs_2O	5,0	20	450	0,180	44,9	44,1	19,8		85,9

T-27/AB122.1	BaO	5,0	20	450	0,180	87,8	54,6	48,0		86,7
T27/AB122.2	BaO	5,0	20	450	0,180	52,4	42,3	22,2		93,8
T-24/AB111.1	0,27 Na_2O	5,0	20	450	0,180	35,8	40,8	14,6	13,26	92,0
T-24/AB111.2	0,27 Na_2O	5,0	20	450	0,180	59,3	58,4	34,6		99,9
T-24/AB111.3	0,27 Na_2O	5,0	20	450	0,180	67,9	53,7	36,5		85,6
T-25/AB112.1	0,5* K_2O	5,0	20	450	0,180	19,5	54,6	10,6	14,79	85,8
T-25/AB112.2	0,5* K_2O	5,0	20	450	0,180	19,6	53,1	10,4		87,8
T-25/AB112.3	0,5* K_2O	5,0	20	450	0,180	44,4	35,6	15,8		97,2
T-26/AB113.1	0,5* Cs_2O	5,0	20	450	0,180	12,5	50,2	6,3	14,74	99,9
T-26/AB113.2	0,5* Cs_2O	5,0	20	450	0,180	17,8	37,0	6,6		89,4
T-26/AB113.3	0,5* Cs_2O	5,0	20	450	0,180	6,6	41,3	2,7		95,4
ZR-6/AB114.1	0,41 Na_2O	5,0	20	450	0,180	9,9	12,7	1,3	9,97	81,0
ZR-6/AB114.2	0,41 Na_2O	5,0	20	450	0,180	12,7	67,8	8,6		88,6
ZR-6/AB114.3	0,41 Na_2O	5,0	20	450	0,180	36,0	45,2	16,2		84,6

Table 3-13: Set-up VI-A using 3,0 g catalyst, 20cc/min N2, approx 18g H_20.

Catalyst/ exp. No.	Doping $[\%]_{ICP}$	N_2 [cc / min]	τ [s]	T [°C]	WHSV [g HDA×h^{-1} / x ml Kat.]	Conversion [%]	Selectivity [%]	Yield [%]	TG weight loss [%]	Mass balance [%]
T-21.4/AB136.2A	0,58	20	0,06	430	0,3	18,6	55,0	10,3	10,4	76,4
T-21.4/AB136.4A	0,58	20	0,05	430	0,3	27,2	25,8	7,0		36,8
T-21.4/AB136.5A	0,58	20	0,06	430	0,3	20,1	45,8	9,2	12,14	65,6
T-21.4/AB136.6A	0,58	20	0,07	430	0,3	11,7	46,4	5,4		86,0
T-22.2/AB146.2A	0,5*	20	0,06	430	0,3	24,5	63,9	15,6		-
T-22.2/AB146.3A	0,5*	20	0,06	430	0,3	36,3	78,4	28,5		-
T-21.4/AB131.1A	0,58	20	0,05	450	0,3	100	45,6	45,6	9,2	73,4
T-21.4/AB131.2A	0,58	20	0,07	450	0,3	93,8	41,8	39,2	12,6	64,1
T-22.2/AB143.1A	0,5*	20	0,06	450	0,3	100	77,7	77,7		80,2
T-22.2/AB143.2A	0,5*	20	0,07	450	0,3	100	70,7	70,7		83,2

In order to decide if the sodium or the potassium catalyst based on Hombifine N is more suitable to investigate the effect of reaction conditions the results are compared in Table 3-13 and Table 3-14 at 430°C and 450°C in set-up VI-A and set-up VI-B. Although the reaction parameters were kept as constant as possible (3,0 g catalyst, 20cc/min N_2, approx 18g H_20) e.g. the repeated experiments AB-136 show variations at temperatures of 430 °C. Because of these fluctuations the results have to be interpreted with caution in this case as well. Generally the sodium impregnated catalyst T-21.4 shows a conversion of around 20 % and a selectivity of more than 45 % using set-up VIA at 430 °C. In contrast, the potassium impregnated catalyst T-22.2 leads to a selectivity of more than 70 % in a single case. The strengths of the basic centres determined by CO_2-TPD are comparable. The higher BET-surface of T-22.2 (84 m^2/g)

could explain the higher conversion in this case. Even at a higher temperature of 450 °C a high selectivity is demonstrated with K_2O loaded material T-22.2. If the temperature is high enough, e.g. at 450 °C, most of the HDA (**4**) had reacted.

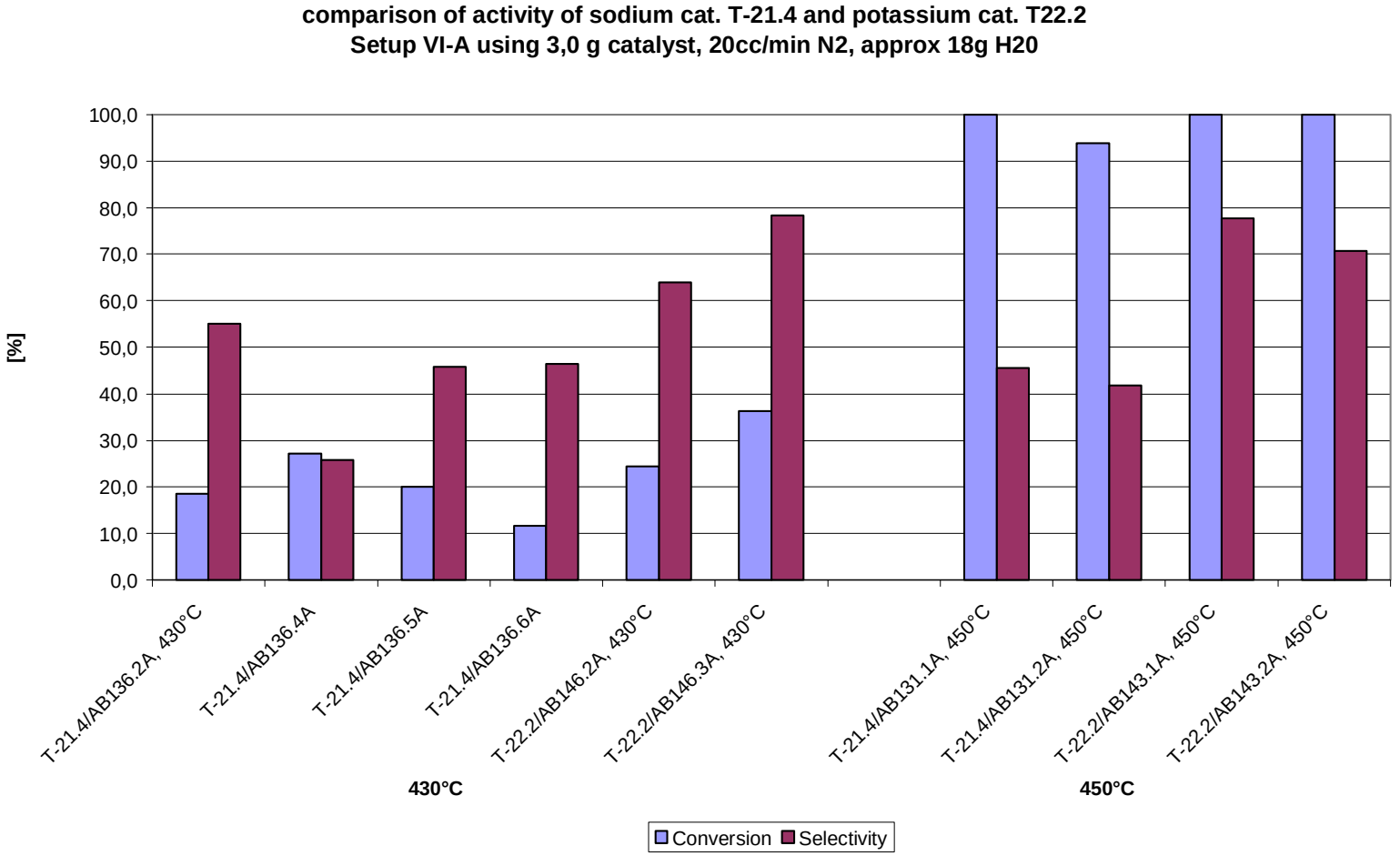

Fig. 3-17: Set-up VI-A using 3,0 g catalyst, 20cc/min N2, approx 18g H_20.

Table 3-14: Set-up VI-B using 3,0 g catalyst, 20cc/min N2, approx 18g H_20.

Catalyst/ exp. No.	Doping $[\%]_{ICP}$	N_2 [cc / min]	τ [s]	T [°C]	WHSV [g HDA×h^{-1} / x ml Kat.]	Conversion [%]	Selectivity [%]	Yield [%]	TG weight loss [%]	Mass balance [%]
T-21.4/AB147.3B	0,58	20	0,05	430	0,3	14,5	39,7	5,8		39,2
T-21.4/AB147.4B	0,58	20	0,05	430	0,3	17,3	57,3	9,9		59,4
T-21.4/AB147.5B	0,58	20	0,05	430	0,3	36,7	9,9	3,6		62,9
T-22.2/AB137.1B	0,5	20	0,06	430	0,3	12,2	56,8	6,9	12,0	79,6
T-22.2/AB137.2B	0,5	20	0,06	430	0,3	11,2	58,7	6,6	10,9	75,1
T-22.2/AB137.3B,	0,5	20	0,05	430	0,3	18,1	34,3	6,2		71,0
T-21.4/AB144.1B	0,58	20	0,06	450	0,3	96,2	78,7	75,6		92,0
T-21.4/AB144.2B	0,58	20	0,05	450	0,3	92,8	67,2	62,3	8,3	81,5
T-22.2/AB132.1B	0,5	20	0,05	450	0,3	14,0	48,1	6,7	12,2	77,9
T-22.2/AB132.2B	0,5	20	0,06	450	0,3	27,3	42,8	11,7	13,0	87,0
T-22.2/AB132.3B	0,5	20	0,05	450	0,3	42,9	33,8	14,5	2,14	41,5

Particularly in set-up VI-B the 0,58 % sodium impregnated catalyst T-21.4 gives a better conversion and selectivity at both temperatures than T-22.2. Although the results are scattered, the potassium impregnated catalyst T-22.2 always reached less than 18 % conversion at 430 °C at a selectivity of around 57 %. In set-up B this results could not be improved like in set-up A. T-21.4 however achieves conversions of more than 92 % and high selectivities of more than 67 % at 450 °C (Exp. AB144.2B). Therefore the experiments mainly on a sodium impregnated catalyst based on Hombifine N support were in the focus. It is obvious that this support has more acidic centres before impregnation than any other used material as measured by NH_3-TPD. The presence of both acidic and basic centres on this catalyst could be the reason of its advantage over other materials.

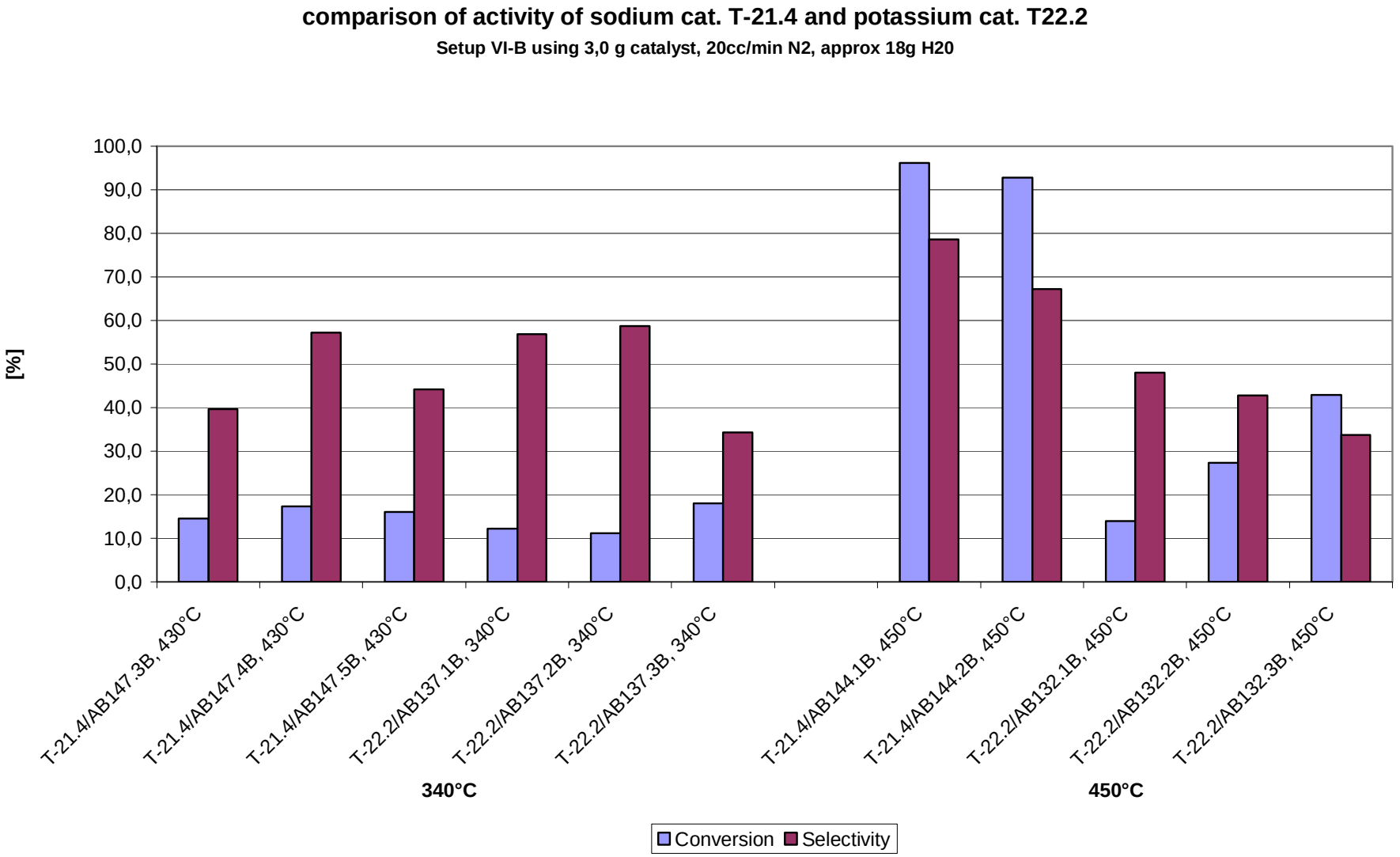

Fig. 3-18: Reproducibility of the experiments with T-21, using 3,0 g catalyst, 20cc/min N2, approx 18g H_20.

Table 3-15: Reproducibility of experimental series using 5,0 g catalyst, 20cc/min N_2, approx 18g H_20.

Catalyst/ exp. No.	Doping Na_2O $[\%]_{ICP}$	Catalyst amount [g]	N_2-flow [cc/min]	T [°C]	WHSV [g HDA×h^{-1} / x ml Kat.]	Conversion [%]	Selectivity [%]	Yield [%]	TG weight loss [%]	Mass balance [%]
T-21/AB104.1	0,74	5,0	20	450	0,180	100	24,6	24,6		-
T-21/AB104.2	0,74	5,0	20	450	0,180	77,0	29,5	22,7		-
T-21/AB104.3	0,74	5,0	20	450	0,180	99,6	26,0	25,9		79,8
T-21/AB104.4	0,74	5,0	20	450	0,180	91,4	31,5	28,8		64,8
T-21/AB104.5	0,74	5,0	20	450	0,180	100	26,5	26,5		99,9
T-21/AB104.6	0,74	5,0	20	450	0,180	100	29,9	29,9	11,86	99,9
T-21/AB105.1*	0,74	5,0	20	450	0,180	100	40,1	40,1		99,9
T-21/AB105.2*	0,74	5,0	20	450	0,180	99,2	28,0	27,8		94,9

feed: 0,2 wt% HDA in THF.

In an early stage of the experiment series the reproducibility of some tests was closely scrutinised. As presented in Table 3-15 the conversion is mostly complete using 5 g T-21 catalyst and 0,5 wt% or just 0,2 wt% HDA/THF solution at a 20 cc/min nitrogen flow and approx 18 g H_20. Selectivities are in the range of 23 % to 30 % using 0,5 wt% HDA/THF solution. These results display a scattering which renders difficult a conclusive interpretation. At higher dilution of the feed a higher selectivity is observed. The alternative intermolecular reaction and the polymerisation are diminished. In the course of the tests most of the runs have been carried out at least twice. As a result of this screening it was focused on catalysts supported on Hombifine N doped with small amounts of sodium like T-21 for the further optimisation of reaction conditions. The target of the following experiments was to identify trends when a single factor was varied.

The amount of water and consequently the residence time have been varied. The sodium and potassium doped anatase materials which showed the highest amount of basic centres, i.e. T-21 and T-22 were used. Catalyst T-21.3 was tested in set-up VI-A and T-22.2 was tested in set-up VI-B.

In these tests if no water was used the results were less good than by adding some water (exp. AB117.1A, AB117.2A); the conversion was lower (70% and 85%), the selectivity was just 25-30% and even the mass balance is extremely low (51-55%). In this case reactants deposited inside the pipes and could not be analysed. By raising the amount of added water to 15 g / h all results can be improved (exp. AB-116.1A, AB-116.2B); conversions of 100 % at selectivities around 52-54 % are possible. The high BET-surface of 80 m^2/g obviously offers enough reactive centres. Using a water rate of 27 g / h the selectivity drops to 43 % (exp. AB-119.1A, AB-119.2A).

Table 3-16: Set-up VI-A using 5,0 g sodium catalyst T-21.3, 20cc/min N2.

catalyst/ exp. No.	doping Na_2O $[\%]_{ICP}$	H_2O [g / h]	τ [s]	T [°C]	WHSV [g HDA×h^{-1} / x ml Kat.]	conversion [%]	selectivity [%]	yield [%]	m loss to TG [%]	mass balance [%]
T-21.3/AB117.1A	0,51	0	0,16	450	0,180	85,4	25,7	22,01	16,4	51,6
T-21.3/AB117.2A	0,51	0	0,16	450	0,180	70,4	30,6	21,52	14,55	54,7
T-21.3/AB116.1A	0,51	15,2	0,06	450	0,180	100	54,3	54,3		99,9
T-21.3/AB116.5A	0,51	15,1	0,06	450	0,180	100	52,2	52,2	13,00	99,9
T-21.3/AB119.1A	0,51	27,1	0,04	450	0,180	98,4	42,9	42,3	12,64	99,9
T-21.3/AB119.2A	0,51	26,9	0,04	450	0,180	98,0	42,7	41,9		87,7

Table 3-17: Set-up VI-B using 5,0 g potassium catalyst T-22.2, 20cc/min N2.

catalyst/ exp. No.	doping K_2O $[\%]_{ICP}$	H_2O [g / h]	τ [s]	T [°C]	WHSV [g HDA×h^{-1} / x ml Kat.]	conversion [%]	selectivity [%]	yield [%]	m loss to TG [%]	mass balance [%]
T-22.2/AB118.2B	0,5	0	0,19	450	0,180	37,7	25,8	9,71	15,88	79,0
T-22.2/AB118.1B	0,5	0	0,25	450	0,180	70,7	10,5	7,4	9,95	40,6
T-22.2/AB120.2B	0,5	16,7	0,06	450	0,180	99,5	47,8	47,55		99,9
T-22.2/AB120.4B	0,5	22,0	0,05	450	0,180	100	45,8	45,76	15,44	99,9
T-22.2/AB120.1B	0,5	22,9	0,05	450	0,180	97,9	59,4	58,16	14,32	38,1
T-22.2/AB120.3B	0,5	23,1	0,05	450	0,180	99,3	34,8	34,58		98,7

A similar situation is observed using catalyst T-22.2 in set-up VI-B (BET-surface of 84 m^2/g). Without water the conversion is not complete (40-70%) and the selectivity is low at 11-25 % (exp. AB-118.1B and AB-118.2B). A complete conversion is achieved by the addition of water. Using a rate of 17 g / h water a selectivity of 48 % is measured (exp. AB-120.2B). The selectivity drops at a rate of 22-23 g / h (exp. AB-120.1B, AB-120.2B). These current results often show complete conversions. To detect differences in activity the amount of catalyst was reduced in further experiments.

Table 3-18: Set-up VI-A using 3,0 g sodium catalyst T-21.4 and T-21.5, 20cc/min N_2.

Catalyst/ exp. No.	Doping Na_2O $[\%]_{ICP}$	H_2O [g / h]	τ [s]	T [°C]	WHSV [g HDA×h^{-1} / x ml Kat.]	Conversion [%]	Selectivity [%]	Yield [%]	TG weight loss [%]	Mass balance [%]
T-21.4/AB136.5A	0,58	15,0	0,06	430	0,3	20,1	45,8	9,2	12,14	65,6
T-21.4/AB136.2A	0,58	15,5	0,06	430	0,3	18,6	55,0	10,3	10,4	76,4
T-21.4/AB136.4A	0,58	16,9	0,05	430	0,3	27,1	25,8	7,0		66,8
T-21.4/AB136.1A	0,58	20,0	0,06	430	0,3	91,6	34,3	31,4	10,1	67,5
T-21.4/AB136.6A	0,58	20,0	0,07	430	0,3	11,7	46,4	5,4		86,1
T-21.5/AB149.2A	0,40	25,0	0,04	430	0,3	18,9	51,3	9,7		88,1
T-21.5/AB149.1A	0,40	25,0	0,04	430	0,3	18,0	54,8	9,9		83,1
T-21.5/AB151.1A	0,40	34,7	0,03	430	0,3	14,1	47,7	6,7		78,4
T-21.5/AB151.3A	0,40	37,8	0,03	430	0,3	15,3	35,6	5,4		79,1

Further experiments with variable water feed rates and consequently different residence times τ have been carried out with just 3 g of catalyst material, to detect differences in catalyst activity. The calculation of residence time τ includes the amount of nitrogen, water and substrate. Because of the volatile output of water and substrate pump a longer residence time τ can be generated although more water has been pumped in the system by a reduced output of substrate (e.g. AB 136.1 and AB 136.4). The experiments have been carried out at 430 °C and 450 °C as well. All other parameters were kept constant: 20cc/min N_2 and a reduced pressure of 280 mbar. In experiments with T-21.4 and T-21.5 at 430 °C (Table 3-18) conversions around 18 % can be realized at any calculated residence time in set-up A. Run 136.1A examplifies the variance. Taking into account the scattering the selectivity ranges from 45% to 55%. However, no clear cut trend can be ascertained from these experimental results.

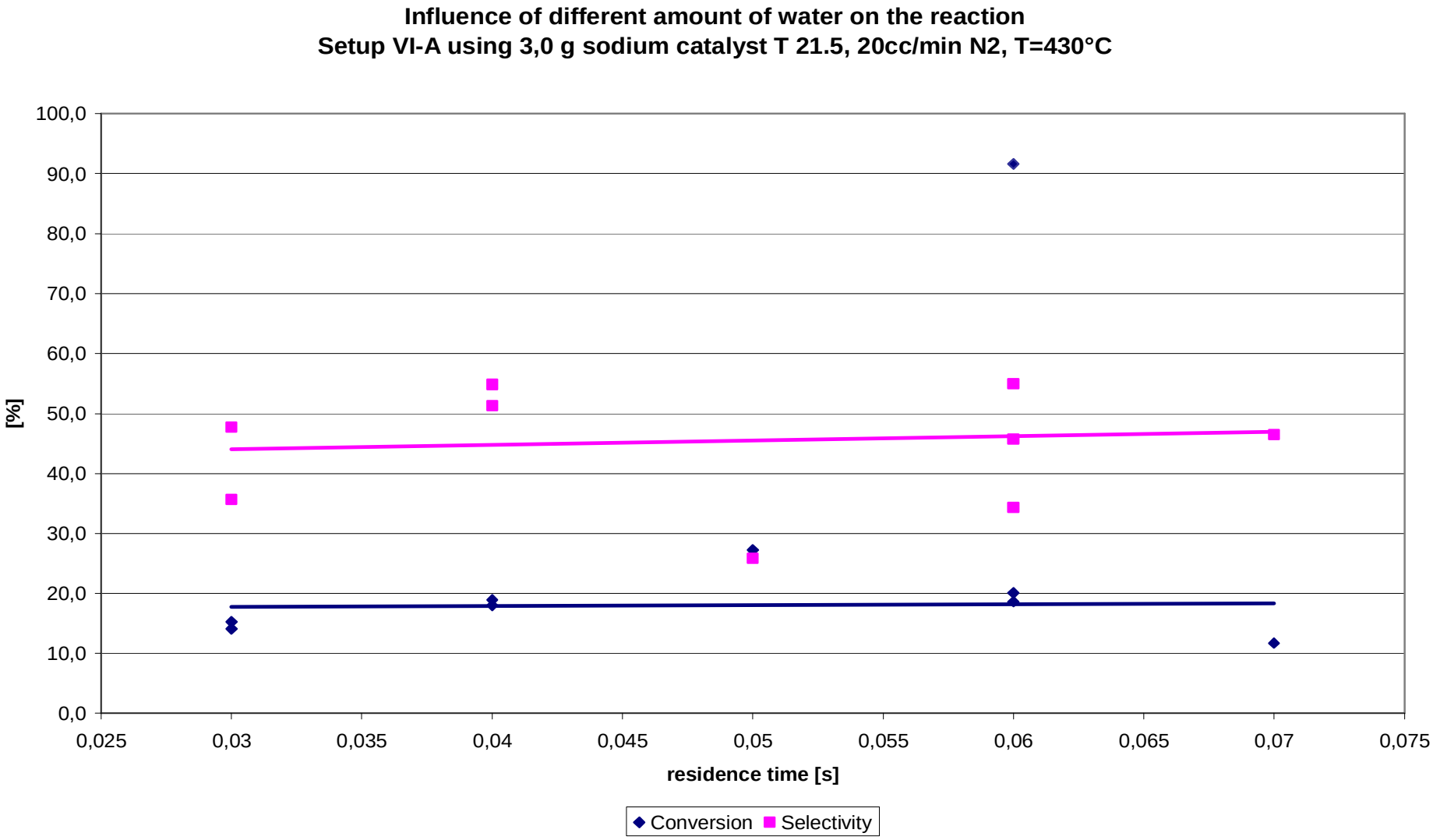

Fig. 3-19: Influence of different amount of water on the reaction.

Table 3-19: Set-up VI-A using 3,0 g catalyst T-21.4, T-21.6 and T-21.7, 20cc/min N2. T=450 °C.

catalyst/ exp. No.	doping Na_2O $[\%]_{ICP}$	H_2O [g / h]	τ [s]	T [°C]	WHSV [g HDA×h^{-1} / x ml Kat.]	conversion [%]	selectivity [%]	yield [%]	m loss to TG [%]	mass balance [%]
T-21.7/AB173.1A	0,66%	12,8	0,07	450	0,3	17,2	31,2	5,4	13,5	79,6
T-21.7/AB173.2A	0,66%	12,9	0,06	450	0,3	17,3	48,8	8,4	14,0	77,7
T-21.4/AB131.2A	0,58%	13,5	0,07	450	0,3	93,8	41,8	39,2	12,6	64,1
T-21.4/AB131.1A	0,58%	16,5	0,05	450	0,3	100,0	45,6	45,6	9,2	73,4
T-21.6/AB156.2A	0,51%	22,3	0,04	450	0,3	16,5	62,3	10,3		52,5
T-21.7/AB175.1A	0,66%	24,0	0,04	450	0,3	16,0	30,7	4,9	11,6	72,8
T-21.6/AB156.1A	0,51%	25,0	0,04	450	0,3	11,7	59,3	7,0	11,1	78,5
T-21.6/AB158.2A	0,51%	35,6	0,03	450	0,3	23,0	45,8	10,5	10,1	80,4
T-21.6/AB158.1A	0,51%	36,3	0,03	450	0,3	8,5	33,6	2,9	11,2	77,5

In experiments at 450 °C (Table 3-19) conversions around 20 % can be attained at any calculated residence time in set-up A. At this temperature some runs e.g. AB131.2A or AB131.1A show higher conversions even though the BET-surface, the amount of doping to ICP and quantity of basic centres to TPD of T-21.4 is lower than of T-21.7. Selectivities range mainly from 34% to 48 %. Two experiments (AB156.1, AB156.2) achieved a high selectivity of 59 % and 62 %, respectively. Barring the fact of a positive influence of water on the reaction system, no definite effect of the amount of added water can be discerned. Exp. AB158.1A/AB158.2A for example show the problem of reproducibility. Conversion and selectivity highly differ. Unsteady results related to the different amount of added water to the system are an additional evidence of the irregular experimental conditions. By scaling up the experimental Set-up dimension blockades and inhomogenities can be reduced probably. The influence of residence time would be more obvious.

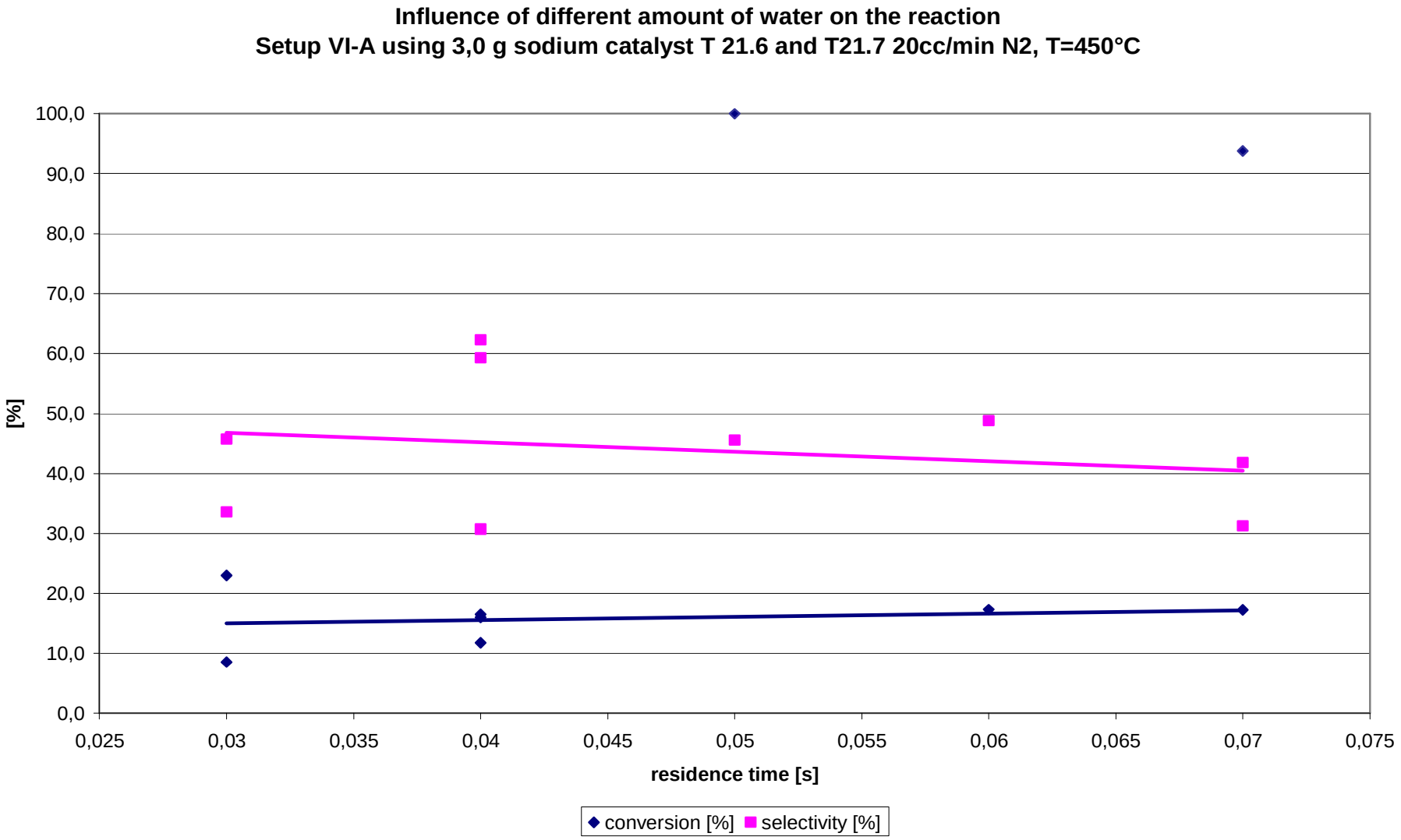

Fig. 3-20: Influence of different amount of water on the reaction.

Influence of different amount of water on the reaction setup A

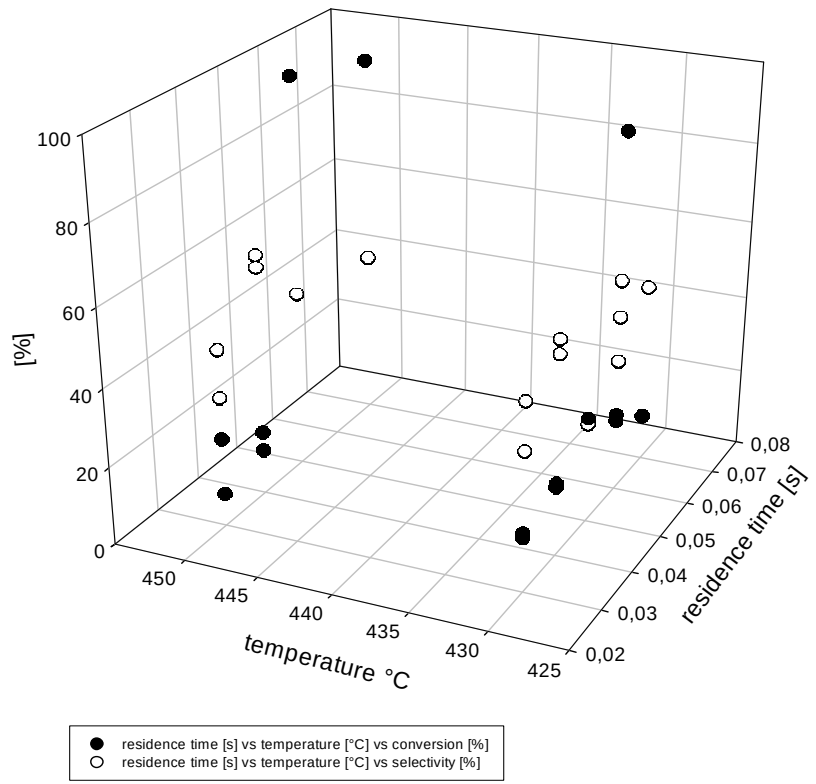

Fig. 3-21: Influence of different amount of water on the reaction at 430 °C and 450 °C using 3,0 g sodium catalyst, 20cc/min N_2.

Table 3-20: Set-up VI-B using 3,0 g catalyst T-21.4, T-21.6 and T-21.7, 20cc/min N_2. T=430 °C.

Catalyst/ Run. No.	Doping Na_2O [%]	H_2O [g / h]	τ [s]	T [°C]	WHSV [g HDA×h^{-1} / x ml Kat.]	Conversion [%]	Selectivity [%]	Yield [%]	TG weight loss [%]	Mass balance [%]
T-21.4/AB147.1B	0,58%	15,1	0,06	430	0,3	69,4	58,2	40,3	16,2	90,4
T-21.4/AB147.2B	0,58%	16,4	0,06	430	0,3	81,3	84,8	68,9		69,1
T-21.4/AB147.4B	0,58%	16,5	0,05	430	0,3	17,3	57,3	9,9		59,4
T-21.4/AB147.3B	0,58%	16,8	0,06	430	0,3	14,5	39,7	5,8		39,3
T-21.4/AB147.5B	0,58%	16,9	0,05	430	0,3	16,0	44,1	7,1		62,9
T-21.5/AB150.1B	0,40%	25,5	0,04	430	0,3	7,9	51,8	4,1		65,7
T-21.5/AB150.2B	0,40%	27,0	0,04	430	0,3	14,0	53,5	7,5		69,8
T-21.5/AB152.2B	0,40%	33,5	0,03	430	0,3	7,9	26,0	2,1		74,8
T-21.5/AB152.1B	0,40%	35,1	0,03	430	0,3	7,7	54,1	4,2		71,0

Table 3-21: Set-up VI-B using 3,0 g catalyst T-21.4, T-21.6 and T-21.7, 20cc/min N_2. T=450 °C.

Catalyst/ Run. No.	Doping Na_2O [%]	H_2O [g / h]	τ [s]	T [°C]	WHSV [g HDA×h^{-1} / x ml Kat.]	Conversion [%]	Selectivity [%]	Yield [%]	TG weight loss [%]	Mass balance [%]
T-21.7/AB174.2B	0,66%	7,7	0,08	450	0,3	6,5	24,4	1,6	13,7	76,0
T-21.7/AB174.1B	0,66%	11,5	0,07	450	0,3	21,1	5,1	1,1	11,5	71,6
T-21.4/AB144.1B	0,58%	15,6	0,06	450	0,3	96,1	78,6	75,6		99,9
T-21.7/AB144.3B	0,66%	17,0	0,06	450	0,3	23,8	34,1	8,1	15,8	65,9
T-21.7/AB144.4B	0,66%	17,7	0,06	450	0,3	7,2	43,8	3,1	13,9	49,3
T-21.4/AB144.2B	0,58%	18,0	0,05	450	0,3	92,8	67,2	62,3	8,3	81,5
T-21.6/AB157.2B	0,51%	25,4	0,04	450	0,3	5,5	48,5	2,6	6,1	36,7
T-21.6/AB159.1B	0,51%	34,4	0,03	450	0,3	28,3	35,2	9,9	10,7	72,5
T-21.6/AB159.2B	0,51%	36,0	0,03	450	0,3	2,2	31,2	0,7		73,0

To check the results above the same experiments have been carried out in set-up B with similar sodium doped catalysts. At 430 °C the conversion rises form 8 % at low residence time of 0,03 s to 17 % at 0,05 s. A longer residence time leads, as expected, to a higher conversion. Runs AB147.1B and AB147.2B are two examples of high conversions being achieved at τ = 0,06 s. The selectivity is in the range of 40 % to 58 % and shows no clear trend. Additional experiments were carried out at 450 °C. The conversion varies widely from 2 % at 0,03 s to 79 % at 0,06 s. The small variations of BET and doping of different reproduced lots can, however, not explain these different results of conversion and selectivity. The best selectivity and conversion in this test series are measured using T-21.4 at τ of 0,05 s and 0,06 s (AB-144.1B and AB-144.2B). The fact that good results have repeatedly been achieved demonstrates the potential of this reaction.

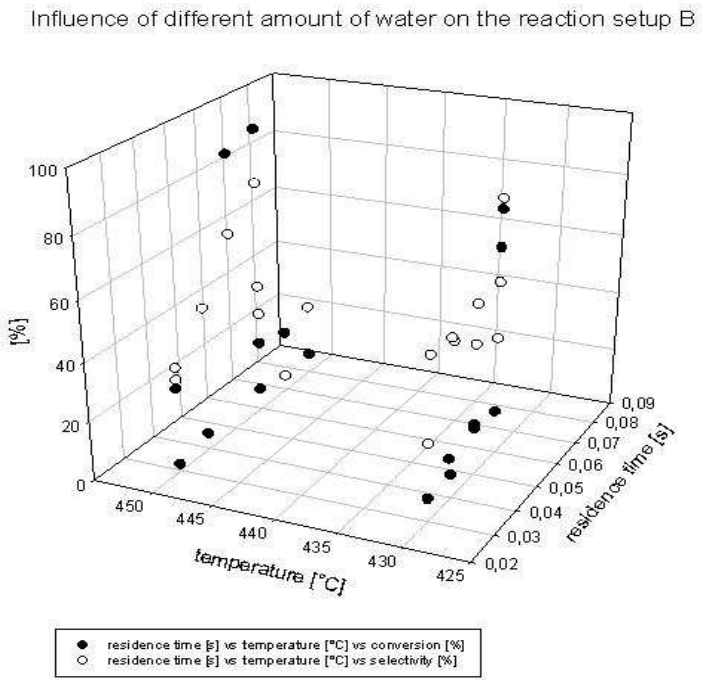

Fig. 3-22: Set-up VI-B using 3,0 g sodium catalysts, 20cc/min N_2 at T=430 °C and T=450 °C.

After the investigation of the effect of adding different amounts of water to the reaction system the residence time τ was varied by changing the nitrogen flow rate. In the absence of the voluminous water steam the residence times τ are significantly higher when using nitrogen rates from 20 cc/min. to 60 cc/min.. As mentioned before a relatively high amount of catalyst (4 g) was used at the beginning of the studies. Carrying out the experiment with sodium doped catalyst at 450 °C, reduced pressure and no water but varying nitrogen flow rates high conversions of more than 92 % have been obtained. Selectivities remain constant at around 32 %. (Table 3-22, Fig. 3-23).
High conversions of more than 90 % even at lower temperature of 430 °C appear sporadically. Generally the conversion lies between 20 % and 40 %. The lower temperature of 430 °C leads to a severe scattering of the results, the selectivity lies again at around 20 % to 28 % again. (Table 3-23, Fig. 3-24). Because of the strong data scattering, a definite trend based on the residence time τ cannot be drawn. However, the chosen nitrogen rates and the consequent high resident times are suitable for complete conversions. Due to the high conversions and the high reactivity of the catalyst, its amount was reduced to just 3 g in further experiments. The variational results in current experiments (Table 3-23, Fig. 3-24) are the result of unsteady pressure conditions as well as small variations in fixed bed charge, reactor geometry, output of the pump and work-up. By scaling up the experimental Set-up dimension blockades and inhomogenities can be reduced probably.

Table 3-22: Set-up VI-A using 4,0 g sodium catalyst T-21.4, no water, T = 450 °C.

Catalyst/ Run No.	Doping Na_2O $[\%]_{ICP}$	N_2 [cc / min]	τ [s]	T [°C]	WHSV [g HDA×h^{-1} / x ml Kat.]	Conversion [%]	Selectivity [%]	Yield [%]	TG weight loss [%]	Mass balance [%]
T-21.4/AB129.1A	0,58%	20	0,31	450	0,225	91,9	27,7	25,5	14,4	78,1
T-21.4/AB125.1A	0,58%	40	0,19	450	0,225	100	27,6	27,6	16,9	77,4
T-21.4/AB125.2A	0,58%	40	0,25	450	0,225	100	35,2	35,3	15,8	81,1
T-21.3/AB127.1A	0,51%	60	0,22	450	0,225	100	32,8	32,8	16,6	58,4
T-21.3/AB127.2A	0,51%	60	0,20	450	0,225	94,0	31,0	28,7	16,3	87,7

Table 3-23: Set-up VI-A using 4,0 g sodium catalyst T-21.4, no water, T = 430 °C.

Catalyst/ Run No.	Doping Na_2O [%]	N_2 [cc / min]	τ [s]	T [°C]	WHSV [g HDA×h^{-1} / x ml Kat.]	Conversion [%]	Selectivity [%]	Yield [%]	TG weight loss [%]	Mass balance [%]
T-21.6/AB160.1A	0,51%	60	0,17	430	0,225	20,9	24,7	5,2	15,3	74,8
T-21.6/AB160.2A	0,51%	60	0,17	430	0,225	29,9	22,6	6,7	15,4	84,3
T-21.6/AB162.2A	0,51%	40	0,18	430	0,225	39,8	15,9	6,3	16,3	89,6
T-21.7/AB164.4A	0,66%	20	0,20	430	0,225	98,3	27,5	27,0	13,9	96,3
T-21.7/AB164.3A	0,66%	20	0,23	430	0,225	97,2	25,7	25,0	14,6	75,9
T-21.6/AB162.1A	0,51%	40	0,24	430	0,225	30,2	28,2	8,5	16,3	74,8
T-21.7/AB160.4A	0,66%	60	0,25	430	0,225	91,1	18,5	16,9		96,5
T-21.6/AB164.1A	0,51%	20	0,28	430	0,225	16,6	27,0	4,5	15,6	99,9
T-21.7/AB164.5A	0,66%	20	0,30	430	0,225	93,8	25,2	23,7		95,5
T-21.6/AB164.2A	0,51%	20	0,41	430	0,225	24,0	26,4	6,3		91,0

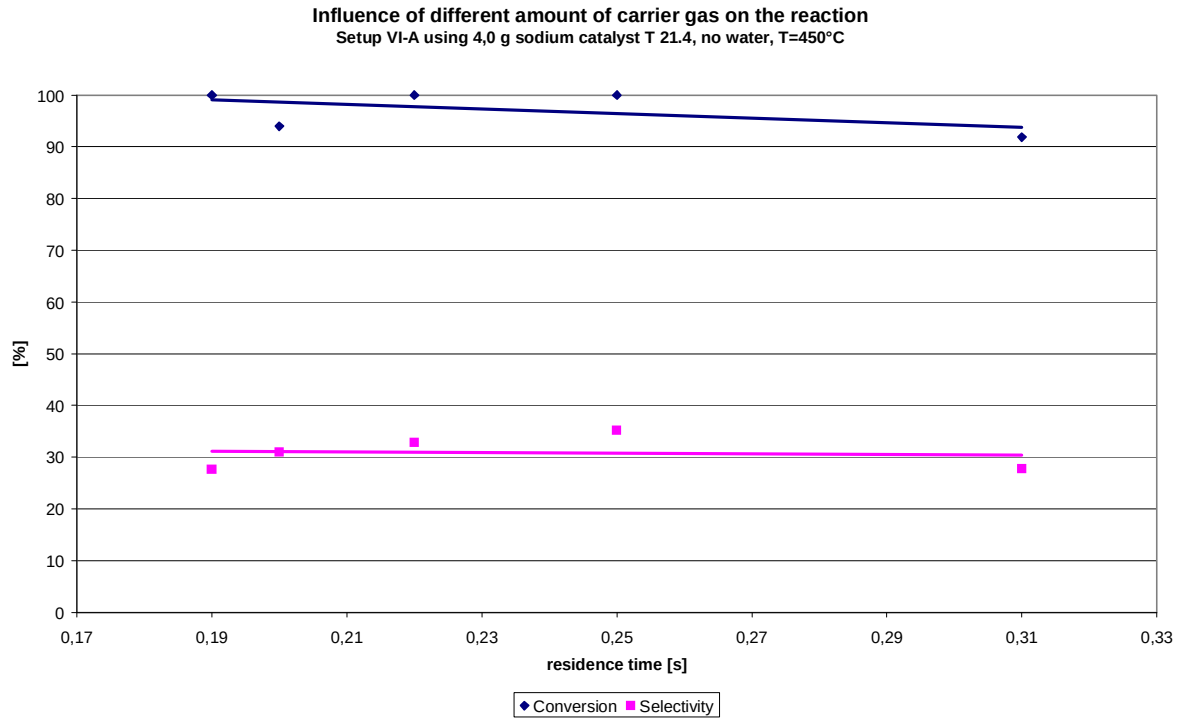

Fig. 3-23: Effect of nitrogen rate on the reaction at 450 °C using 4,0 g sodium catalyst, no water in set-up VIA.

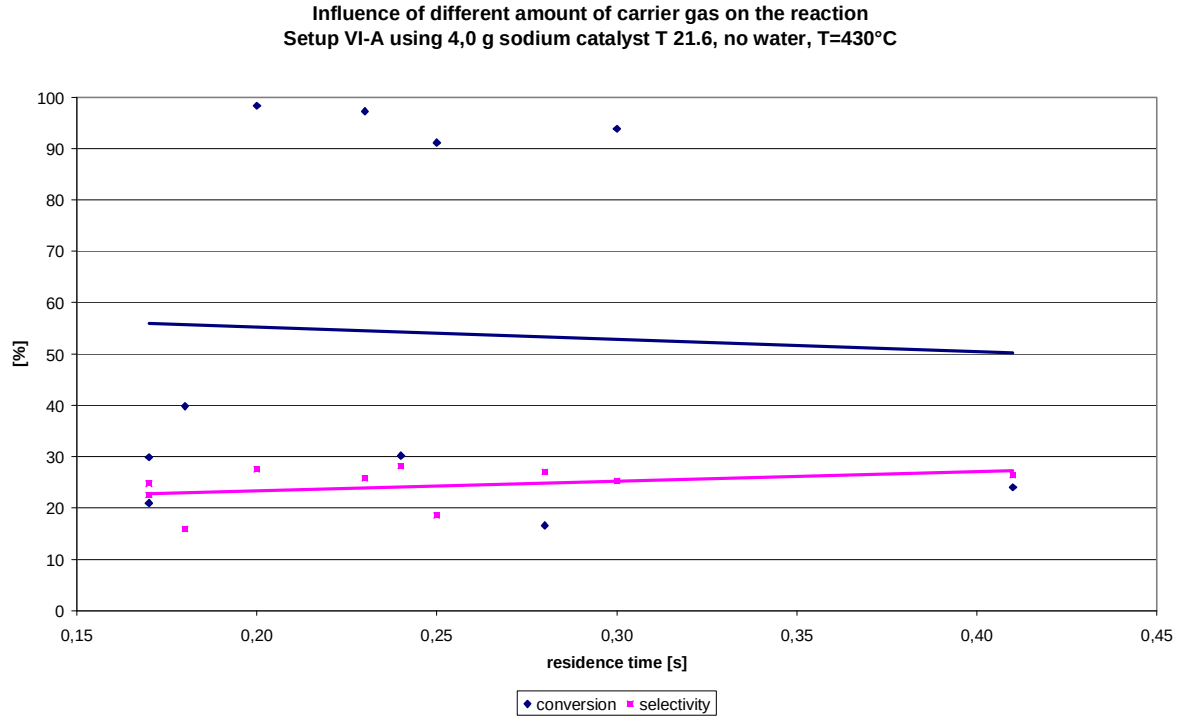

Fig. 3-24: Effect of nitrogen rate on the reaction at 430 °C using 4,0 g sodium catalyst, no water in set-up VIA.

Table 3-24: Set-up VI-B using 4,0 g potassium catalyst T-22.2, no water, T = 450 °C.

Catalyst/ exp. No.	Doping K_2O [%]	N_2 [cc / min]	τ [s]	T [°C]	WHSV [g HDA×h^{-1} / x ml Kat.]	Conversion [%]	Selectivity [%]	Yield [%]	TG weight loss [%]	Mass balance [%]
T-22.2/AB130.1B	0,5%	20	0,27	450	0,225	52,6	24,8	13,0	15,5	37,4
T-22.2/AB130.2B	0,5%	20	0,29	450	0,225	35,0	36,4	12,7		39,2
T-22.2/AB126.1B	0,5%	40	0,24	450	0,225	93,9	15,4	14,4	15,8	96,7
T-22.2/AB126.2B	0,5%	40	0,23	450	0,225	51,8	23,1	12,0	16,1	85,7
T-22.2/AB126.3B	0,5%	40	0,25	450	0,225	94,6	45,0	42,5	18,72	42,7
T-22.2/AB128.1B	0,5%	60	0,18	450	0,225	18,2	32,0	5,8	15,7	80,8
T-22.2/AB126.4B	0,5%	40	0,19	450	0,225	94,5	25,0	23,6		37,6
T-22.2/AB128.2B	0,5%	60	0,19	450	0,225	16,0	18,1	2,9	16,2	90,3
T-22.2/AB128.3B	0,5%	60	0,19	450	0,225	59,5	40,2	23,9		29,3

Additionally the influence of nitrogen flow rate on the reaction with potassium doped catalyst T-22.2 (BET-surface 84 m^2/g) was tested under the same conditions in set-up VIB. At 450 °C the results show a strong scattering. The sodium-impregnated catalysts were more active at this high temperature (Table 3-22). With the exception of a singular high conversion above 90 %, relatively low conversions of less than 20 % is observed if the residence time τ is too short. Increasing the residence time τ to 0,27 s conversions of over 50 % can be attained. This run is coherent.

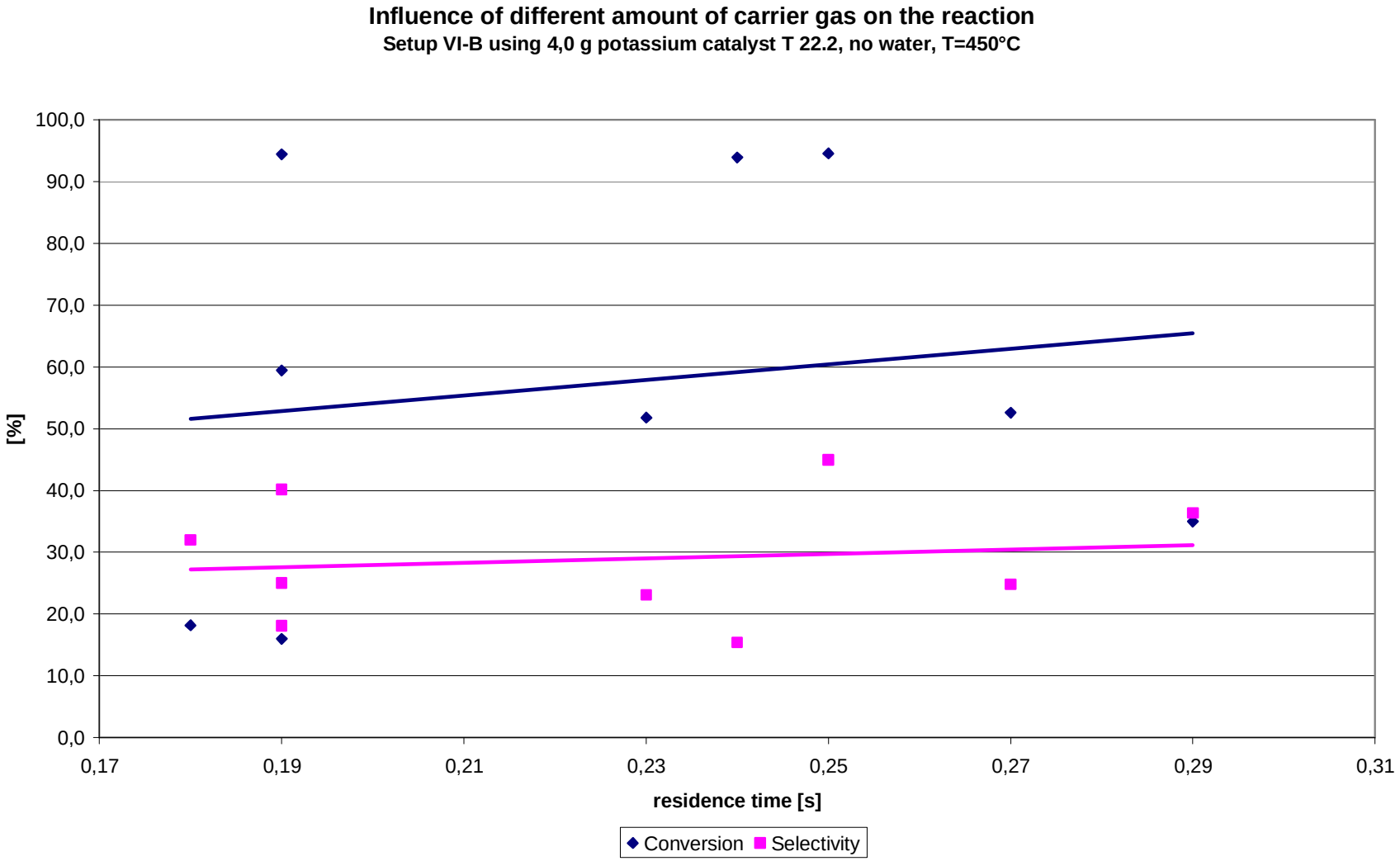

Fig. 3-25: Effect of nitrogen rate on the reaction at 450 °C using 4,0 g potassium catalyst T-22.2, no water in set-up VIB.

The gas phase is taken to be close to ideality. Anyhow, changing the temperature in the experiments listed in Table 3-25 and Table 3-26 has but a minor influence on residence time τ. The variations of residence time τ are caused by the inconstancy of the pump flow rate. Catalyst T-21.4 (Table 3-25) has been tested in set-up VI A and catalyst T-22.2 (Table 3-26) has been tested in set-up VI B by changing the temperature. The reaction conditions (20cc/min N_2 and approx. 18 g H_2O) are kept constant. In each case just 3 g of catalytic material was used in the experiment. The conversion of HDA (**4**) is favoured at the higher temperature of 450 °C (100% in AB131.1A and 27% in AB132.2B) and declines at the lower temperature of 400 °C (24% in AB139.1A and 11% in AB140.1B). A lower catalytic activity at lower temperatures has a positive effect on selectivity (55% at 430 °C in AB 136.2A and 65% at 400 °C in AB140.1B). The trend lines document, as expected, a higher conversion at higher temperatures. In these two run series the problem of reproducibility is obvious again. Inconstant results are evident in several runs at 430 °C and 440 °C using T-21.4 in set- VI A (Table 3-25).

Table 3-25: Set-up VI-A using 3,0 g sodium catalyst T-21.4, 20cc/min N2, approx 18g H_20.

Catalyst/ exp. No.	Doping Na_2O $[\%]_{ICP}$	N_2 [cc / min]	τ [s]	T [°C]	WHSV [g HDA×h^{-1} / x ml Kat.]	Conversion [%]	Selectivity [%]	Yield [%]	TG weight loss [%]	Mass balance [%]
T-21.4/AB131.1A	0,58%	20	0,05	450	0,3	100	45,6	45,6	9,2	73,4
T-21.4/AB131.2A	0,58%	20	0,07	450	0,3	93,8	41,8	39,2	12,6	64,1
T-21.4/AB141.3A	0,58%	20	0,06	440	0,3	11,1	29,0	3,2	14,8	69,3
T-21.4/AB141.4A	0,58%	20	0,06	440	0,3	12,5	36,6	4,6		37,3
T-21.4/AB141.5A	0,58%	20	0,06	440	0,3	23,1	37,4	8,6		80,4
T-21.4/AB141.6A	0,58%	20	0,06	440	0,3	17,5	29,4	5,1		72,2
T-21.4/AB141.7A	0,58%	20	0,04	440	0,3	23,6	42,6	10,1	16,4	75,8
T-21.4/AB136.2A	0,58%	20	0,06	430	0,3	18,6	55,0	10,3	10,4	76,4
T-21.4/AB136.4A	0,58%	20	0,05	430	0,3	27,2	25,8	7,0		36,8
T-21.4/AB136.5A	0,58%	20	0,06	430	0,3	20,1	45,8	9,2	12,1	65,6
T-21.4/AB136.6A	0,58%	20	0,07	430	0,3	11,7	46,4	5,4		86,0
T-21.4/AB139.1A	0,58%	20	0,06	400	0,3	24,1	42,8	10,3	13,4	68,6

Experimental reproduction would average the present inconsistent results. An exponential function of temperature influence due to *Arrhenius* equation is expected. The huge deviation reveals the complexity to control the experimental conditions.

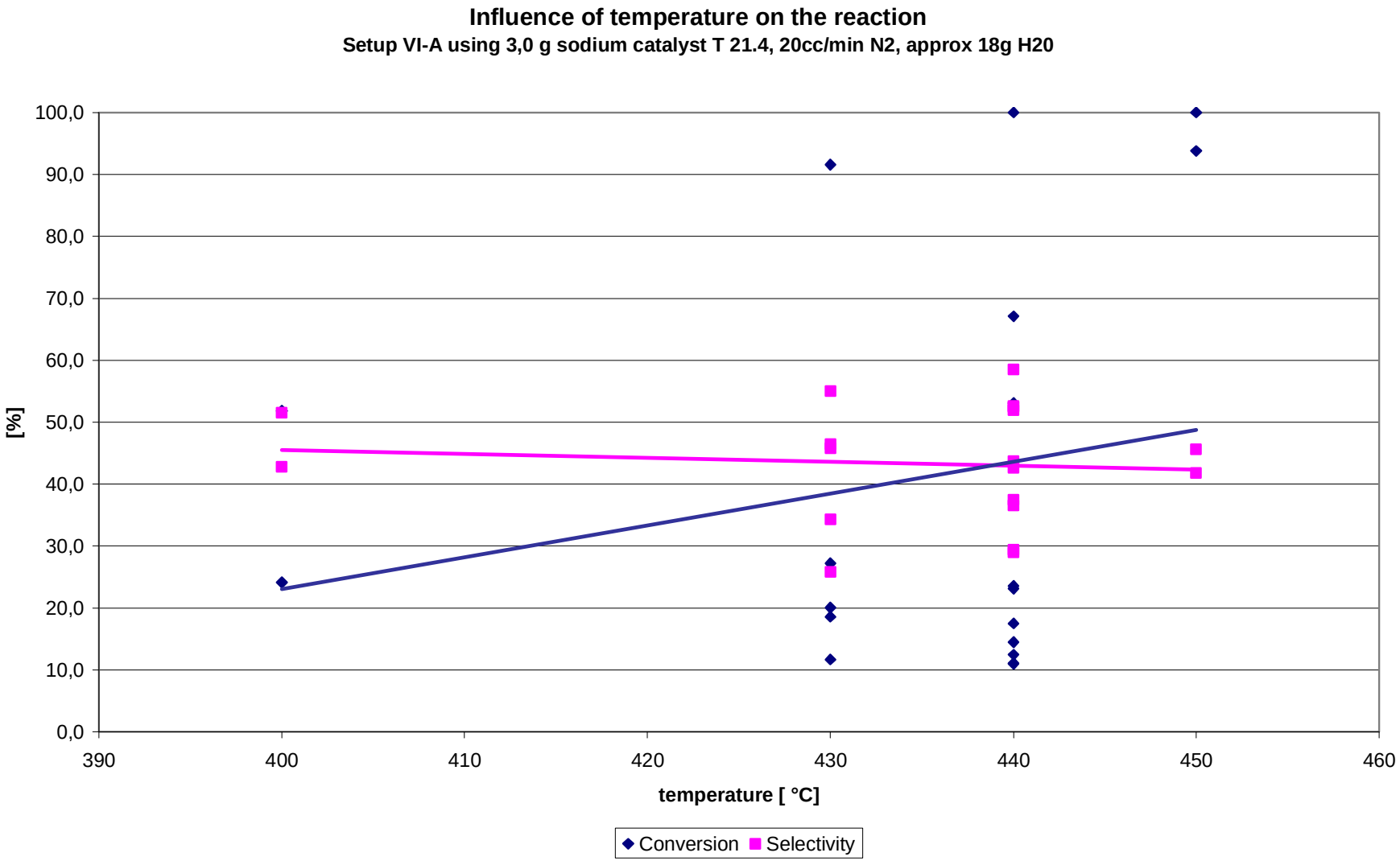
Influence of temperature on the reaction
Setup VI-A using 3,0 g sodium catalyst T 21.4, 20cc/min N2, approx 18g H20
100,0
90,0
80,0
70,0
60,0
50,0
40,0
30,0
20,0
10,0
0,0
[%]
390
400
410
420
430
440
450
460
temperature [°C]
Conversion
Selectivity

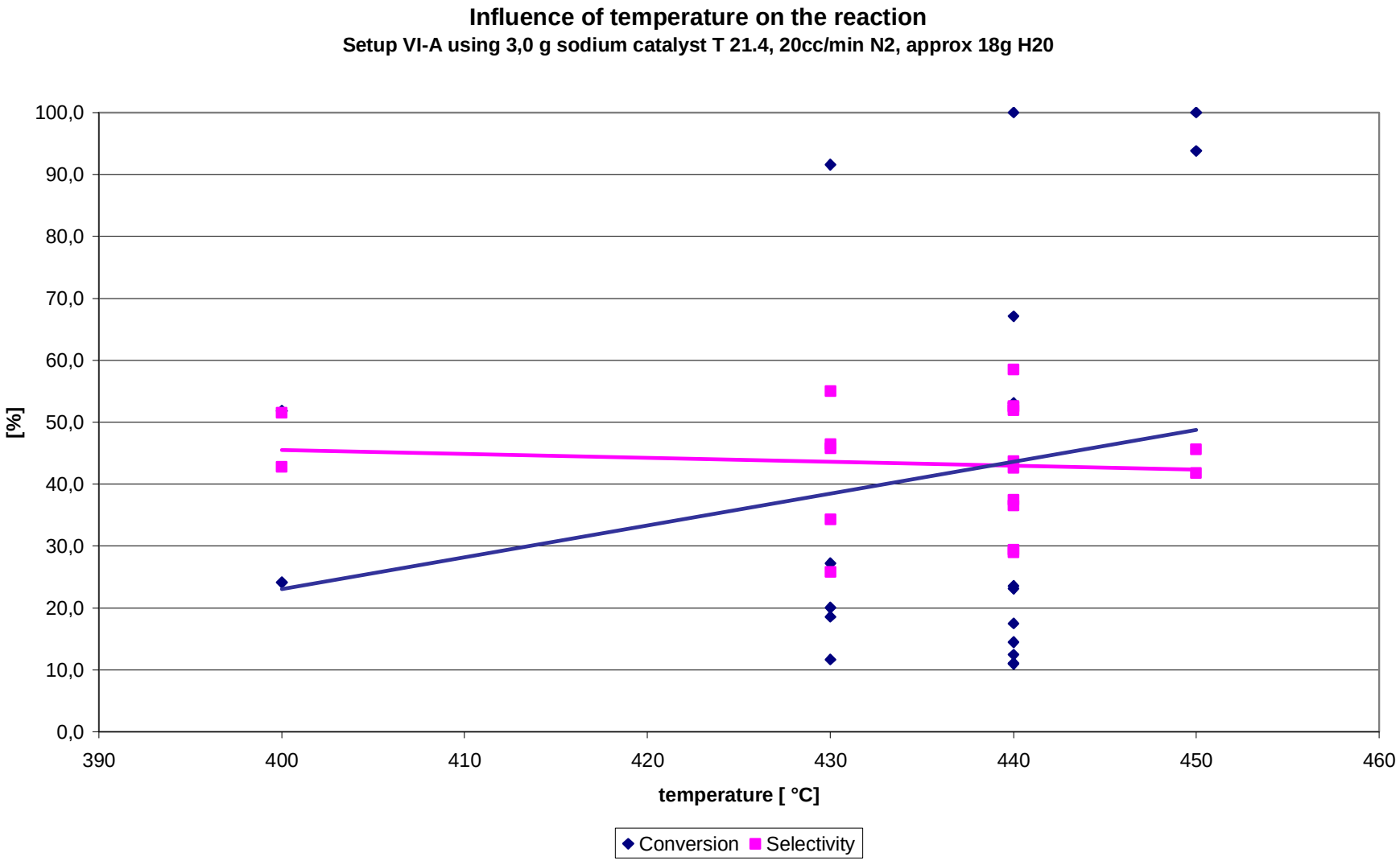

Fig. 3-26: Influence of temperature on the reaction using 3,0 g sodium catalyst T-21.4, approx 18g H_20 in set-up VIA.

Table 3-26: VI-B using 3,0 g potassium catalyst T-22.2, 20cc/min N2, approx 18g H_20.

Catalyst/ exp. No.	Doping K_2O [%]	N_2 [cc / min]	τ [s]	T [°C]	WHSV [g HDA×h^{-1} / x ml Kat.]	Conversion [%]	Selectivity [%]	Yield [%]	TG weight loss [%]	Mass balance [%]
T-22.2/AB132.1B	0,5%	20	0,05	450	0,3	14,0	48,1	6,7	12,2	77,9
T-22.2/AB132.2B	0,5%	20	0,06	450	0,3	27,3	42,8	11,7	13,0	87,0
T-22.2/AB132.3B	0,5%	20	0,05	450	0,3	42,9	33,8	14,5	2,1	41,5
T-22.2/AB137.1B	0,5%	20	0,06	430	0,3	12,2	56,8	6,9	12,0	79,6
T-22.2/AB137.2B	0,5%	20	0,06	430	0,3	11,2	58,7	6,6	10,9	75,1
T-22.2/AB137.3B	0,5%	20	0,05	430	0,3	18,1	34,3	6,2		71,0
T-22.2/AB140.1B	0,5%	20	0,07	400	0,3	11,0	65,7	7,2		92,2
T-22.2/AB140.2B	0,5%	20	0,06	400	0,3	9,1	62,7	5,7		62,3
T-22.2/AB140.3B	0,5%	20	0,06	400	0,3	21,9	63,6	13,9		33,7
T-22.2/AB140.4B	0,5%	20	0,06	400	0,3	4,1	40,3	1,7		71,3

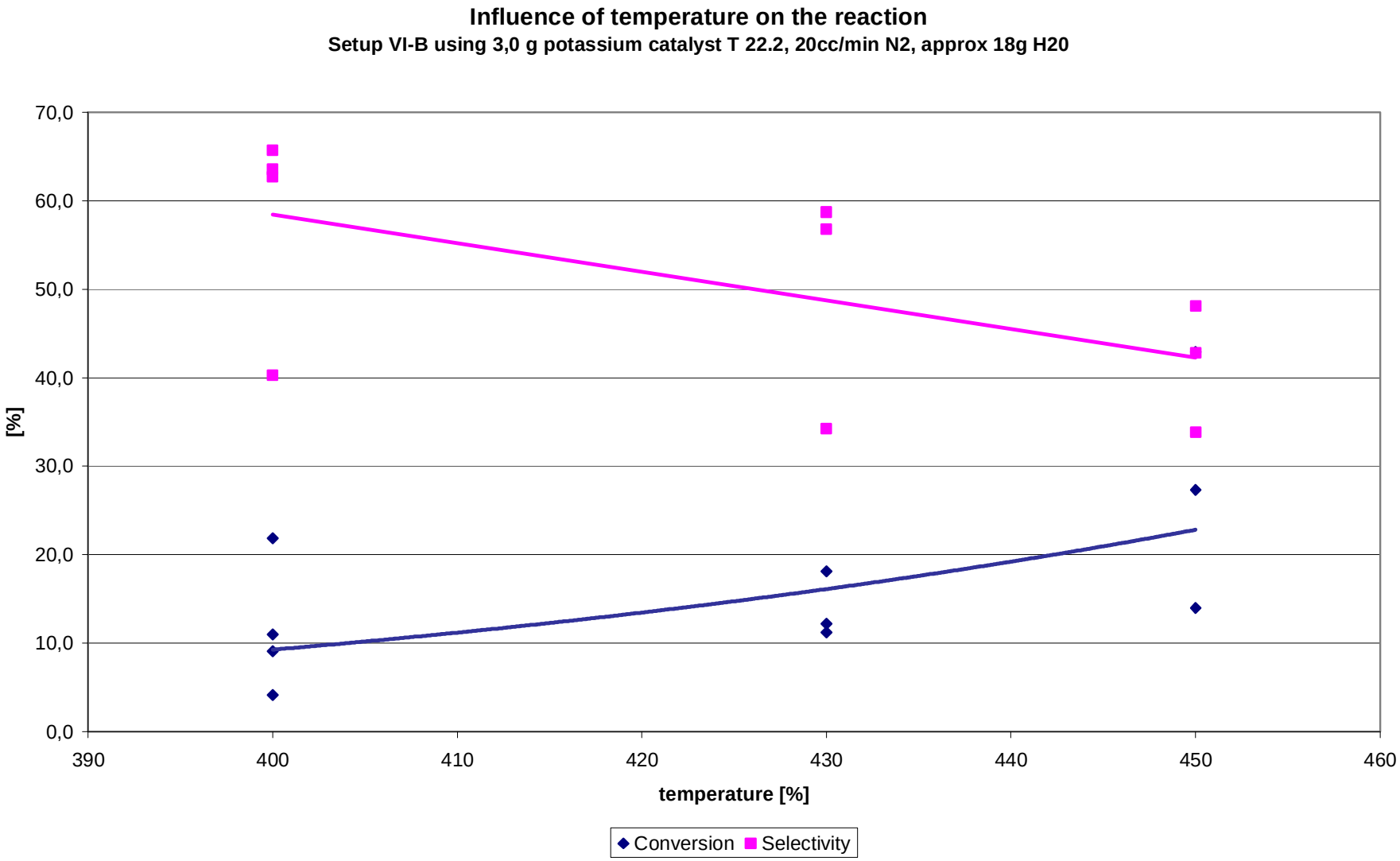

Fig. 3-27: Effect of temperature on the reaction using 3,0 g potassium catalyst T-22.2, approx 18g H_20 in set-up VIB.

In some regeneration experiments with sodium catalyst T-21.5 and potassium catalyst T-22.3 the decline of activity was scrutinised. T-21.5 was tested in set-up VI A and the potassium catalyst T-22.3 was tested in set-up VI B. The experiment was carried out with 3 g catalytic material, 20 cc/min N_2, approx 18 g H_20 and a temperature of 440 °C. After the first run of 300 min. and flushing with pure solvent, the reactor was heated up to 500 °C under a slow stream of compressed air over night. On the next day the reactor was cooled down to reaction temperature and the second run (marked “R” – rerun - in the run number) was carried out like the first one. In both cases the conversion and the selectivity decreased after the first run.

Table 3-27: Regeneration experiments of sodium catalyst T-21.5 and potassium catalyst T-22.3.

Catalyst/ Run No.	Doping Na_2O [%]	N_2 [cc / min]	τ [s]	T [°C]	WHSV [g HDA×h^{-1} / x ml Kat.]	Conversion [%]	Selectivity [%]	Yield [%]	TG weight loss [%]	Mass balance [%]
T-21.5/AB141.8A	0,40	20	0,06	440	0,3	44,6	40,8	18,2		
T-21.5/AB141.8AR	0,40	20	0,06	440	0,3	15,3	13,1	2,0		
T-21.5/AB141.9A	0,40	20	0,06	440	0,3	52,6	51,7	27,2		
T-21.5/AB141.9AR	0,40	20	0,05	440	0,3	47,9	44,4	21,3		
Catalyst/ Run No.	**Doping K_2O [%]**	**N_2 [cc / min]**	**τ [s]**	**T [°C]**	**WHSV [g HDA×h^{-1} / x ml Kat.]**	**Conversion [%]**	**Selectivity [%]**	**Yield [%]**	**TG weight loss [%]**	**Mass balance [%]**
T-22.3/AB142.2B	0,5	20	0,07	440	0,3	14,5	43,7	6,3		
T-22.3/AB142.2BR	0,5	20	0,07	440	0,3	16,5	19,6	3,2		
T-22.3/AB142.3B	0,5	20	0,05	440	0,3	11,0	58,5	6,4		
T-22.3/AB142.3BR	0,5	20	0,05	440	0,3	9,5	26,2	2,5		

In the first run of T-21.5 in set-up-VIA at 440 °C conversions of 44,6 % (52,6 %) and respectively selectivities of 40,8 % (51,7 %) could be attained. After regeneration as described, conversions of 15,3 % (47,9 %) and respectively selectivities of 13,1 % (23,3 %) have been measured. Less active than T-21.5 is the potassium doped catalyst T-22.3. In the first run conversions of 14,5 % (11,0 %) and respectively selectivities of 19,6 % (26,2 %) were possible. After regeneration conversions of 16,5 % (9,5 %) and respectively selectivities of 19,6,1 % (26,6 %) were measured.
Probably oxidation products of regeneration process concentrate inside the reactor and on the catalyst. The harsh conditions of 500 °C and hotspots could have destroyed the catalytic activity of the impregnated materials. Another possibility is the leaching effect during the first run.

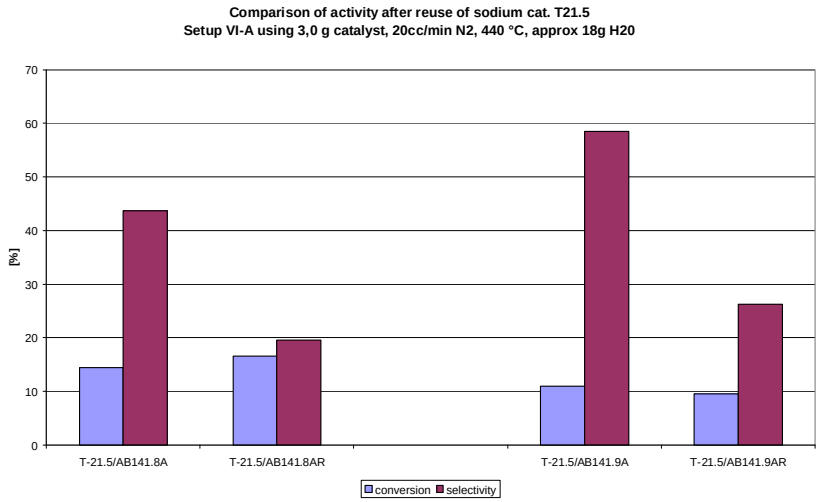

Fig. 3-28: Regeneration experiments of 3,0 g sodium catalyst T-21.5, approx 18g H_20 in set-up VIA.

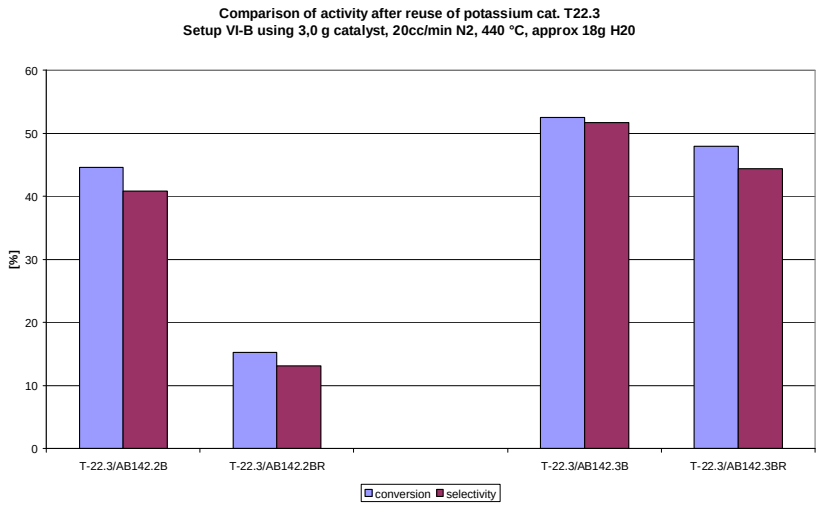

Fig. 3-29: Regeneration experiments of 3,0 g potassium catalyst T-22.3, approx 18g H_20 in set-up VIB.

As reported in chapter 2.3.2 an alternative variation of the ring closing reaction is the intramolecular ester condensation of e.g. alkyl substituted diesters (*Dieckmann*-condensation). Using the same experimental set-ups (VI A and VI B) and similar reaction conditions as reported before, the diester was tested with the current catalytic system T-21.6 or T-21.7, respectively. In the patent WO 2004/009524 A1 *BASF* described the use of TiO2 + 2 % K_2O at 350 °C and claimed a selectivity of 90 % and a yield of 78 %. The tests were carried out at 450 °C and 430 °C at a carrier gas flow of 20 cc/min. The ester usually was solved in THF and occasionally water was added to the system. In two cases toluene was used as solvent instead (AB172B). The results are presented below.

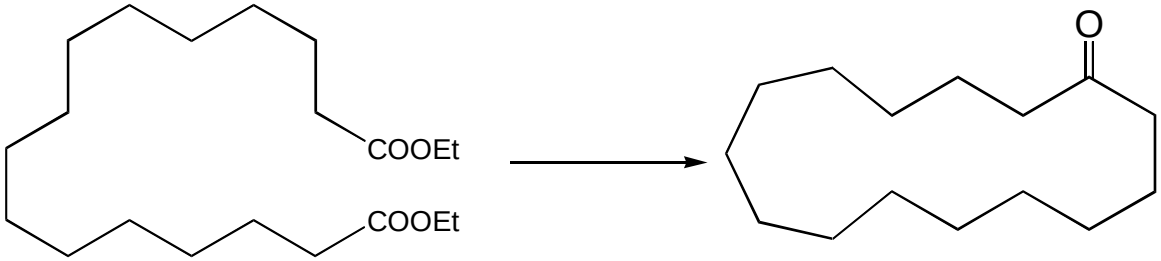

Hexadecanedioicdiester Cyclopentadecanone

Fig. 3-30: *Dieckmann*-condensation of hexadecanedioic diester to *exaltone* (2).

Generally comparable reaction conditions as before have been used. Using 3 g of catalyst T-21.6 a nitrogen rate of 20 cc/min at 430 °C and no additional water conversions from 4,8 % to 18,2 % and selectivities from 20,3 % to 54,8 % have been measured (Table 3-28). By increasing the reaction temperature to 450 °C and the amount of catalyst the conversion could not be decisively enhanced. The maximum conversion of 23,1 % is noticed in AB-169.1B. The addition of water has a positive influence even on this reaction. Thus, a high conversion of 63,3 % (56,9 %) at a selectivity of 42,2 % (43,3 %) was possible in the run AB-170.1 (AB-170.2). If toluene is used as a solvent the conversion can even be higher in these conditions.

Table 3-28: Results of the *Dieckmann*-condensation of Hexadecanedioic diester to *exaltone* (2).

Catalyst/ Run No.	Doping [%]	Cat. [g]	N_2[cc / min]	T [°C]	Water [ml/h]	Conversion [%]	Selectivity [%]	Yield [%]	TG weight loss [%]	Mass balance [%]
T-21.6/ AB166.1A	0,51%	3	20	430	0	8,4	29,9	2,5	15,5	81,1
T-21.6/ AB166.2A	0,51%	3	20	430	0	11,9	54,8	6,5	16,5	62,5
T-21.6/ AB167.1B	0,51%	3	20	430	0	18,2	21,8	4,0	18,1	61,1
T-21.6/ AB167.2B	0,51%	3	20	430	0	17,9	20,3	3,6	19,4	62,8
T-21.7/ AB168.1A	0,66 %	4	20	450	0	13,1	15,9	2,1	18,1	82,2
T-21.7/ AB169.1B	0,66 %	4	20	450	0	23,1	13,6	3,2	16,7	99,9
T-21.7/ AB171.1B	0,66 %	4	20	450	0	8,8	25,2	2,2		67,4
T-21.7/ AB171.2B	0,66 %	4	20	450	0	6,8	25,6	1,7		67,8
T-21.7/ AB170.1B	0,66 %	4	20	450	14,2	63,3	42,2	26,7	13,7	88,1
T-21.7/ AB170.2B	0,66 %	4	20	450	14,5	56,9	43,3	24,6	15,15	99,9
T-21.7/ AB172.1B*	0,66 %	4	20	450	13,2	69,3	30,9	21,1		90,3
T-21.7/ AB172.2B*	0,66 %	4	20	450	14,0	82,1	30,9	22,3		40,4

* Solvent: toluene. Pressure: 280 mbar

3.6 Analysis of by-products

If the reaction is carried out with sufficient amount of catalyst and temperature no educt peak is detected in the GC. The reactant can be converted completely. In all presented experiments the formation of by-products reduces the selectivity. The different factors which affect selectivity have already been mentioned. Attempts were made to separate the collected and reduced reaction products by different thin layer chromatography experiments (TLC). Numerous solvents and eluent mixtures have been tried out on silica gel and aluminium oxide stationary phases. Because of the large number of by-products and their similar solubility and physical properties the different compounds did not separate well, preventing thus the application of column chromatography. Peak bundles detected by GC with a constant gap interval of around one minute result from a difference of one methyl group in the molecule. GCMS-method was used as an alternative way to identify the by-products. Beside the generated *exaltone* (**2**) and the silylated educt HDA (**4**) different silylated carbonic acids in various lengths were detected. Additionally, fragments of silylated carboxylic acids and alcohols were found by this method. Furthermore the formation of di-, tri-, and oligomers is plausible in these reaction conditions. If the reaction temperature is high enough, higher boiling substances can desorb from the catalyst surface and leave the reactor. In these experiments a certain amount of reactants always remain undetected.

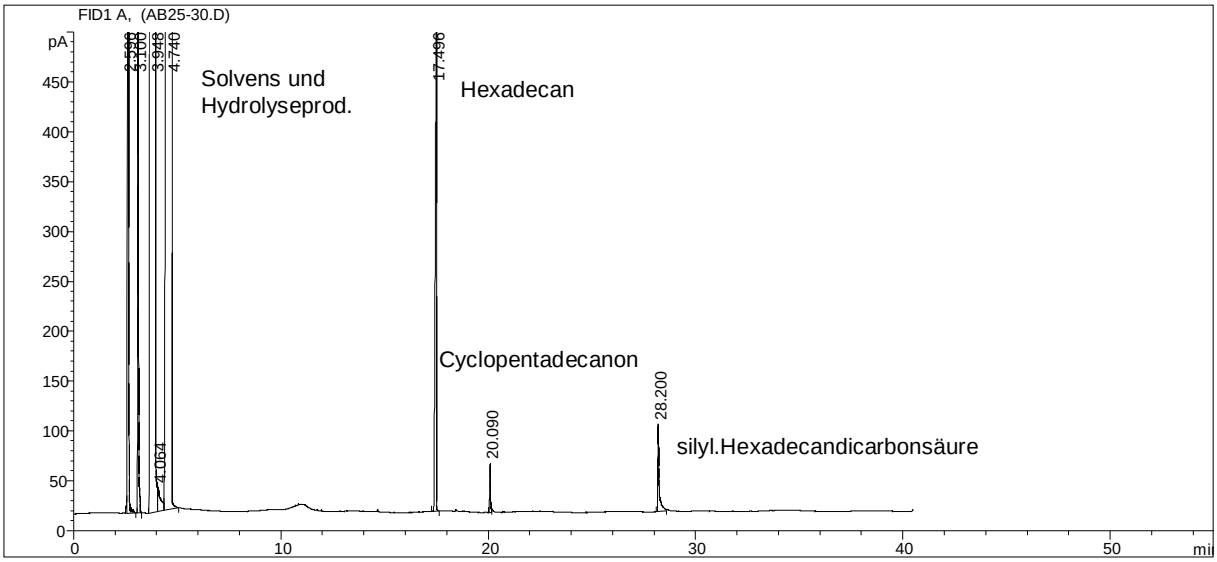

Fig. 3-31: Typical GC scan.

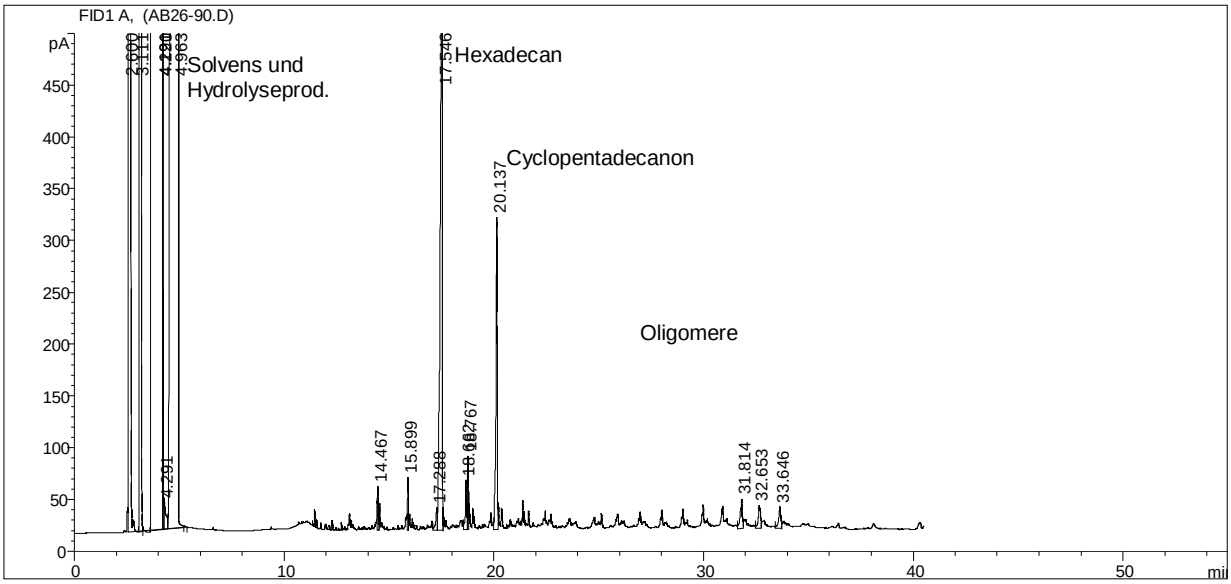

Fig. 3-32: Formation of crack byproducts at, 450 °C.

3.7 Examination of used catalyst materials

Used catalysts have been examined by XRD. There was no change of modification in a single measurement. An irreversible deactivation by a change of modification can be excluded. Attempts to extract the grey or dark brown deposits on the catalysts surface with different solvents like THF, toluene or ethanol were fruitless; the deposits were totally insoluble and no by-product was detected in GC. Also, thermogravimetric measurements (TG) have been carried out. In TG-measurements a sample changes its weight by undergoing a temperature-time profile in a defined atmosphere (here air). Because these measurements are time intensive not all of the used samples could be examined. In some cases the used catalyst could not be removed from the reactor. The relative amount of organic deposits is mentioned in the presented tables. Usually 8 % to 18 % of the used catalyst is organic material. No valid correlation linking this to the catalytic activity could be found. Additionally the amount of deposits at higher temperatures (e.g. 500 °C) is in the range of measurements taken after the reaction has taken place at lower temperatures.

Under the milder reaction conditions employed in the diploma thesis non converted educt was identified by this method. The DTG plot of current experiments shows, however, no deposition of HDA (**4**) on the catalyst surface.

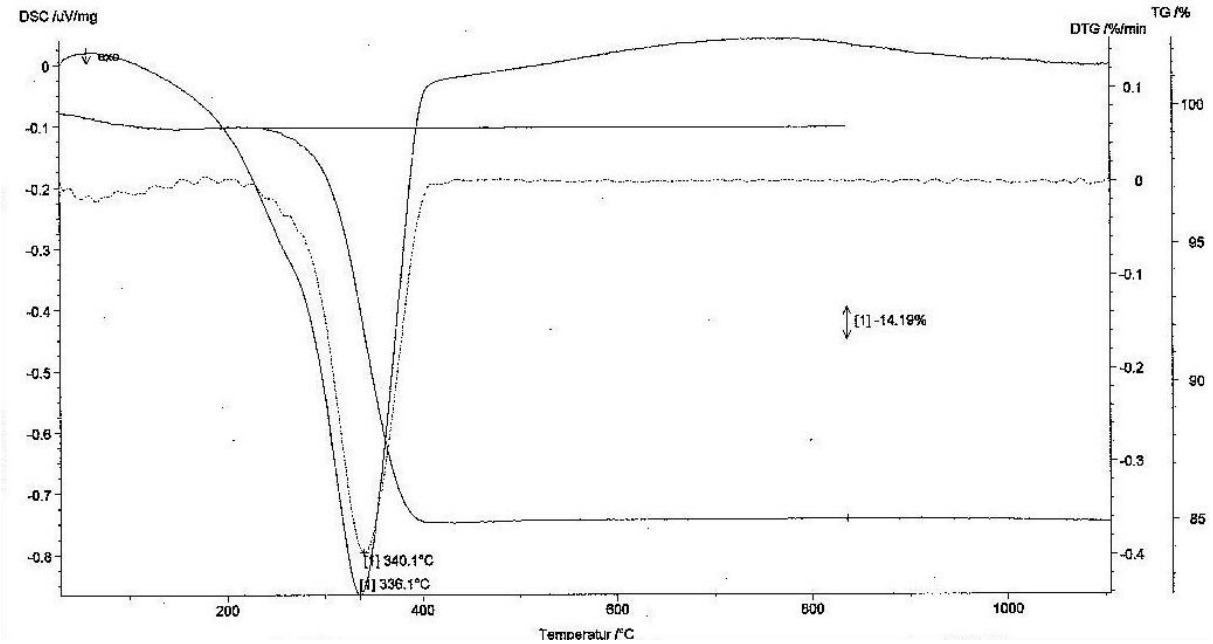

Fig. 3-33: TG-plot of a used catalyst.

4 Conclusions and outlook

The subject of present thesis is the heterogeneous synthesis of macrocyclic ketones, specifically *exaltone* (**2**) (cyclopentadecanone) starting from of a relatively cheaply available feedstock - a long chain, aliphatic dicarboxylic acid (here hexadecane dicarboxylic acid HDA (**4**)). These macrocyclic ketones are valuable, ecologically harmless fragrances, which have industrial relevance. A direct conversion of HDA (**4**) to *exaltone* (**2**) would be an enormous progress compared to other synthetic methods like ring enlargements or the *Diekmann*-condensation on basic TiO_2-catalysts published by *BASF*.[160]

To realise this kind of cyclization basic loaded titanium dioxide- and zirconium dioxide materials with high BET-surfaces were tested, along with a few experiments with silica or alumina based materials. One focus was the preparation of basic and bifunctional catalysts, based on high BET-area support materials. In the context of this project catalysts with different basic materials and different amounts of loading had been prepared, characterised (by XRD, BET, CO_2-TPD, ICP) and tested on their catalytic performance. Basic loaded anatase catalysts of 80 to 100 m^2/g BET-areas have been prepared. SEM and EDX-experiments revealed problems with the homogeneous distribution of active material on the support if the amount of impregnated base was too high.

After catalyst preparation and characterisation, the application in an intramolecular decarboxylation-dehydratisation reaction of hexadecane dicarboxylic acid (**4**) followed. An important objective was the improvement of previously used reaction conditions, including the optimisation of the reactor set-up. A liquid feed gas phase continuous flow reactor connected to a vacuum pump seems to be the best configuration yet. The vacuum helps to facilitate the desorption of products from the catalyst surface. In addition the reactant mobility and desorption of the educt and products from the catalyst surface and from the reactor walls can be influenced by water addition and high temperatures. Other parameters investigated were the amount of catalyst or carrier gas nitrogen (and therefore the residence time τ) or the catalyst loading. In all of the self-made reactor set-ups these parameters can be

varied but the fouling of the reactor with unidentifiable solid products could never be completely avoided.

Straight from the beginning of the preparative work it became obvious that reduced pressure and temperature over 400 °C were needed to carry out the reaction and transport the highly boiling reactants. This view was supported by thermodynamic calculations relying on computer-assisted simulation of molecular geometry and calculation of *Gibbs* enthalpies of competing reactions at different temperatures.

The educt HDA (**4**) is hardly soluble. Just ethanol (approximately 2 wt%), pyridine and tetrahydrofuran (approximately 5 wt%) are able to solve the dicarboxylic acid. The low solubility in ethanol supports the high dilutions effect which prevents oligomerization but affects low output. Pyridine is harmful to health and therefore experiments have been carried out with the less harmful THF at a moderate solubility of 5 wt%.

With a sufficient amount of catalyst (4,0 g, WHSV < 0,225 HDA×h^{-1}/ x ml cat.) the complete conversion of HDA (**4**) is possible at temperatures high enough (450 °C). TG-measurements show, as expected, a better desorption of high boiling organic compounds from the catalytic surface at higher temperatures. The most favourable temperature interval to carry out this reaction lies between approximatively 400 °C and 450 °C. The amount of catalytically active dopant (ca. 2,7 wt% to 6,6 wt%) had only a small effect in tests with sodium oxide loaded catalyst based on P25, Hombifine N or Hombikat Typ II. Within these tests at 450 °C 50 % selectivity was sporadically possible at 100 %conversion. Later experiments using 3,0 g sodium or potassium catalyst (ca. 0,5 wt%), 20cc/min N_2 and approx, 18g/h H_20 confirm the rising conversion and decreasing selectivity at higher temperatures.

Further runs with a loading of just around 0,5 wt% sodium oxide achieved the best results because the agglomeration of the catalytic active sides on the surface could be prevented. The basic oxides such as Li_2O, K_2O, Cs_2O as well as BaO and CaO have shown catalytic activity in this reaction as well. A rising trend towards better selectivity from potassium to cesium is not sure. Calcium doped catalyst on anatase materials with high BET-surface of 146 m^2/g (84 m^2/g,) have two different

strong basic centres and show conversions of 84 % (60 %) but only low selectivities of 11 %. Although Hombifine N based materials show a smaller BET-surface area and have less basic groups (according to CO_2-TPD measurements,) they provide a better selectivity, independent of the loaded material compared with catalysts based on Hombikat Typ II. In the work ca. 0,5 wt% sodium or potassium oxide on Hombifine N were used to for further experiments. For investigating the effect of water amount (and consequently of the residence time) 4 g sodium oxide or potassium oxide doped catalysts have been applied. If these tests were performed without adding water the results were less satisfactory than in the presence of water. The conversion was lower (40% and 85%), the selectivity was just 11-30% and the mass balance was extremely low (51-55%.) By raising the amount of added water to 15 g / h all results can be improved; conversions of 100 % at selectivities around 50 % are possible. Using a larger water rate of 27 g / h the selectivity drops. Reducing τ by addition of water is followed by an increase of selectivity and conversion. This is the consequence of a better desorption of organic compounds from the catalyst surface. If less catalyst was used (3 g, WHSV 0,3 g HDA×h^{-1}/ x ml cat.) the catalytic activity could be better observed. Using just 3 g catalyst the residence time becomes too short to reach high conversions. Experiments have been carried out at 430 °C and 450 °C as well, all other parameters remaining constant. At these temperatures conversions of around 20 % and selectivities of around 50 % were obtained with both catalysts. In most cases a longer residence time causes a higher conversion and a lower selectivity, as expected.

After investigating the effect of adding different amounts of water to the reaction system, the residence time τ was varied by adjusting the nitrogen flow rate, without water. In the absence of the very voluminous water steam the residence time τ was significantly higher when using nitrogen rates from 20 cc/min. to 60 cc/min. By carrying out the experiment with 4 g sodium doped catalyst at 450 °C, reduced pressure and no water at all but at variable nitrogen flow rates, high conversions of more than 92 % have been obtained. Selectivity remains constant at around 32 %. High conversions of more than 90 % even at lower temperature (430 °C) are only sporadically encountered. Generally conversion lies between 20 % and 40 %. The lower temperature of 430 °C causes a strong scattering of the results. The selectivity stays again at around 20 % to 28 %. A definite correlation with residence time τ

cannot be established because of the strong data scattering. The sodium impregnated catalysts were more active at this high temperature than the potassium doped ones: With the exception of incidentally high conversions above 90 %, relatively low conversions of less than 20 % were observed if the residence time τ was too short. By increasing the residence time τ to 0,27 s conversions of over 50 % can be realized.
Used akali impregnated catalysts can be regenerated by heating in oxidising atmosphere. The conditions of regeneration process have to be optimised. If the catalysts are recycled in the process a lower yield is observed. The conversion as well as the selectivity of the first run can not be achieved anymore. Further experiments are necessary to improve the recyclability.

The *Dieckmann*-condensation of hexadecanedioic diester to *exaltone* (2) has also successfully been tested with the reported catalytic systems. The addition of water has a positive effect on this reaction too. Yields over 20 % are directly reproducible even without running in the optimum of temperature and pressure.

The current work has been rendered somewhat difficult by the relatively poor reproducibility of the runs and the data scattering, even when using two experimental set-ups identically in construction. For this reason it is problematic at this stage to draw clear-cut conclusions.

The future challenge is to increase the yield of macrocyclic ketones by improving reaction conditions. Along screening new catalysts a process optimisation has to be considered. Not all of the products were detected, either because they remained trapped in the reactor system or passed uncondensed into the attached vacuum pump. With the currently employed set-ups reproducible experimental conditions are difficult to achieve. Larger diameter pipes and other engineering measures would probably avoid the occasional blocking. A longer activation time of catalysts before the running the experiment could also have a positive effect on the reaction. The acquired knowledge could then, at a later stage, be applied to other substrates like octadecene dicarboxylic acid (**5**). The most challenging problem in the future is to achieve reproducibility. A scale up can improve the reproducibility.

If a sample collecting is possible during the run, measurements of conversion and selectivity depending on TOS can be taken. Current set-ups were safety-related not suitable for sampling any time.

One approach of further research is the testing of new titanium dioxide materials, e.g. mesoporous Ti oxides. Such materials, which fully retain their mesostructure up to 300 °C, 400 °C and 600 °C respectively, have been extensively developed and these materials are now commercially available. An initial report of the synthesis of mesoporous TiO_2 appeared in1995.[180] This material was synthesized by a modified sol–gel route with phosphate surfactants that combined the principles of liquid crystal templating with the sol-gel chemistry of titanium alkoxides.[181] Another mesoporous titania synthesis by ligand-assisted templating with amine surfactants yields surface areas of up to 900 $m^2\ g^{-1}$.

Moreover, the preparative methods of the basic catalysts can be optimised. Strong basic sites like K_2O or Na_2O can also be formed by activation on the composites resulting from the decomposition of loaded nitrate or iodide in air. All in all a optimised catalytic system could reduce side reactions (e.g. cracking) and enhance selectivity. Additionally, a detailed investigation of the influence of calcination temperature and time on the specific surface of the catalysts will be required.

Another potential way to reduce the deposits on the catalyst surface (beside the addition of water to the system) is to reduce the feed rate. However, this would impair the economics of this process even further.

5 Experimental

5.1 Remarks to the analytics

5.1.1 Instrument and detection technique

Analytic capillary gas chromatography (GC):

The quantitative analysis of catalytic experiments is based on gas chromatography. To quantify conversion (C), selectivity (S) and yield (Y) following equations were used:

$$C_{Ed.}[\%] = \frac{A\_Ed._{transformed}[\%]}{A\_Ed._{transformed}[\%] + A\_Ed._{nontransformed}[\%]} \times 100\%$$

$$S_{Prod.}[\%] = \frac{A\_Prod.[\%]}{A\_Ed._{transformed}[\%]} \times 100\%$$

$$Y_{Prod.}[\%] = \frac{S \times C}{100}\%$$

C_{Ed} = conversion of educt
A Ed.$_{transformed}$ = Area percent of products after reaction
A Ed.$_{nontransformed}$ = Area percent of non transformed educt after reaction
$S_{Prod..}$ = selectivity of product
A Prod. = Area percent of desired product
$Y_{Prod.}$ = yield of desired product

The calculation of conversion and selectivity bears on the area-percent of detected substances in the GC-trace of examined product mixtures. No external standard (e.g. hexadecane) has been used.

Cyclization of hexadecanoic diacid (**4**):

Instrument	HP 6890 Plus
Column	FS-SE-54; 25m x 0,25 mm ID;
Temperature programme	50 °C; 5 min iso; 8 °C/min; 270 °C; 8 min iso
Injection volume	1 µL
Carrier gas	N_2, 0,5 bar; 10 min iso; 1 bar/min; 1,5 bar; 32 min iso
Injector	350 °C
Detector	300 °C

D. Das also used no external standard and relied on a calibration curve instead. A quantification bases on a calibration curve plots the peak area against the concentration of the component. This method turned out to be inexact.

Mass spectroscopy (GC-MS):

Unknown side products were identified by mass spectroscopy.

GC	Varianstar 3400 CX
MS	Varian Saturn 3
Electron energy	70 eV
Ionisation	electrical; 0,7 mA
Column	30 m x 0,25 DB5MS
Column temperature	50 °C; 5 min iso; 8 °C/min; 270 °C; 8 min iso
Evaporation temperature	350 °C
Carrier gas	1 bar Helium

High Performance Liquid Chromatography (HPLC):

A *Merck Hitachi* Co. instrument was used for HPLC analytics.

Instrument	La Chrom
Detectors	RI 7490 und DAD L4500 (UV 213 – 290 nm
Column	RP 18e (100 – 4,6 mm) und RP 18
Eluent	acetonitrile / ethanol (70 : 30); 0,6 ml / min
Temperature	35 °C
Injection load	10 µL

Inductively Coupled Plasma atomic emission spectrometry (ICP-AES):

The sodium concentration on the support materials TiO_2 and ZrO_2 were detected by a Spectroflame Modula FTM18 of *Spectro.* The samples have been disintegrated by a mixture of H_2SO_4, HF und HNO_3.

X-ray powder diffraction (XRD):

For XRD-measurements a *Siemens* diffractometer D 5000 with a 40 sample changer was available. The comminuted samples were loaded in a plastic sample holder before measuring.

X-ray tube	copper, long fine-focus (FL Cu 4KE)
Heating current	40 mA
Acceleration voltage	40 kV
Monochromator	secundary monochromator
Aperture	variable aperture set V 20
Filter	Ni
Wavelength	CuKα1 = 1,5406 Å;

	CuKα2 = 1,5444 Å; CuKα1,2 = 1,5419 Å;
Angular range	0,5 – 90 °
Angular speed	1,2 °/min

BET-surface area analysis:

The specific areas of the support materials and the prepared catalysts were measured with a *Micromeritics* ASAP 2000 instrument. Each sample was heated out at 300 °C under HV and the dead volume (void volume) was defined with helium before each measurement. The adsorption- and desorption isotherms were detected at 77,15 K with N_2.

FTIR-pyridine-adsorption spectroscopy (pyridine-FTIR)

The FTIR-pyridine-adsorption measurements have been carried out with the Protégé 460 of *Nicolet* company. The measuring cell, constructed in the Institute's workshop, includes a KBr-window, a heating facility and is suitable for working in vacuum. The samples were pressed in self-supporting pellets of 16 mg / cm^2 size. Samples prepared by this method were calcined at 400 °C and 10^{-3} torr and cooled to 50 °C under vacuum after two hours. Within this time the background spectrum was recorded at 400, 300, 200 and 100 °C. After the cooling process the adsorption of pyridine was started over a *Schlenk* flask. The measuring cell was heated to 100, 200, 300 und 400 °C after this loading. Each temperature was held for one hour. Scans have been recorded by 100 scans and a resolution of four.

Temperature programmed desorption (TPD):

NH_3-TPD measurements were carried out with a *Thermofinion* TPD 1100 instrument. Samples were heated at 400 °C in N_2-atmosphere for 3 hours and loaded with 3 Vol% NH_3 in argon for 3-4 hours afterwards. To minimize the physisorption the samples were flushed with N_2 at 120 C for one hour. The measuring proper was performed at a temperature ramp of 10 °C / min from RT to 900 °C in an argon stream of 20 ml / min. The amount of desorbed NH_3 was registered by a TCD detector.

CO_2-TPD measurements were carried out with the same instrument. The samples were heated at 500 °C in N_2 atmosphere for 3 hours and loaded with pure CO_2 at 80 °C for 3-4 hours afterwards. To minimize the physisorption the samples were flushed with N_2 at 80 C for one hour. The measuring was carried out at a temperature ramp of 10 °C / min from RT to 500 °C in an argon stream of 20 ml / min. The amount of desorbed CO_2 was registered by a TCD-detector.

Thermogravimetry / Differential scanning calorimetry (TG/DSC):

Used, coked catalysts were analysed by thermogravimetry with the STA 409C instrument of *Netsch* Co. Al_2O_3 was used as a reference sample. The measurement started at RT with a heating rate of 2 K / min to 1010 °C in air. To get homogeneous samples the material was ground with an agate mortar before measurement.

5.2 Remarks on the preparative work

5.2.1 Chemicals:

The catalyst materials were company donations. Substrates were provided by *Mitsubishi (MCC)* Co. Further chemicals were purchased at *Aldrich*, *Merck* and *Fluka* in synthesis grade and used without purification. Deionised water was used.

5.2.2 Preparation of catalysts by the incipient wetness method

The support material weighed and dried over night (e.g. TiO_2 UV100, TiO_2 K 03, TiO_2 Hombifine N, TiO_2 Hombikat Typ II, TiO_2 P25, VP ZrO_2) was elutriated with a minimal amount of deionised water. The necessary amount of water was determined in a preliminary test, by adding water dropwise to a small quantity of support material until slurrying. The slurry water (by weight difference) was then extrapolated to the whole catalyst batch. By constant stirring the slurried material was alkalinised with e.g. sodium hydroxide. This suspension was stirred overnight, then dried and calcined. The detailed preparations are given below:

a) 2% Na_2O on Titania (Hombifine N) support (T-10):
The support material, titanium oxide (BET surface area = 315 m^2/g) from Sachtleben, Germany (400,0 g) was intensively mixed with a minimum amount of water and 20 g dissolved oxalic acid. The ductile mass was pressed with a force of 120 tonnes through a nozzle of 2 mm in diameter. The pressed material was dried overnight at 110 ^oC in an air oven and then calcined in air at 250 ^oC for 1 hour. The white solid was crushed and sieved to 1,0-2,0 mm sized particles. For impregnation a smaller amount of these particles (80 g) was treated with a solution of sodium hydroxide and one drop of dimethyl amine to get the desired metal oxide loading. After drying in a rotary evaporator and then in air oven at 100^oC for one hour the pellets were finally calcined in air at 500^oC for 1 hour. This catalyst is designated as T-10.

b) 6% Na_2O on Titania (Hombifine N) support (T-10B):

This precursor was already used also for the preparation of T-10. Unimpregnated particles have been used to prepare this catalyst. 40 g of these particles were treated with a solution of 3,295 g sodium hydroxide and one drop of dimethyl amine to get the desired metal oxide loading. After drying in a rotary evaporator and then in air oven at 100^oC for one hour the pellets were finally calcined in air at 500^oC for 1 hour. This catalyst is designated as T-10B.

c) 2% Na_2O on Titania (P25) support (T-11):

The support material, titanium oxide (BET surface area = 50 m^2/g) from Degussa, Germany (150,0 g) was intensively admixed with a minimum amount of water and 7,5 g solved Oxalic acid. The ductile mass was pressed with a force of 60 tonnes through a 2 mm. nozzle The pressed material was dried overnight at 110 ^oC in an air oven and then calcined in air at 250 ^oC for 1 hour. The white solid was crushed and sieved to 1,0-2,0 mm sized particles. For impregnation a smaller amount of these particles (30 g) was treated with a solution of sodium hydroxide and one drop of dimethyl amine. After drying in a rotary evaporator and then in air oven at 100^oC for one hour the pellets were finally calcined in air at 500^oC for 1 hour. This catalyst is designated as T-11.

d) 6% Na_2O on Titania (P25) support (T-11):

This precursor was already used also for the preparation of T-11. Unimpregnated particles have been used to prepare this catalyst. 37 g of these particles were treated with a solution of 3,048 g sodium hydroxide and one drop of dimethyl amine to get the desired metal oxide loading. After drying in a rotary evaporator and in air oven at 100^oC for one hour the pellets were finally calcined in air at 500^oC for 1 hour. This catalyst is designated as T-11B.

e) 2% Na_2O on Titania (Hombikat Typ II, Lot.: 1570019) support (T-12):

The support material, titanium oxide (BET surface area = 107 m^2/g) from Sachtleben, Germany (400,0 g) was intensively mixed with a minimum amount of water and 20 g dissolved oxalic acid. The ductile mass was pressed with a force of 60 tonnes through a 2 mm nozzle. The pressed material was dried overnight at 110 ^oC in an air oven and then calcined in air at 250 ^oC for 1 hour. The white solid was crushed and

sieved to 1,0-2,0 mm sized particles. For impregnation a smaller amount of these particles (80 g) were treated with a solution of sodium hydroxide and one drop of dimethylamine to get the desired metal oxide loading. After drying in a rotary evaporator and in air oven at 100^{o}C for one hour the pellets were finally calcined in air at 500^{o}C for 1 hour. This catalyst is designated as T-12

f) 6% Na_2O on Titania (Hombikat Typ II, Lot.: 1570019) support (T12-B):

This precursor was already used also for the preparation of T-12. Unimpregnated particles have been used to prepare this catalyst. 40 g of these particles were treated with a solution of 3,295 g sodium hydroxide and one drop of dimethyl amine to get the desired metal oxide loading. After drying in a rotary evaporator and in air oven at 100^{o}C for one hour the pellets were finally calcined in air at 500^{o}C for 1 hour. This catalyst is designated as T-12B.

g) 2% K_2O on Titania (Hombikat Typ II, Lot.: 1570019) support (T-13):

This precursor was already used also for the preparation of T-12 and T-12B. Unimpregnated particles have been used to prepare this catalyst. 40 g of these particles were treated with a solution of 0,49 g potassium hydroxide and one drop of dimethyl amine to get the desired metal oxide loading. After drying in a rotary evaporator and in air oven at 100^{o}C for one hour the pellets were finally calcined in air at 500^{o}C for 1 hour. This catalyst is designated as T-13.

h) 2% Li_2O on Titania (Hombikat Typ II, Lot.: 1570019) support (T-14):

This precursor was already used also for the preparation of T-12 and T-12B. Unimpregnated particles have been used to prepare this catalyst. 40 g of these particles were treated with a solution of 1,15 g lithium hydroxide and one drop of dimethyl amine to get the desired metal oxide loading. After drying in a rotary evaporator and in air oven at 100^{o}C for one hour the pellets were finally calcined in air at 500^{o}C for 1 hour. This catalyst is designated as T-14.

i) 2% Cs_2O on Titania (Hombikat Typ II, Lot.: 1570019) support (T-15):

This precursor was already used also for the preparation of T-12 and T-12B. Unimpregnated particles have been used to prepare this catalyst. 40 g of these particles were treated with a solution of 0,49 g caesium hydroxide and one drop of

dimethyl amine to get the desired metal oxide loading. After drying in a rotary evaporator and in air oven at 100^{o}C for one hour the pellets were finally calcined in air at 500^{o}C for 1 hour. This catalyst is designated as T-15.

j) 2% K_2O on Titania (Hombifine N, Lot.: 1780034) support (T-16):

This precursor was already used also for the preparation of T-10 and T-10B. Unimpregnated particles have been used to prepare this catalyst. 40 g of these particles were treated with a solution of 0,49 g potassium hydroxide and one drop of dimethyl amine to get the desired metal oxide loading. After drying in a rotary evaporator and in air oven at 100^{o}C for one hour the pellets were finally calcined in air at 500^{o}C for 1 hour. This catalyst is designated as T-16.

k) 2% Li_2O on Titania (Hombifine N, Lot.: 1780034) support (T-17):

This precursor was already used also for the preparation of T-10 and T-10B. Unimpregnated particles have been used to prepare this catalyst. 40 g of these particles were treated with a solution of 1,15 g lithium hydroxide and one drop of dimethyl amine to get the desired metal oxide loading. After drying in a rotary evaporator and in air oven at 100^{o}C for one hour the pellets were finally calcined in air at 500^{o}C for 1 hour. This catalyst is designated as T-17.

l) 2% Cs_2O on Titania (Hombifine N, Lot.: 1780034) support (T-18):

This precursor was already used also for the preparation of T-10 and T-10B. Unimpregnated particles have been used to prepare this catalyst. 40 g of these particles were treated with a solution of 0,49 g caesium hydroxide and one drop of dimethyl amine to get the desired metal oxide loading. After drying in a rotary evaporator and in air oven at 100^{o}C for one hour the pellets were finally calcined in air at 500^{o}C for 1 hour. This catalyst is designated as T-18.

m) 2% CaO on Titania (Hombikat Typ II, Lot.: 1570019) support (T-19):

The support material, titanium oxide (BET surface area = 107 m^2/g) from Sachtleben, Germany (130 g) was intensively mixed with 2,7 g calcium oxide, a minimum amount of water and 6,5 g dissolved oxalic acid. The ductile mass was pressed with a force of 60 tonnes through a 2 mm nozzle. The pressed material was dried overnight at 110 ^{o}C in an air oven and then calcined in air at 500 ^{o}C for 1 hour. The white solid

was crushed and sieved to 1,0-2,0 mm sized particles. This catalyst is designated as T-19.

n) 2% CaO on Titania (Hombifine N, Lot.: 1780034) support (T-20):

The support material, titanium oxide (BET surface area = 315 m^2/g) from Sachtleben, Germany (130 g) was intensively mixed with 2,7 g calcium oxide, a minimum amount of water and 6,5 g dissolved oxalic acid. The ductile mass was pressed with a force of 60 tonnes through a 2 mm nozzle. The pressed material was dried overnight at 110 ^oC in an air oven and then calcined in air at 500 ^oC for 1 hour. The white solid was crushed and sieved to 1,0-2,0 mm sized particles. This catalyst is designated as T-20.

o) 0,5% Na_2O on Titania (Hombifine N, Lot.: 1780034) support (T-21):

This precursor was already used also for the preparation of T-10, T-10B, T-16, T-17 and T-18. Unimpregnated particles have been used to prepare this catalyst. 50 g of these particles were treated with a solution of 0,32 g sodium hydroxide and one drop of dimethyl amine to get the desired metal oxide loading. After drying in a rotary evaporator and in air oven at 100 ^oC for one hour the pellets were finally calcined in air at 500 ^oC for 1 hour. This catalyst is designated as T-21.

p) 0,5% Na_2O on Titania (Hombifine N, Lot.: 1780034) support (T-21.2):

The support material, titanium oxide (BET surface area = 315 m^2/g) from *Sachtleben*, Germany (400,0 g) was intensively mixed with a minimum amount of water and 20 g dissolved oxalic acid. The ductile mass was pressed with 120 tonnes through a nozzle of 2 mm diametre. The pressed material was dried overnight at 110 ^oC in an air oven and then calcined in air at 250 ^oC for 1 hour. The white solid was crushed and sieved to 1,0-2,0 mm sized particles. For impregnation a smaller amount of these particles (40 g) was treated with a solution of sodium hydroxide (0,259 g) and one drop of dimethyl amine to get the desired metal oxide loading. After drying in a rotary evaporator and in air oven at 100 ^oC for one hour the pellets were finally calcined in air at 500 ^oC for 1 hour. This catalyst is designated as T-21.2.

q) 0,5% K_2O on Titania (Hombifine N, Lot.: 1780034) support (T-22):

This precursor was already used also for the preparation of T-21.2. Unimpregnated particles have been used to prepare this catalyst. 40 g of these particles were treated with a solution of 0,239 g potassium hydroxide and one drop of dimethyl amine to get the desired metal oxide loading. After drying in a rotary evaporator and in air oven at 100 ^oC for one hour the pellets were finally calcined in air at 500 ^oC for 1 hour. This catalyst is designated as T-22.

r) 0,5% Cs_2O on Titania (Hombifine N, Lot.: 1780034) support (T-23):

This precursor was already used also for the preparation of T-21.2 and T-22. Unimpregnated particles have been used to prepare this catalyst. 40 g of these particles were treated with a solution of 0,240 g caesium hydroxide and one drop of dimethyl amine to get the desired metal oxide loading. After drying in a rotary evaporator and in air oven at 100 ^oC for one hour the pellets were finally calcined in air at 500 ^oC for 1 hour. This catalyst is designated as T-23.

s) 0,5% Na_2O on Titania (Hombikat Typ II, Lot.: 1570019) support (T-24):

The support material, titanium oxide (BET surface area = 315 m^2/g) from *Sachtleben*, Germany (400,0 g) was intensively mixed with a minimum amount of water and 20 g dissolved oxalic acid. The ductile mass was pressed with 120 tonnes through a 2 mm nozzle. The pressed material was dried overnight at 110 ^oC in an air oven and then calcined in air at 250 ^oC for 1 hour. The white solid was crushed and sieved to 1,0-2,0 mm sized particles. For impregnation a smaller amount of these particles (40 g) were treated with a solution of sodium hydroxide (0,259 g) and one drop of dimethyl amine to get the desired metal oxide loading. After drying in a rotary evaporator and in air oven at 100 ^oC for one hour the pellets were finally calcined in air at 500 ^oC for 1 hour. This catalyst is designated as T-24.

t) 0,5% K_2O on Titania (Hombikat Typ II, Lot.: 1570019) support (T-25):

This precursor was already used also for the preparation of T-24. Unimpregnated particles have been used to prepare this catalyst. 40 g of these particles were treated with a solution of 0,239 g potassium hydroxide and one drop of dimethyl amine to get the desired metal oxide loading. After drying in a rotary evaporator and in air oven at 100 ^oC for one hour the pellets were finally calcined in air at 500 ^oC for 1 hour. This catalyst is designated as T-25.

u) 0,5% Cs_2O on Titania (Hombikat Typ II, Lot.: 1570019) support (T-26):

This precursor was already used also for the preparation of T-24 and T-25. Unimpregnated particles have been used to prepare this catalyst. 40 g of these particles were treated with a solution of 0,240 g caesium hydroxide and one drop of dimethyl amine to get the desired metal oxide loading. After drying in a rotary evaporator and in air oven at 100 ^oC for one hour the pellets were finally calcined in air at 500 ^oC for 1 hour. This catalyst is designated as T-26.

v) 0,5% BaO on Titania (Hombifine N, Lot.: 1780034) support (T-27):

This precursor was already used also for the preparation of T-21.2. Unimpregnated particles have been used to prepare this catalyst. 40 g of these particles were treated with a solution of 0,248 g barium hydroxide and one drop dimethylamine to get the desired metal oxide loading. After drying in a rotary evaporator and in air oven at 100^oC for one hour the pellets were finally calcined in air at 500^oC for 1 hour. This catalyst is designated as T-27.

w) Hydrotalcite $Mg_8Al_2(OH)_2CO_3xmH_2O$ (Mg/Al = 4) (HY-1):

To prepare a hydrotalcite material (Mg/Al = 4) a mixture of 63,28 g $Mg(NO_3)_2x6H_2O$ in 310 ml water and 23,12 g $Al(NO_3)_3x9H_2O$ in 310 ml water was added dropwise to a Na_2CO_3 solution (3,26 g in 310 ml water) under permanent stirring. The pH-value was kept at 9 to 9,5 by dropwise addition of a 1 M NaOH solution. After stirring for 24 h the white product was filtered and washed several times with water. After drying in a rotary evaporator and in air oven at 100^oC for one hour, the material was finally calcined in air at 450^oC for 1 hour. This catalyst is designated as Hy-1.

x) 0,5% Na_2O on silica stabilized zirkonia (Saint-Gobain, Lot.: Dms2007-0012) support (ZR-6):

This precursor from *Saint-Gobain* was already available as 3 mm particles. Unimpregnated particles have been used to prepare this catalyst. 40 g of these particles were treated with a solution of 0,259 g sodium hydroxide and one drop of dimethyl amine to get the desired metal oxide loading. After drying in a rotary evaporator and in air oven at 100 ^oC for one hour the pellets were finaly calcined in air at 500 ^oC for 1 hour. This catalyst is designated as ZR-6.

5.2.3 Experimental set-ups and execution of the tests

Reactions have already been carried out in the liquid phase as well as under gas-phase conditions as reported before. The catalyst test for cyclization of hexadecane dicarboxylic acid (**4**) to *exaltone* (**2**) (cyclopentadecanone) have been carried out in an integral packed bed - coiled tubing reactor. In the course of this thesis the experimental set up has been constantly improved. In all used set-ups the process was operated continuously, isothermally and under reduced pressure. The numbering of set-ups follows quarterly reports of the Institute during this project. In Fig. 5-1and Fig. 5-2 the flow-sheet of set-up V is presented. Two of those units were in function.

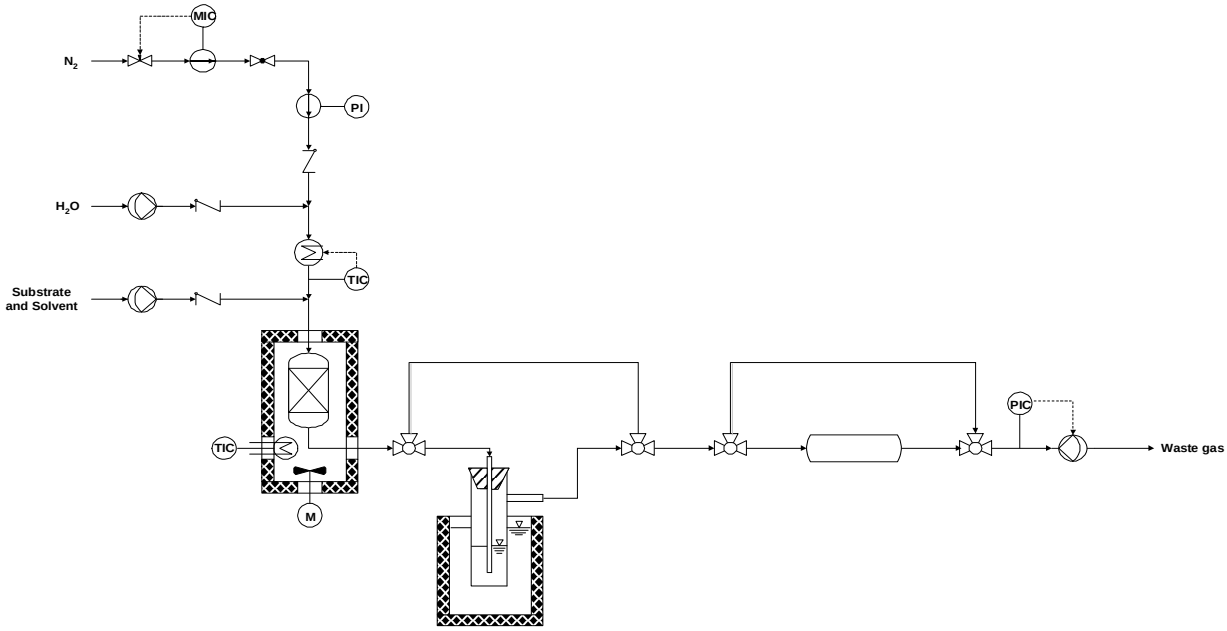

Fig. 5-1: Set-up V: Flow sheet of liquid feed gas phase continuous flow reactor with reduced pressure.

Fig. 5-2: Set-up V - liquid feed gas phase continuous flow reactor with reduced pressure.

In these set-ups the 5 wt % substrate solution in THF was fed into the reactor entry with a calibrated *Telab* metering pump[182] usually adjusted to a flow rate of 18 cc/h (0,9 g HDA / h). Through a capillary with an inner diameter of 1 mm the solution was introduced into a heated coiled tubing reactor in which it evaporated and was brought to the required reaction temperature. Dried and degreased nitrogen carrier gas was fed at the same site. By dint of A constant volume flow was adjusted with the help of a calibrated mass-flow controller of *Brooks* Co. fitted with a control module. Water was injected into the reaction system through the same heated line as nitrogen. A constant volume stream of liquid water was pumped by a *Telab* metering pump[182] and, together with the carrier gas nitrogen, it was heated and evaporated in a tube (ø 8 mm) filled with glass balls. This heating tube is wrapped with a heating tape and isolated. Just like the oven the temperature of this tube is controlled by a PID unit of *Eurotherm*[183].

The air-circulation oven was heated to the required reaction temperature at a rate of 10 °C / min. The temperature was controlled by a *Eurotherm*[183] PID unit. A ventilator inside the oven provides a uniform temperature throughout the oven space. The coiled tubing reactor with an inner diameter of 6 mm has 2.5 coils of 90 mm diameter. At 100 mm from the reactor outlet is located a woven wire mesh holder, which supports the catalyst bed. The catalyst particles used were a sieve fraction between 1.0 and 2.0 mm in size. In set-up V the process gas was passed into a cooled

separating funnel (which can be emptied during the experiment,) fitted with a reflux condenser. Cooling trap and condenser were thermostatted with a cryostat to - 10 °C. Gaseous products were not collected and analysed but rather exhausted into a pump. This pump and the control module (electronic or needle valve) were connected to the reflux condenser. The results are presented in chapter 3.5.

To improve the experimental set-up the construction of the reactor outlet in set-up VI was modified. Instead of a cooled separating funnel with reflux condenser a heated reactor outlet was connected to a glass cooling trap immersed in a Dewar vessel. The parts of the reactor outlet are made of solid metal and heated with heating sleeves. The temperature of these parts was controlled by a *Eurotherm*[183] PID unit.

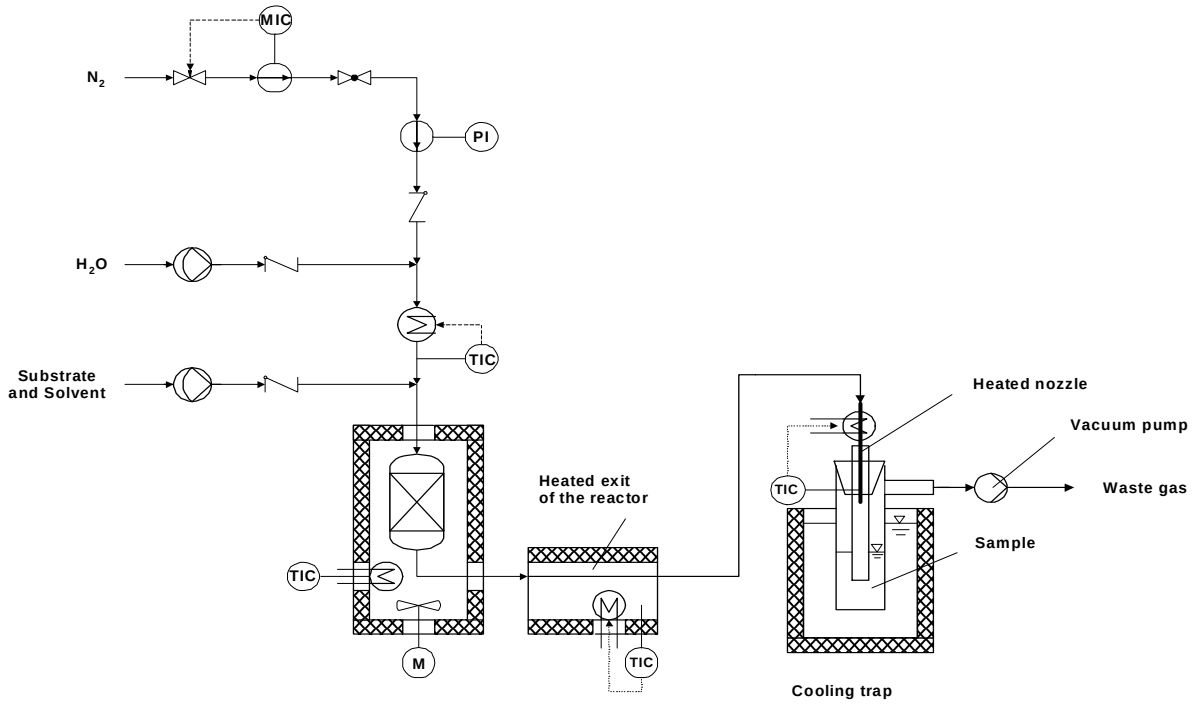

Fig. 5-3: Set-up VI: Flow chart of liquid feed gas phase continuous flow reactor with reduced pressure and heated reactor outlet.

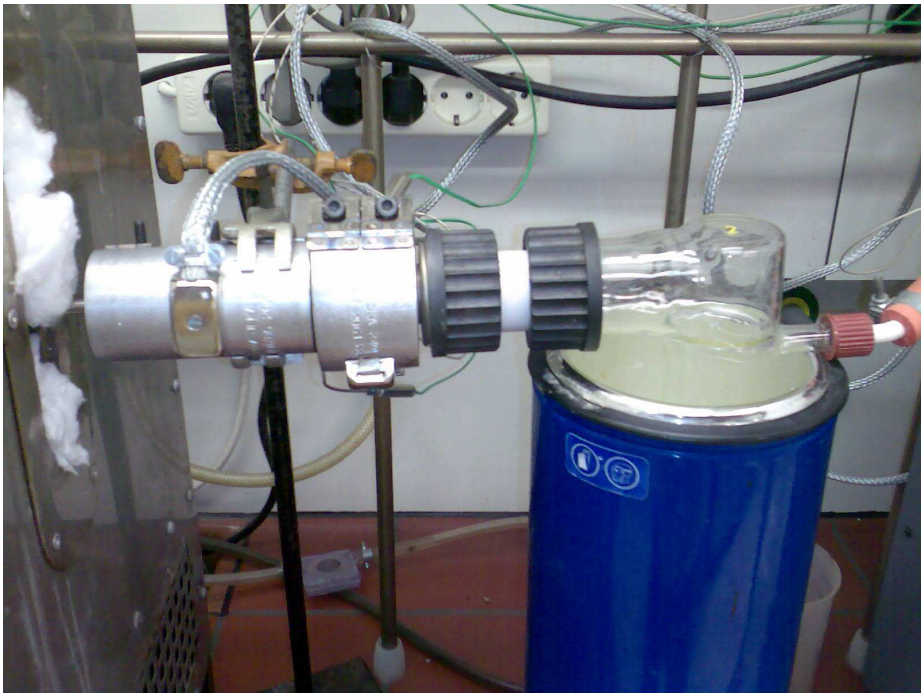

Fig. 5-4: Reactor outlet Set-up VI - liquid feed gas phase continuous flow reactor with reduced pressure

In all experiments a standardised time interval was allowed after heating the reactor to the prescribed temperature the rector and starting the *Telab* pumps, to ensure the complete filling of all feed pipes with substrate or water. After running the experiment substrate feeding was stopped and the pipes were flushed with pure solvent for 30 min. The amount of fed substrate and water was measured by the weight difference of the feeding reservoirs. Because of pressure variations a constant feed rate was not always achieved. The condensed material was worked up in following steps.

The standardized work-up of samples:

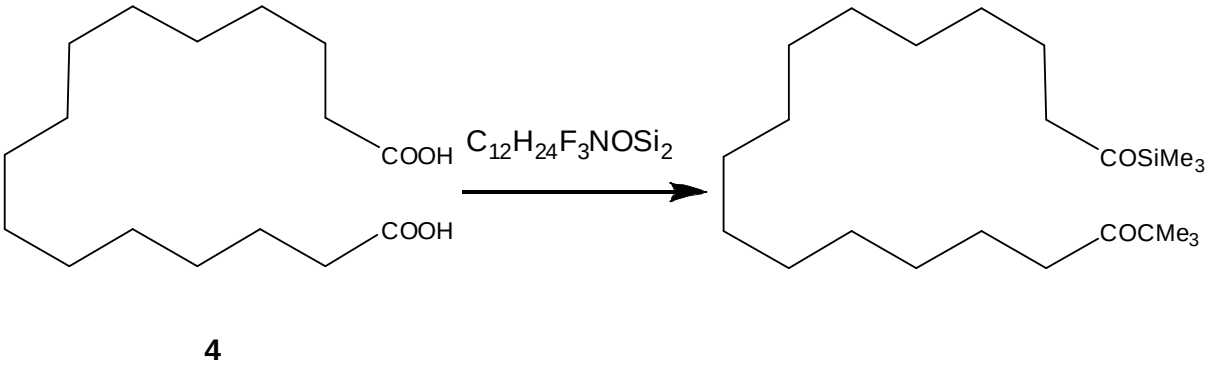

4

Fig. 5-5: Silylation of unreacted HDA (4**).**

Due to the mentioned reasons it was necessary to derivatise the unreacted HDA (**4**) to the homologue silyl ester. Before silylation water and solvent were separated from the samples in a rotary evaporator under high vacuum. The remaining dry solid was dissolved in small amount of pyridine (approx. 10 ml). A known amount of this mixture was treated with approx. 0,1 ml N,O-bis(allyl dimethyl silyl)-2,2,2-trifluoro acetamide in a GC vial. After heating the filled and closed GC vial for 15 min at 50 °C the reaction mixture was analysed by GC-chromatography.

6 Annex

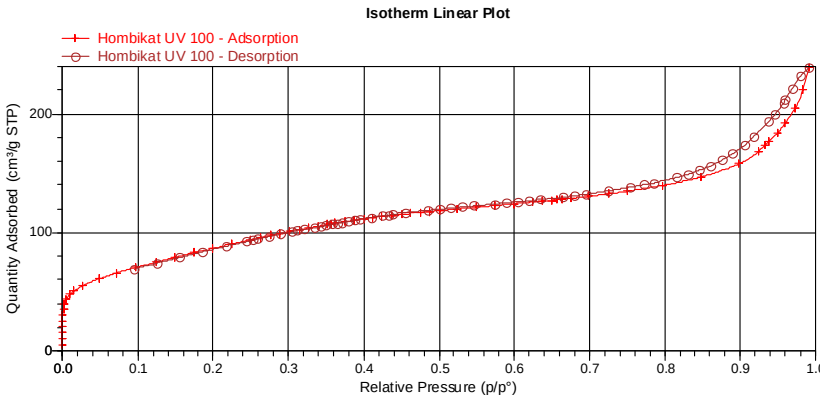

Fig. 6-1: BET-Isotherm of Hombikat UV100

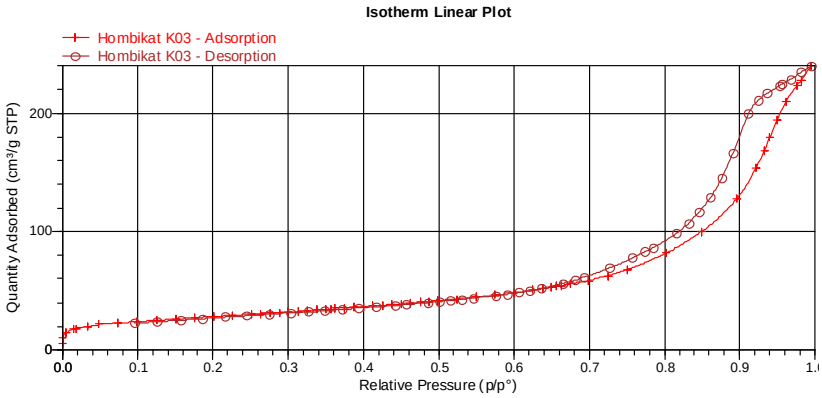

Fig. 6-2: BET-Isotherm of Hombikat K03

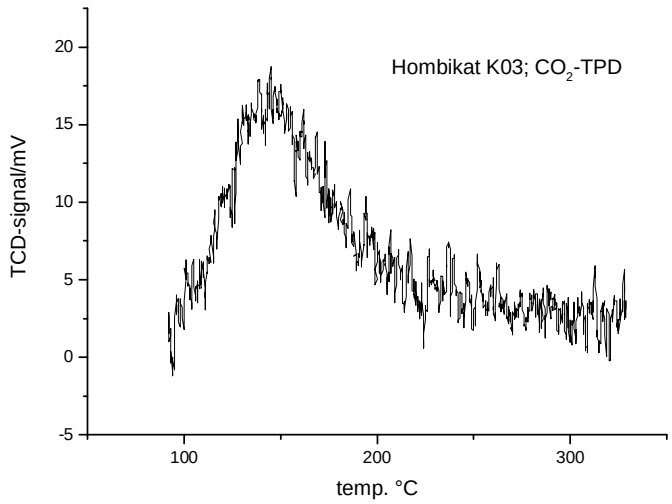

Fig. 6-3: CO_2-TPD of Hombikat K03.

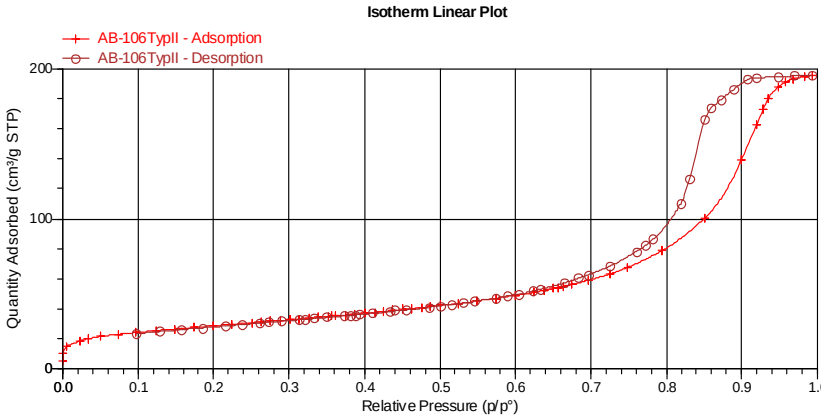

Fig. 6-4: BET-Isotherm of Hombikat Typ-II.

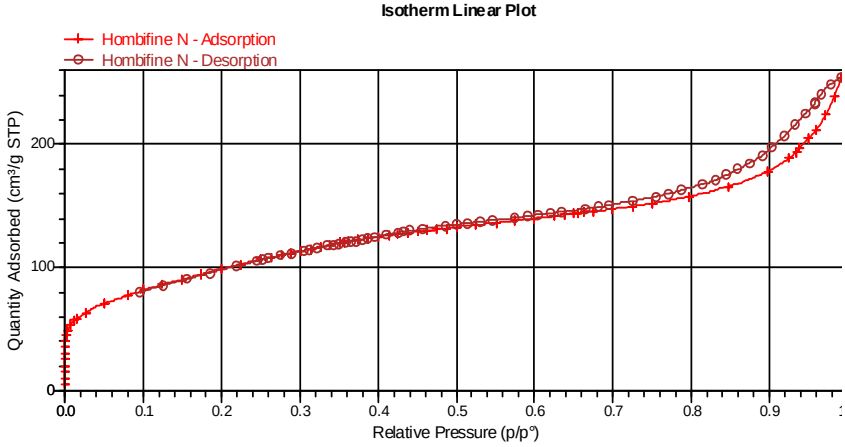

Fig. 6-5: BET-Isotherm of Hombifine N.

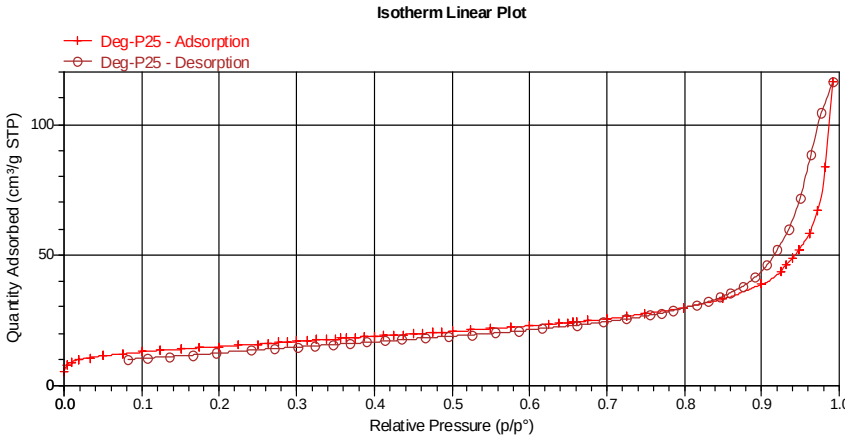

Fig. 6-6: BET-Isotherm of P-25.

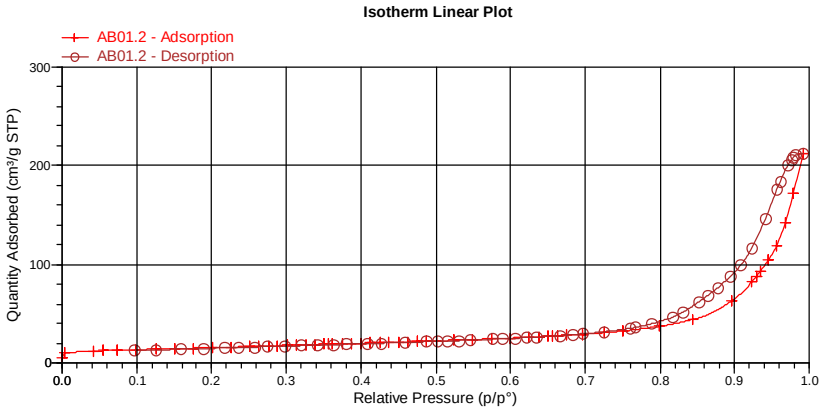

Fig. 6-7: BET-Isotherm of T-8.

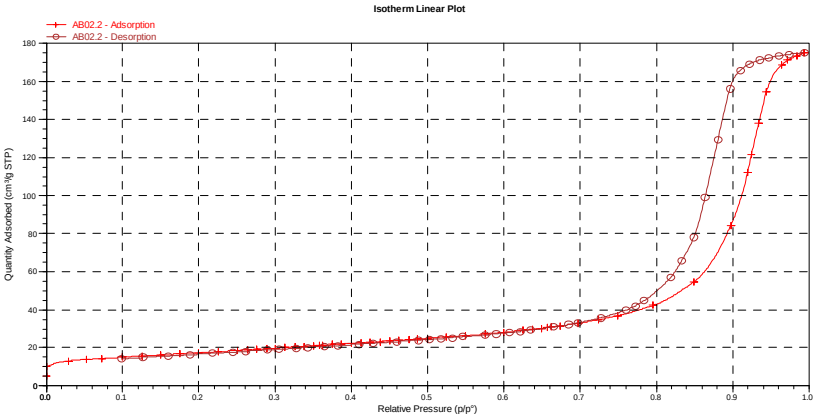

Fig. 6-8: BET-Isotherm of T-9.

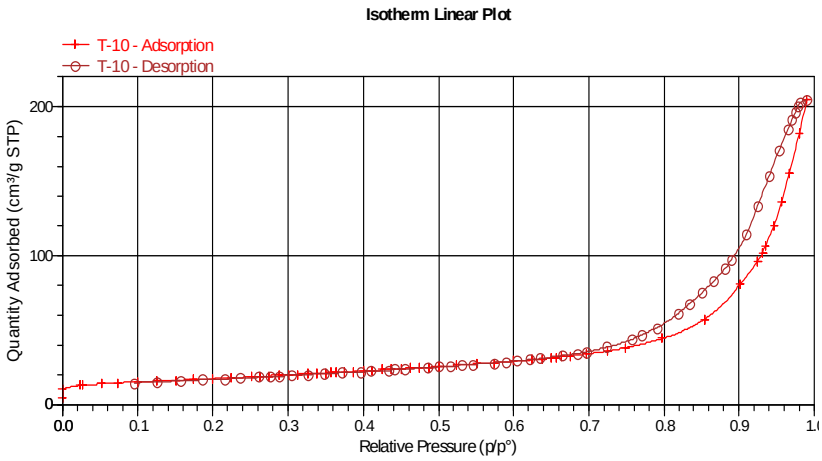

Fig. 6-9: BET-Isotherm of T-10.

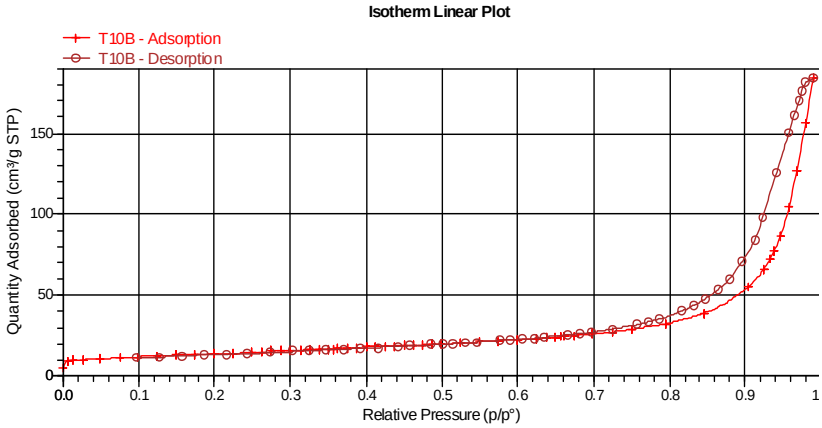

Fig. 6-10: BET-Isotherm of T-10B.

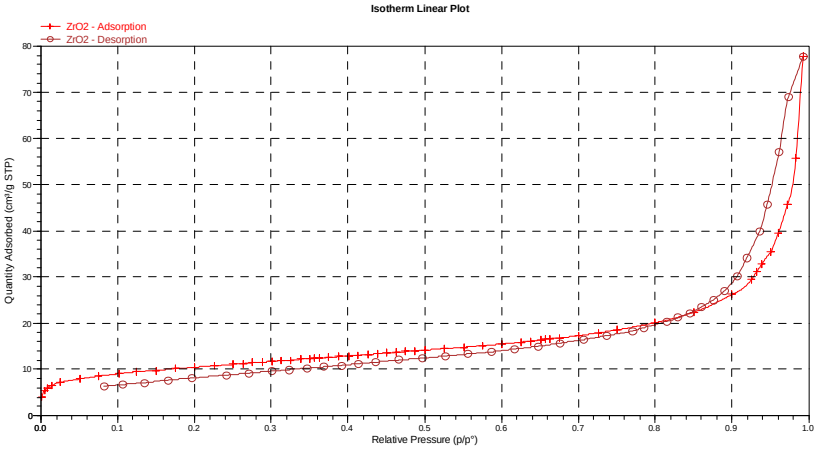

Fig. 6-11: BET-Isotherm of ZR-5.

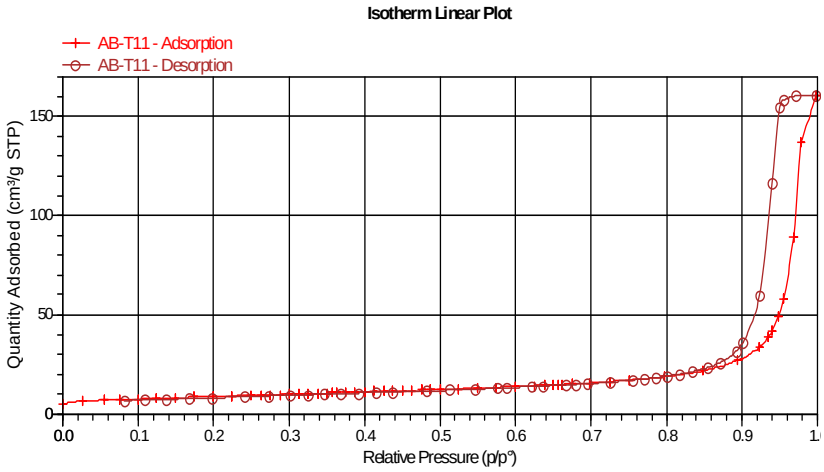

Fig. 6-12: BET-Isotherm of T-11.

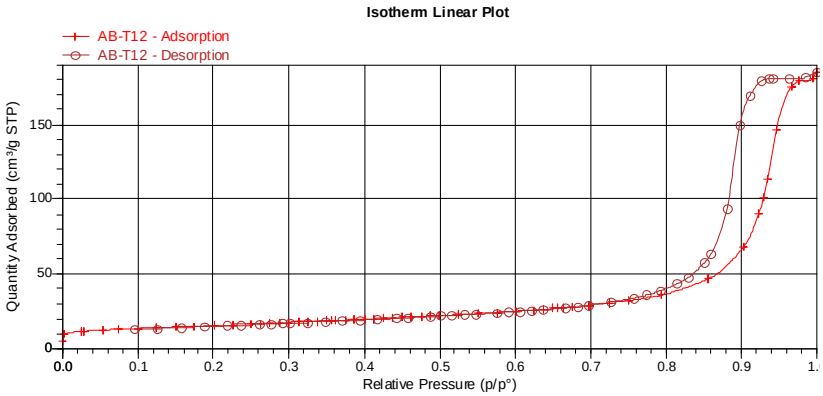

Fig. 6-13: BET-Isotherm of T-12.

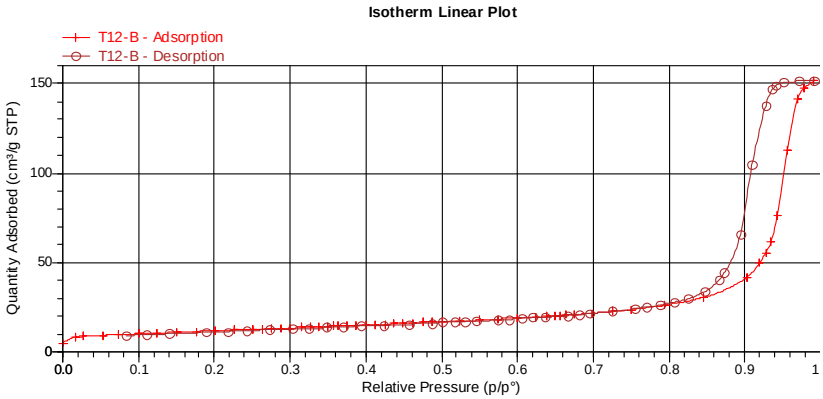

Fig. 6-14: BET-Isotherm of T-12B.

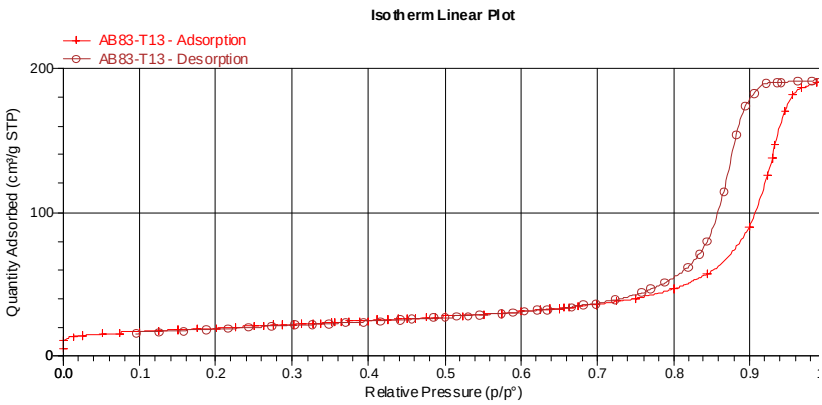

Fig. 6-15: BET-Isotherm of T-13.

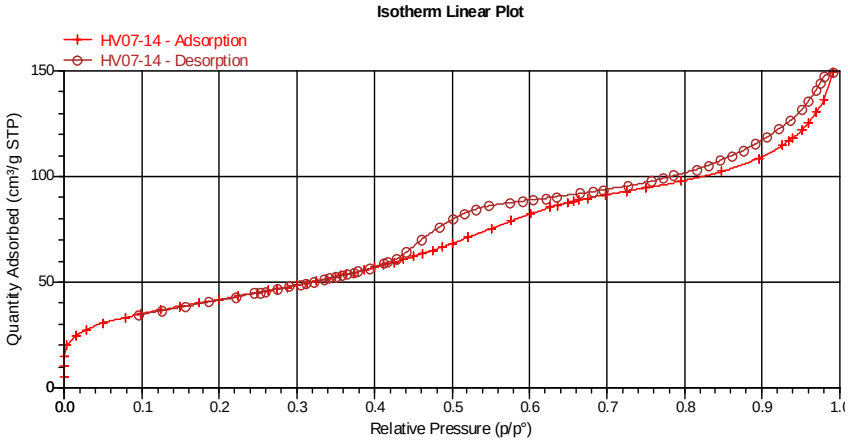

Fig. 6-16: BET-Isotherm of T-14.

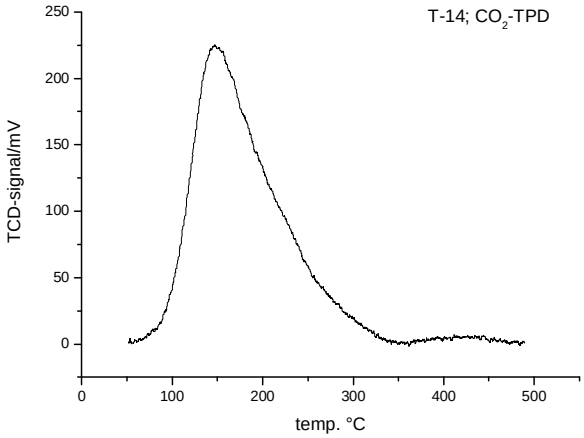

Fig. 6-17: CO_2-TPD of T-14.

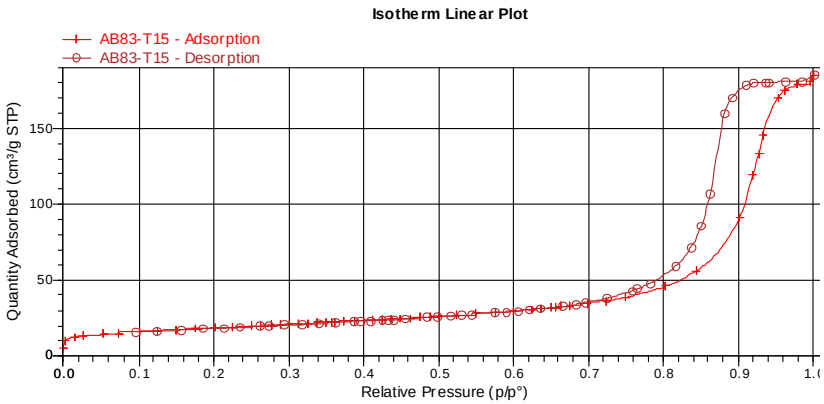

Fig. 6-18: BET-Isotherm of T-15.

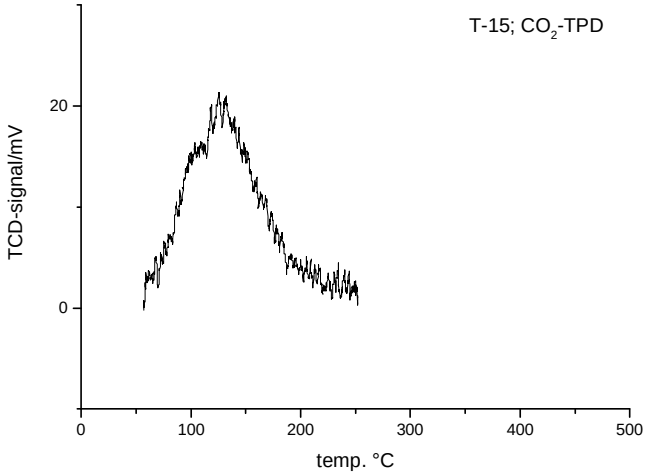

Fig. 6-19: CO_2-TPD of T-15.

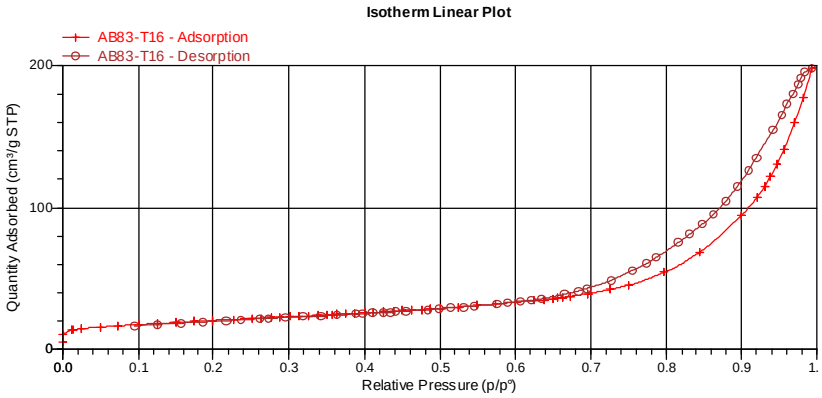

Fig. 6-20: BET-Isotherm of T-16.

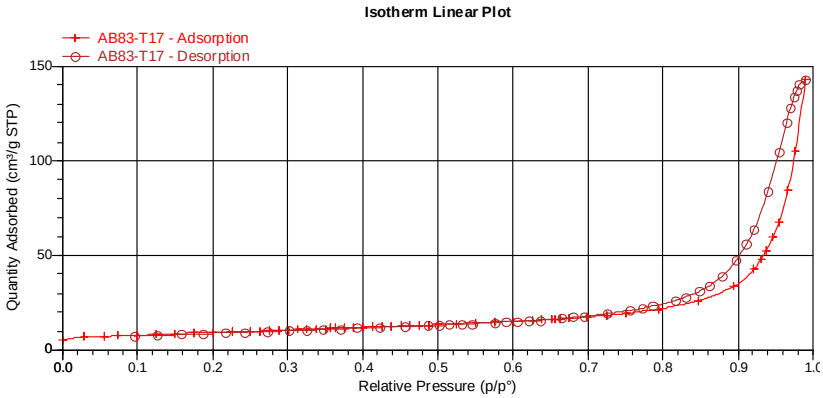

Fig. 6-21: BET-Isotherm of T-17.

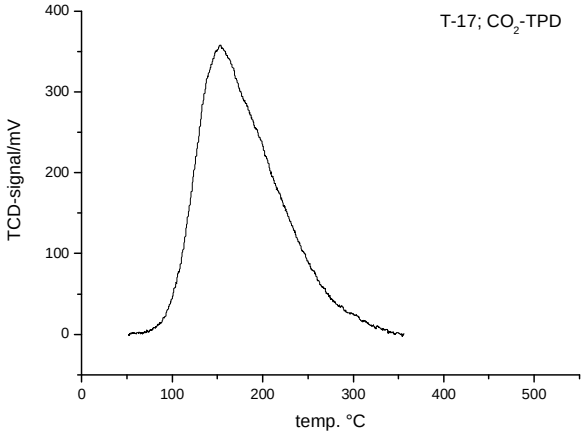

Fig. 6-22: CO_2-TPD of T-17.

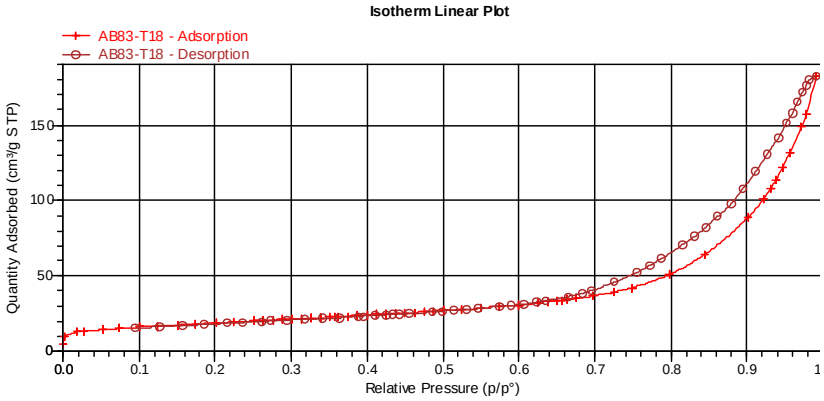

Fig. 6-23: BET-Isotherm of T-18.

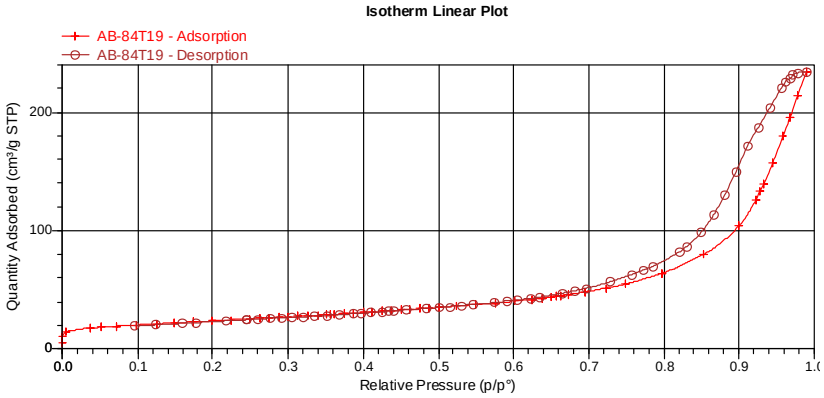

Fig. 6-24: BET-Isotherm of T-19.

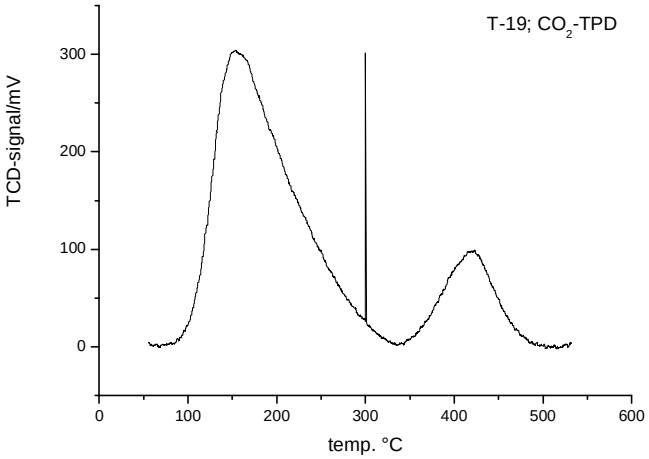

Fig. 6-25: CO_2-TPD of T-19.

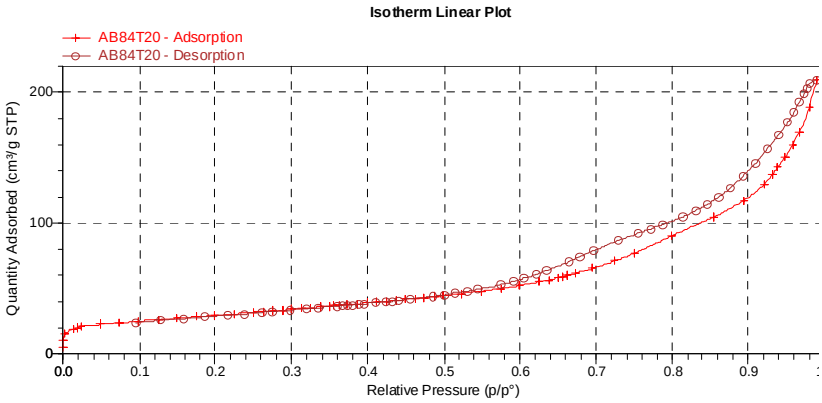

Fig. 6-26: BET-Isotherm of T-20.

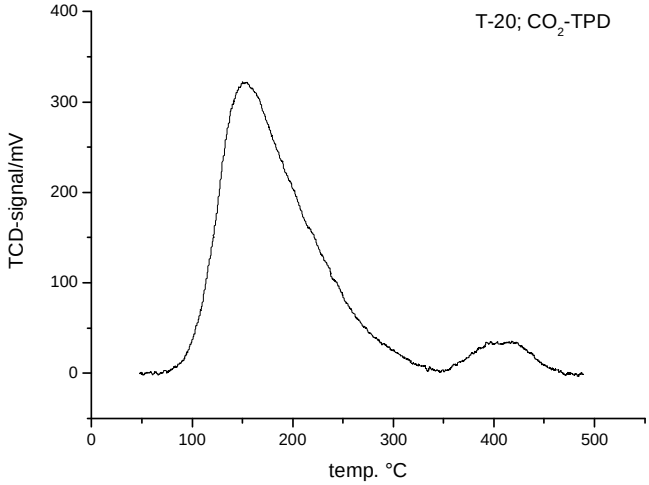

Fig. 6-27: CO_2-TPD of T-20.

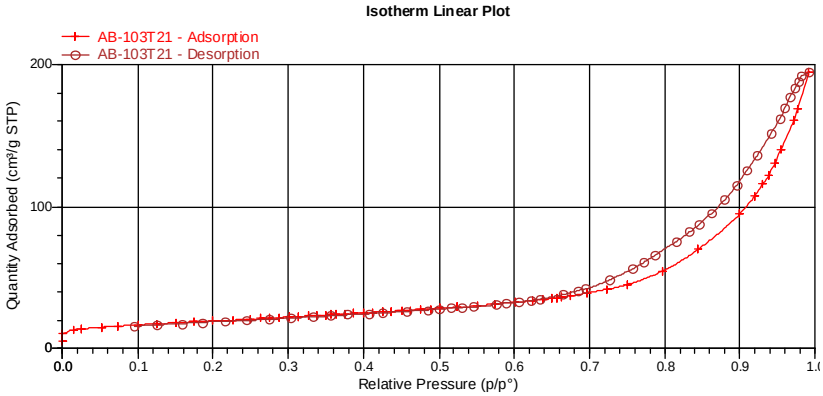

Fig. 6-28: BET-Isotherm of T-21.

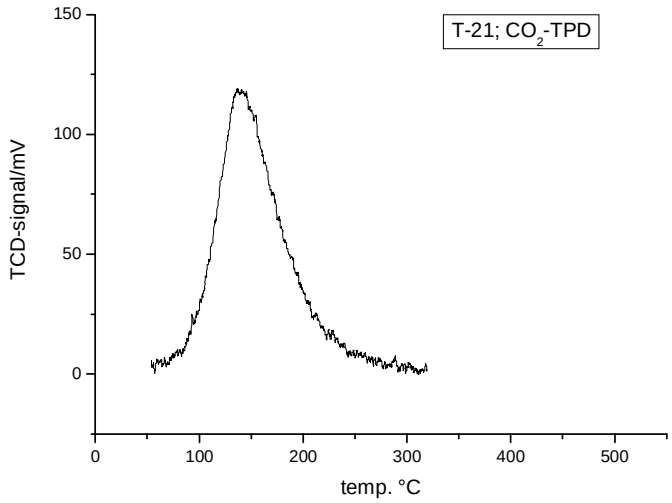

Fig. 6-29: CO_2-TPD of T-21.

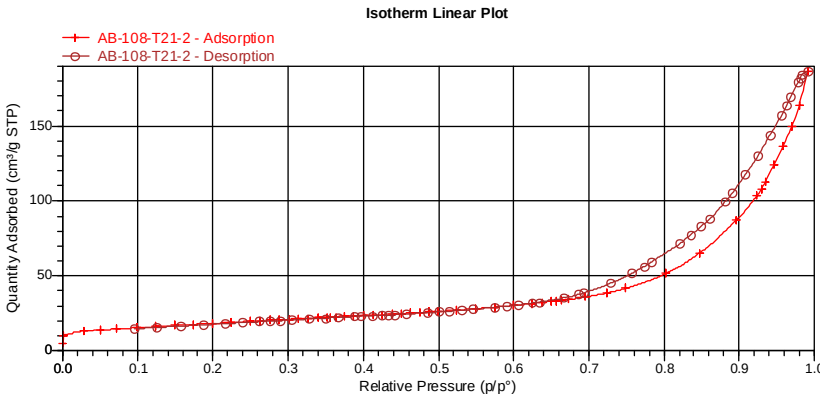

Fig. 6-30: BET-Isotherm of T-21.2.

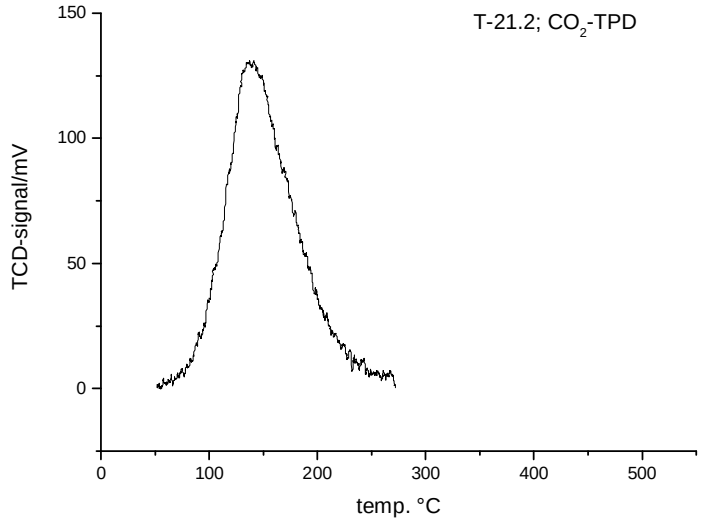

Fig. 6-31: CO_2-TPD of T-21.2.

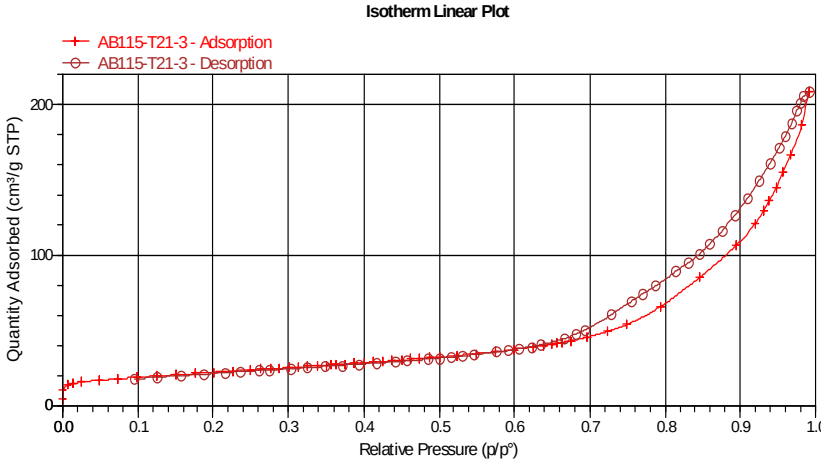

Fig. 6-32: BET-Isotherm of T-21.3.

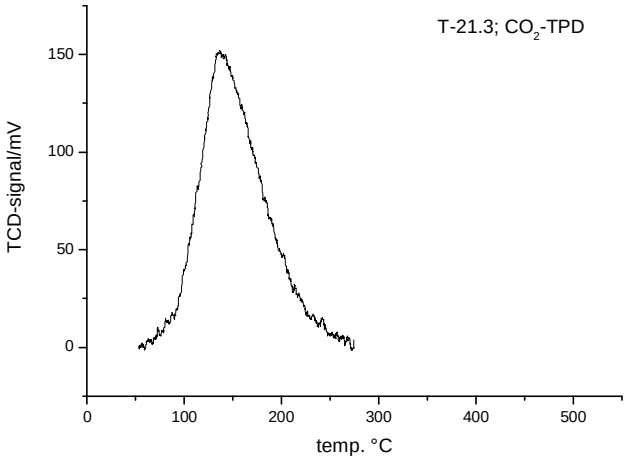

Fig. 6-33: CO_2-TPD of T-21.3.

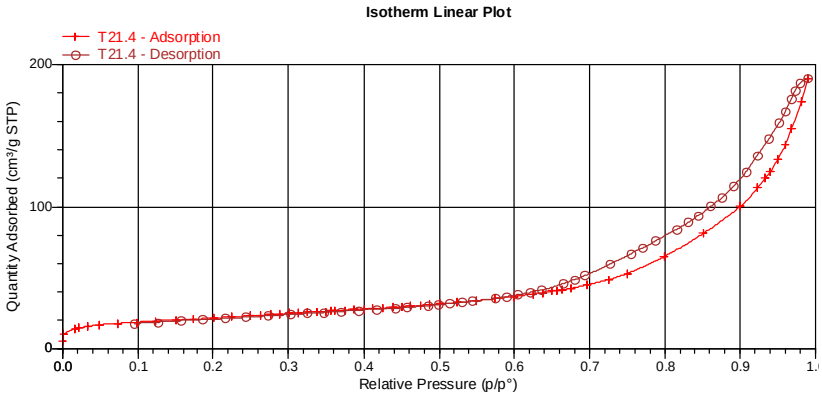

Fig. 6-34: BET-Isotherm of T-21.4.

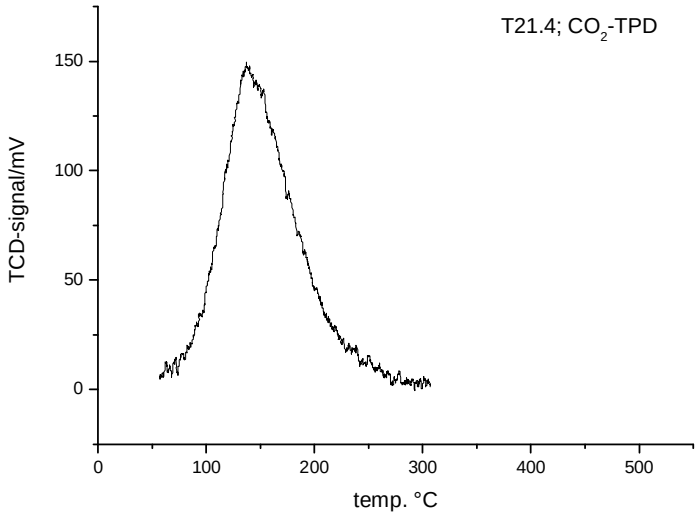

Fig. 6-35: CO_2-TPD of T-21.4.

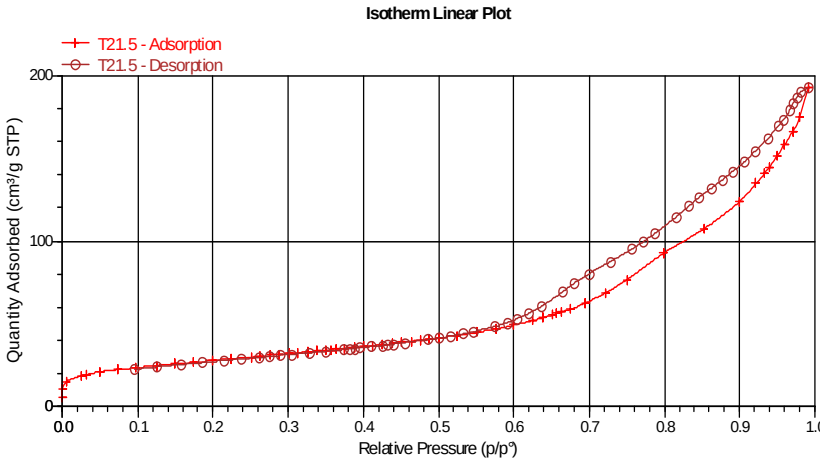

Fig. 6-36: BET-Isotherm of T-21.5.

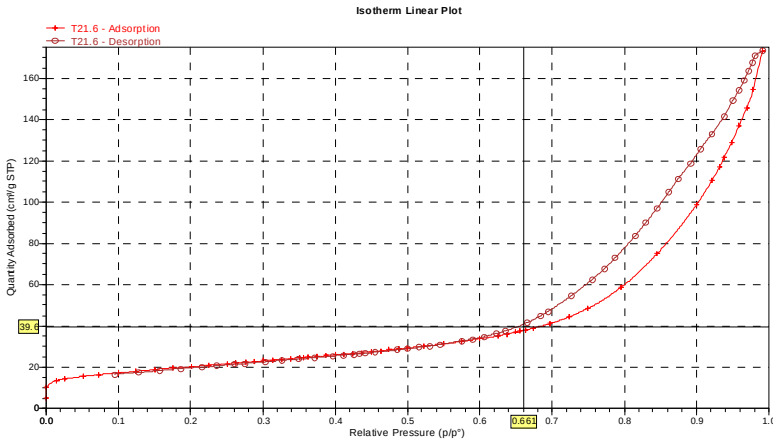

Fig. 6-37: BET-Isotherm of T-21.6.

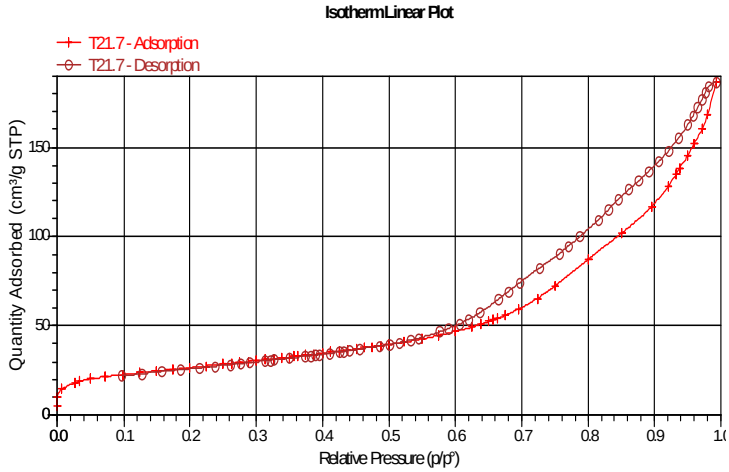

Fig. 6-38: BET-Isotherm of T-21.7.

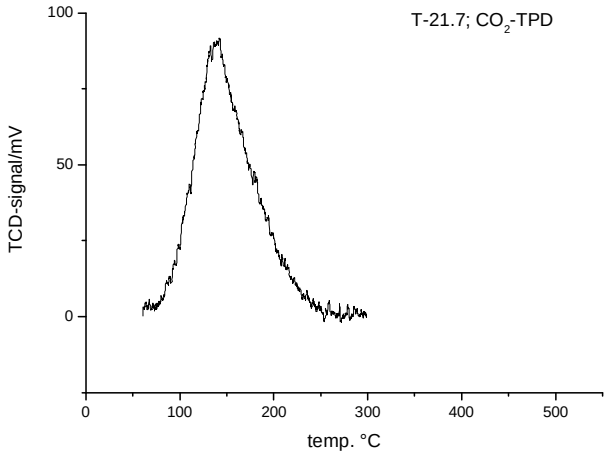

Fig. 6-39: CO_2-TPD of T-21.7.

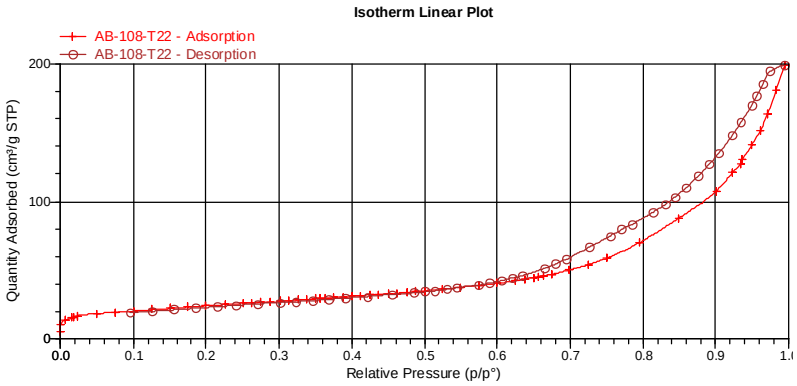

Fig. 6-40: BET-Isotherm of T-22.

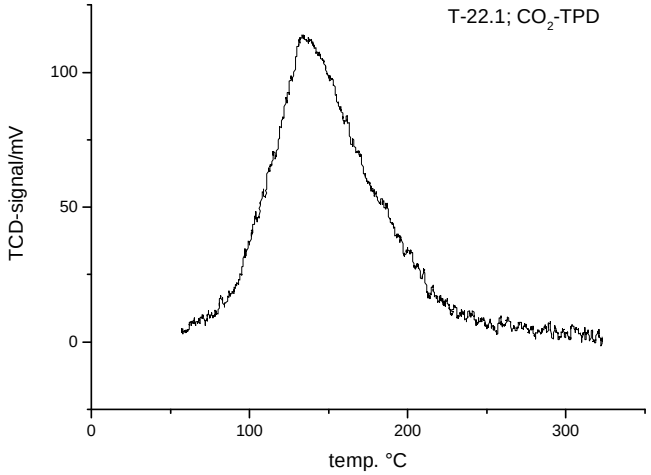

Fig. 6-41: CO_2-TPD of T-22.

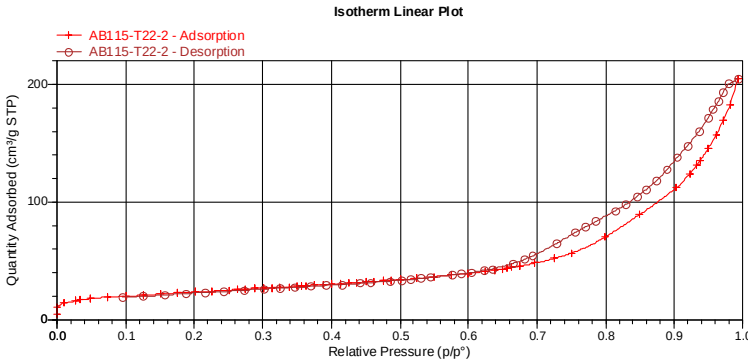

Fig. 6-42: BET-Isotherm of T-22.2.

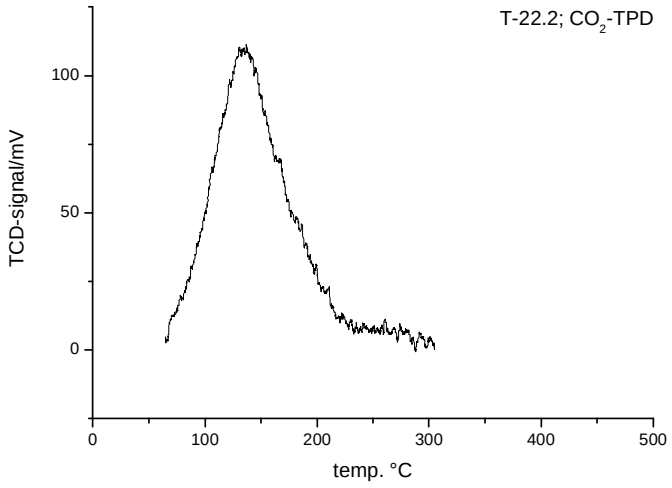

Fig. 6-43: CO_2-TPD of T-22.2.

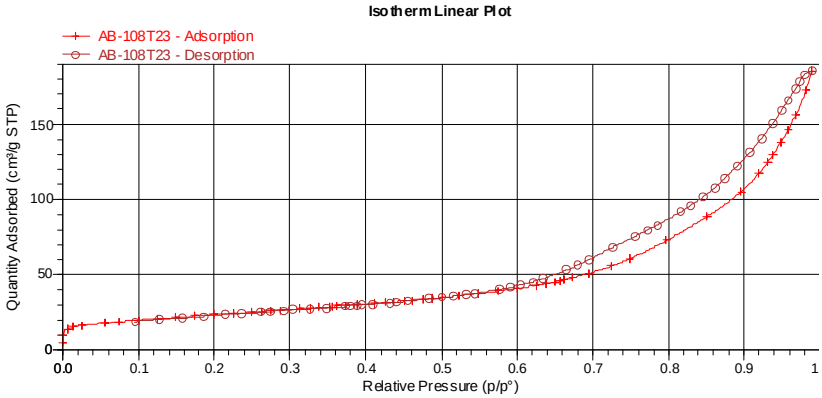

Fig. 6-44: BET-Isotherm of T-23.

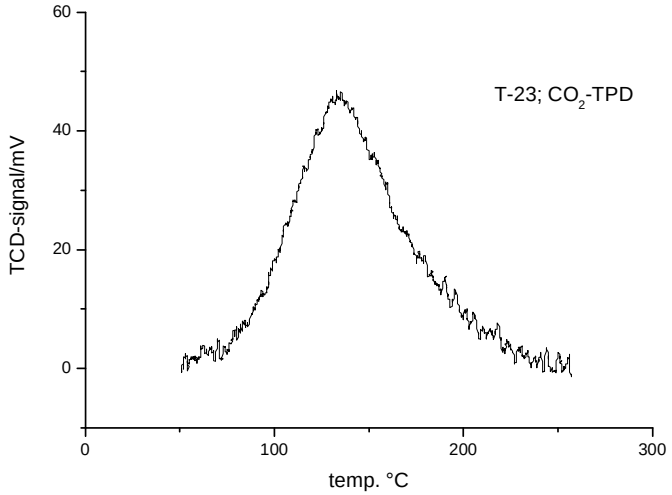

Fig. 6-45: CO_2-TPD of T-23.

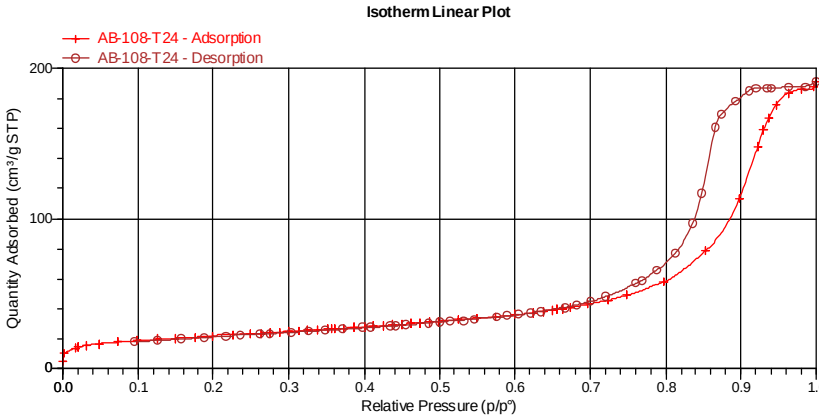

Fig. 6-46: BET-Isotherm of T-24.

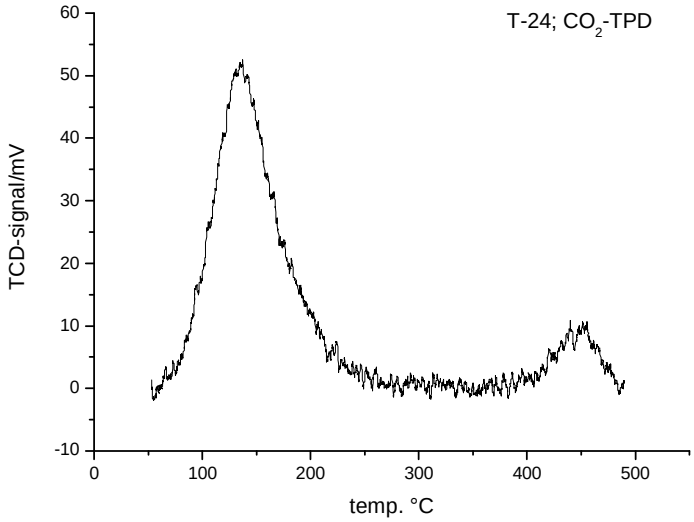

Fig. 6-47: CO_2-TPD of T-24.

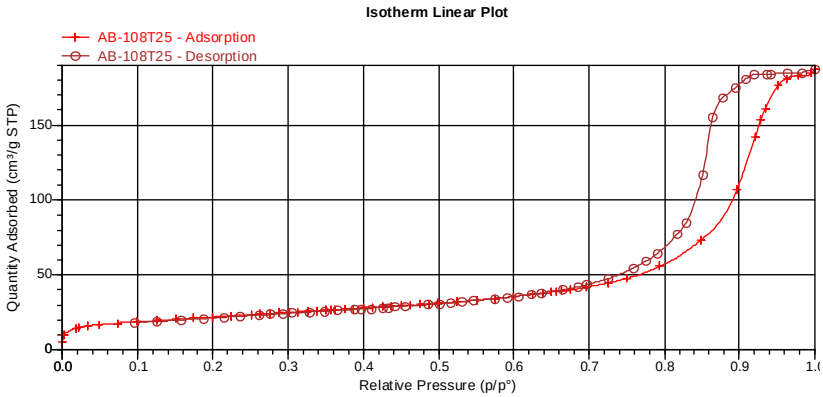

Fig. 6-48: BET-Isotherm of T-25.

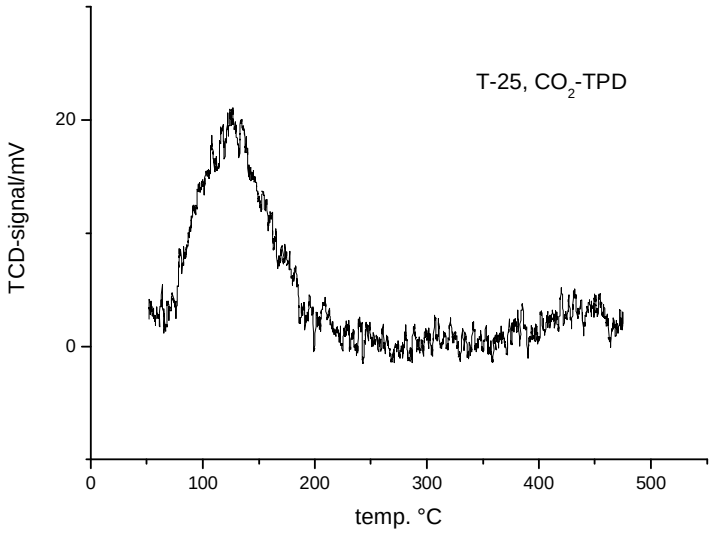

Fig. 6-49: CO_2-TPD of T-25.

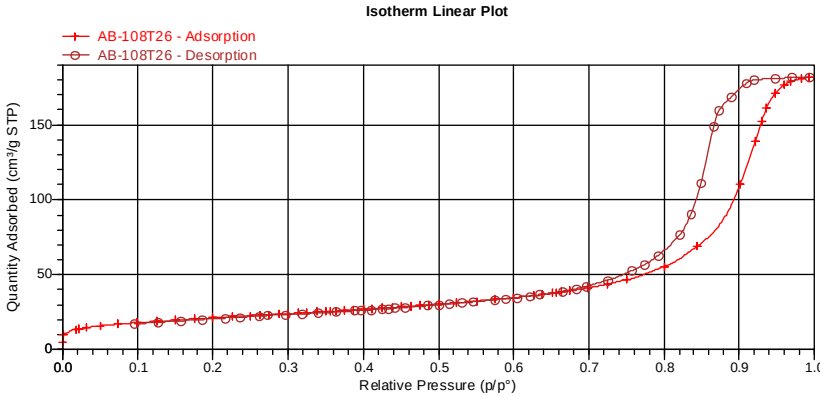

Fig. 6-50: BET-Isotherm of T-26.

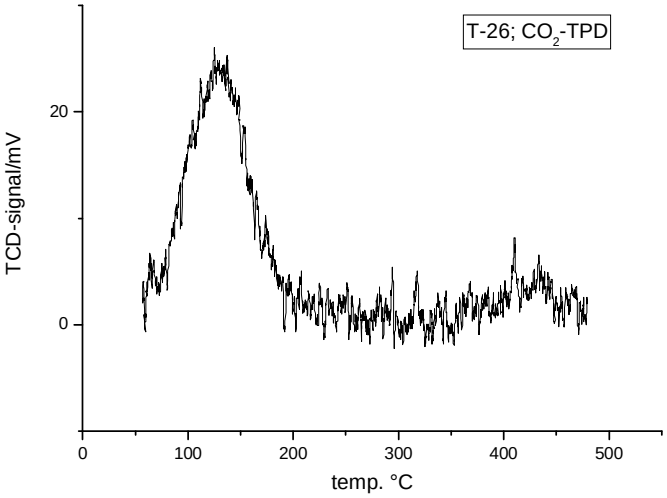

Fig. 6-51: CO_2-TPD of T-26.

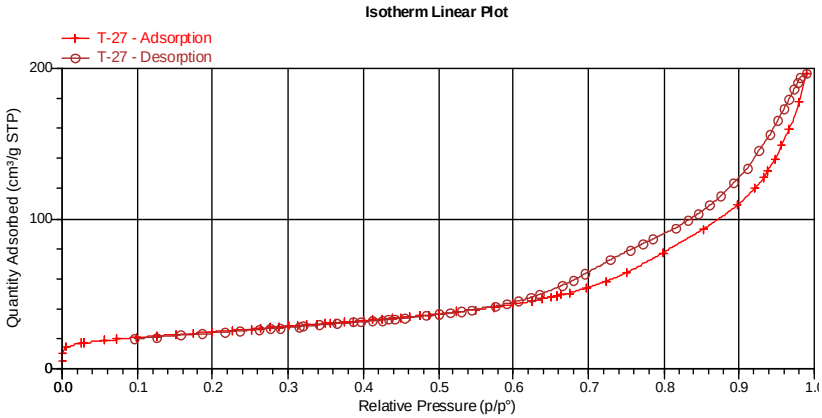

Fig. 6-52: BET-Isotherm of T-27.

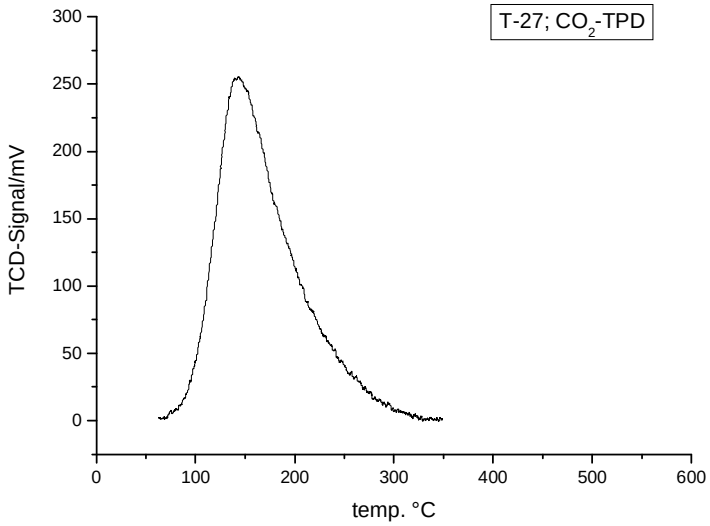

Fig. 6-53: CO_2-TPD of T-27.

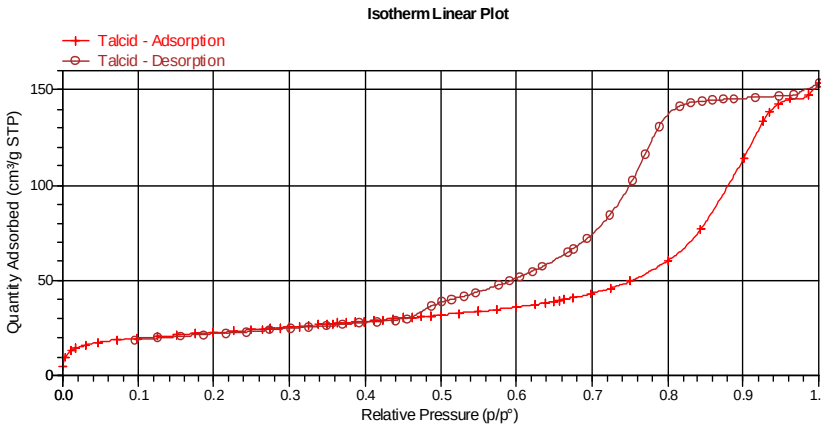

Fig. 6-54: BET-Isotherm of Talcid.

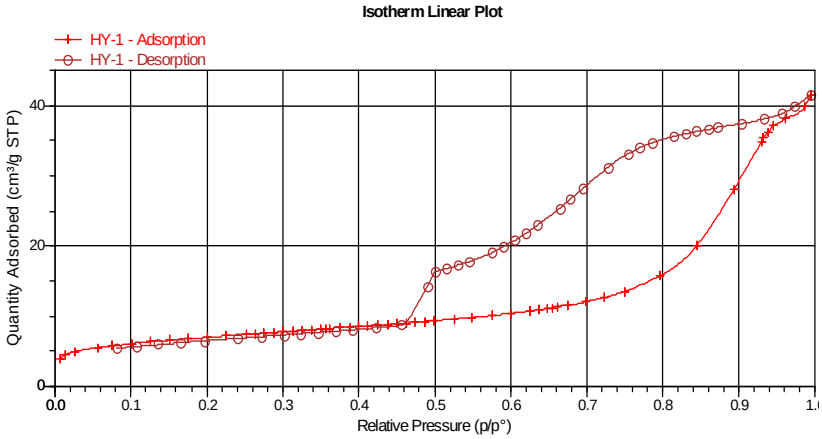

Fig. 6-55: BET-Isotherm of Hy-1.

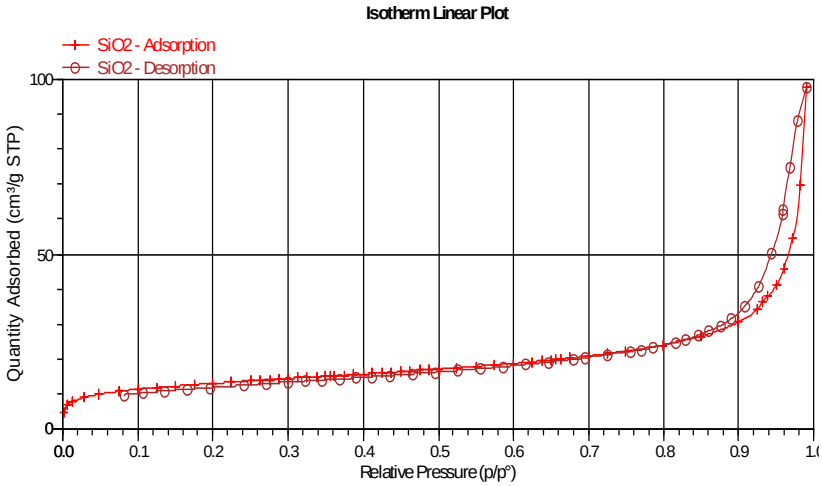

Fig. 6-56: BET-Isotherm of SiO_2.

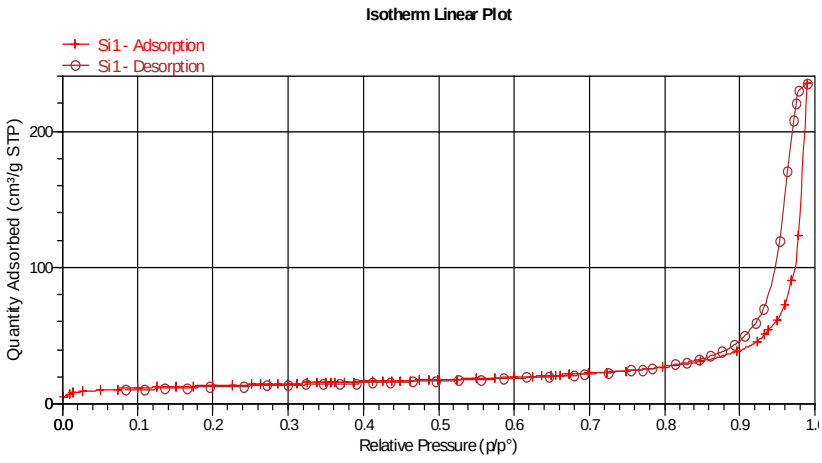

Fig. 6-57: BET-Isotherm of Si-1.

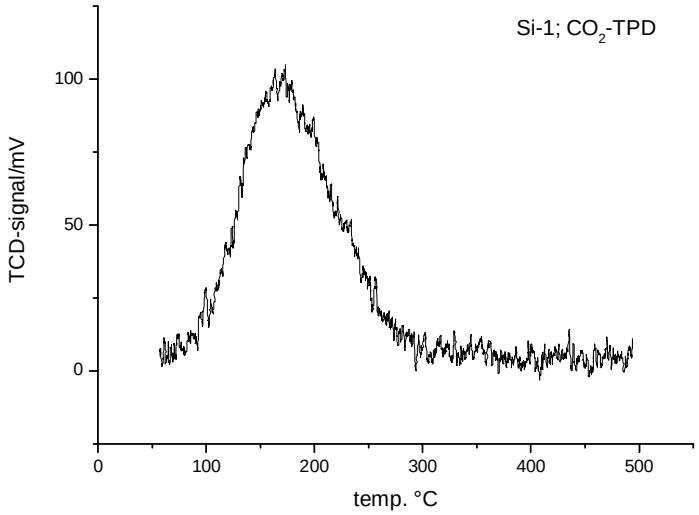

Fig. 6-58: CO_2-TPD of Si-1.

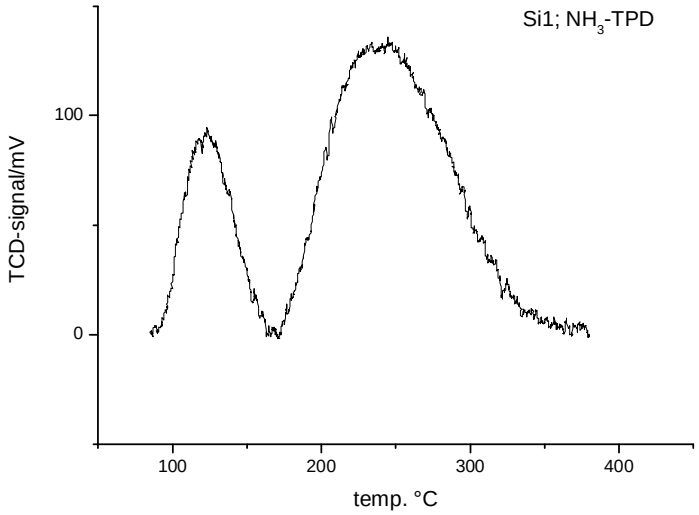

Fig. 6-59: NH_3-TPD of Si-1.

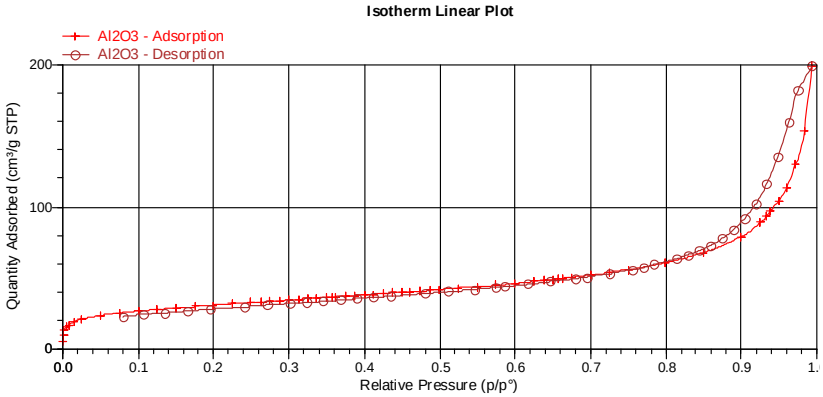

Fig. 6-60: BET-Isotherm of Al_2O_3.

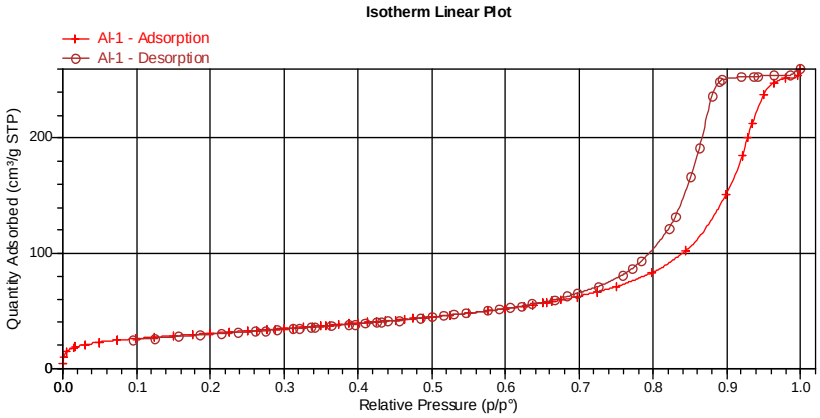

Fig. 6-61: BET-Isotherm of Al-1.

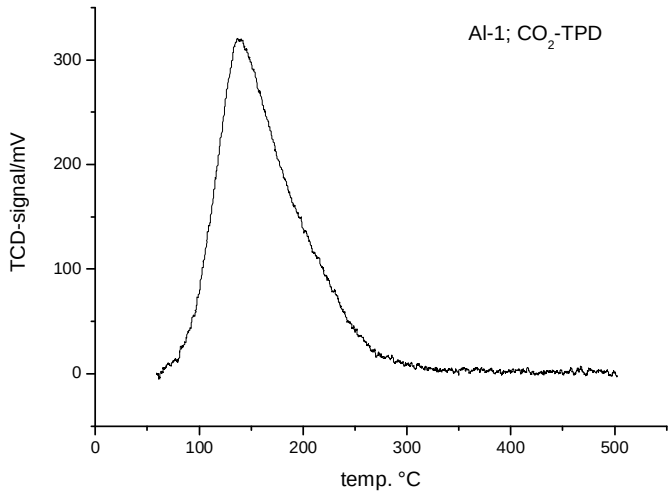

Fig. 6-62: CO_2-TPD of Al-1.

[1] P. Kraft; J. A. Bajgrowicz, C. Denis, G. Fráter, *Angew. Chem., Int. Engl. Ed.* **2000**, *39*, 2980.

[2] G. Fráter, J.A. Bajgrowicz, P. Kraft, *Tetrahedron* **1998**, *54*, 7633.

[3] M. Gautschi, J.A. Bajgrowicz, P. Kraft, *Chimia* **2001**, *55*, 379.

[4] T.F. Wood, *Fragrance Chemistry: The Science of the Sense of Smell*; Theimer, E. T., *Ed.;Academic Press*: New York **1982**, 495.

[5] B.D. Mookherjee, R.A. Wilson, *Fragrance Chemistry: The Science of the Sense of Smell*;E.T. Theimer, *Ed.; Academic Press*: New York **1982**, 434.

[6] P.R. Story, P. Busch, *Advances in Organic Chemistry: Methods and Results*; E.C. Taylor ,Ed.; Wiley-Interscience: Princeton, New Jersey, Vol. 8. **1972**.

[7] A.S. Williams, *Synthesis* **1999**, 1707.

[8] Ohloff, G., *Riechstoffe und Geruchssinn*, Springer Verlag, Berlin, Heidelberg, New York **1990**.

[9] H.J. Borschberg, B. Brauckmann, *Der Struktur von Düften und Aromen auf der Spur*, ETH-Zürich, http://e-collection.ethbib.ethz.ch/ecol-pool/bericht/bericht_181_html.html

[10] http://www.birr-partner.de/?TASK=GLAESER_SHOW_SENSORIKSEMINAR_6

[11] H. Walbaum, *J. Prakt. Chem. [2]* **1906**, *73*, 488.

[12] W. Klyne, J. Buckingham, *Atlas of Stereochemistry*, Chapman a. Hall London **1974**, 36.

[13] D.A. van Dorp, R. Klok, D.H. Nugteren, *Recueil* **1972**, *92*, 915.

[14] Y. Kenichi, Y. Misao, EP1820842A1, *34*, **2007**.

[15] V.R. Mamdapur, P.P. Pai, K.K. Chakravarti, U.G. Nayak, S.C. Bhattacharyya, *Tetrahedron* **1964**, *20*, 2601.

[16] Q. Branca, A. Fischli *Helv. Chim. Acta* **1977**, *60*, 925.

[17] K. Utimoto, M. Tanaka, M. Kitai, H. Nosaki *Tetrahedron Letters* **1978**, *26*, 2301.

[18] K.A. Nelson, E.A. Mash *J. Org. Chem.* **1986**, *51*, 2721.

[19] D. Terunuma, M. Motegi, M. Tsuda, T. Sawada, H. Nozawa, H. Nohira *J. Org. Chem.* **1987**, *52*, 1630.

[20] Z.F. Xie, H. Suemune, K. Sakai *J. Chem. Soc. Chem. Commun.* **1988**, 1638.

[21] N.A. Porter, B. Lacher, V.H.T. Chang, D.R. Magnin *J. Am. Chem. Soc.* **1989**, *111*, 8309.

[22] Z.F. Xie, K.J. Sakai *J. Org. Chem.* **1990**, *55*, 820.

[23] K. Tanaka, H. Ushio, H. Suzuki *J. Chem. Soc., Chem. Commun.* **1990**, 795.

[24] K. Tanaka, H. Suzuki *J. Chem. Soc., Chem. Commun.* **1991**, 101.

[25] K. Tanaka, J. Matsui, Y. Kawabata, H. Suzuki, A. Watanabe *J. Chem. Soc., Chem. Commun.* **1991**, 1632.

[26] P. Dowd, S.C. Choi *Tetrahedron Lett.* **1991**, *32*, 565.

[27] T. Ogawa, C.L. Fang, H. Suemune, K. Sakai *J. Chem. Soc. Chem. Commun.* **1991**, 1438.

[28] W. Oppolzer, R.N. Radinov *J. Am. Chem. Soc.* **1993**, *115*, 1593.

[29] K. Tanaka, J. Matsui, K. Somemiya, H. Suzuki *Synlett* **1994**, 351.

[30] M. Yamaguchi, T. Shiraishi, M. Hirama *J. Org. Chem.* **1996**, *61*, 3520.

[31] Y. Matsumura, H. Fukawa, Y. Terao Chem. Pharm. Bull. 1998, 46, 1484.

[32] A. Alexakis, C. Benhaim, X. Fournioux, A. Heuvel, J.M. Leveque, S. March, S. Roset *Synlett* **1999**, 1811.

[33] Y. Tanabe, N. Matsumoto, T. Higashi, T. Misaki, T. Itoth, M. Yamamoto, K. Mitarai, Y. Nishii Tetrahedron **2002**, *58*, 8269.

[34] Y.H. Choi, J.Y. Choi, H.Y. Yang, Y.H. Kim *Tetrahedron: Asymmetry* **2002**, *13*, 801.

[35] P. Scafato, S. Labano, G. Consolo, C. Rosini *Tetrahedron: Asymmetry* **2003**, *14*, 3873.

[36] C. Fehr, J. Galindo, I. Farris, A. Cuenca *Helv. Chim. Acta* **2004**, *87*, 1737.

[37] T. Misaki, R. Nagase, K. Matsumoto, Y. Tanabe *J. Am. Chem. Soc.* **2005**, *127*, 2854.

[38] M. Morita, N. Mase, H. Yoda, K. Takabe *Tetrahedron: Asymmetry* **2005**, *16*, 3176.

[39] http://www.uni-bayreuth.de/departments/didaktikchemie/umat/duefte/duefte7-9.htm

[40] G. Ohloff, *Riechstoffe und Geruchssinn*, Springer Verlag, Berlin, Heidelberg, New York **1990**, 196.

[41] M. Kerschbaum, *Ber.* **1927**, *60B*, 902.

[42] L.F. Trueb, *Lavoslav Ružička (1887 - 1976) Zum 100. Geburtstag Leopold Ružičkas* Neue Züricher Zeitung, Ebmatingen-Zürich **11.09.1987** www.croatia.ch/kultura/znanost/ruzicka_de.php .

[43] Nobel Lectures, Chemistry 1922-1941, Elsevier Publishing Company, Amsterdam **1966**, 966. www.nobelprize.org/chemistry/laureates/1939/press.html .

[44] L. Ružička, Helv. **1926**, *9*, 230, 715, 1008.

[45] A. Baeyer, *Ber. Dtsch. Chem Ges.* **1885**, *18*, 2269.

[46] K. Biemann, G.Büchi, B.H. Walker *J.Amer.chem.Soc*. **1957**, *79*, 5558.

[47] A. Bauer, *Ber. Dtsch. Chem Ges.* **1891**, *24*, 2832.

[48] www.chemheritage.org/classroom/chemach/plastics/carothers.html .

[49] K.A. Bauer, A.K. Körber, *Influence of molekular structure upon the musk odor characteristics of macrocyclic ketones*, Fragrance and flavor substances **1980**, 155.

[50] J. Müller, W. Böhmer, Fraunhofer-Institut für Molekularbiologie und Angewandte Oeko logie (IME); *annual report 2001*, **2001**, 34.

[51] U. Schwegler, *Untersuchung zu Moschusverbindungen in der Muttermilch*, Bayerisches Landesamt für Gesundheit und Lebensmittelsicherheit **2005**, www.lgl.bayern.de/de/left/fachinformationen/gesundheit/umweltmedizin/moschusverbindungen.htm .

[52] G.G. Rimkus, R. Gatermann, H. Huhnerfuss, *Toxicol. Lett.* **1999**, *111*, 510.

[53] G.G. Rimkus, *Toxicol. Lett*. **1999**, *111*, 37.

[54] H.D. Eschke, J. Traud, H.J.Z. Dibowski *Umweltchem. Ökotox.* **1994**, *6*, 183.

[55] H.D. Eschke, H.J.Z. Dibowski, J. Traud *Umweltchem. Ökotox.* **1995**, *7*, 131.

[56] B. Liebl, S. Ehrenstorfer, *Chemosphere* **1993**, *27*, 2253.

[57] W. Ostwald, *Z. Physik. Chem.* **1894***. 15*, 706.

[58] A.F. Hollemann, E. Wieberg, *Lehrbuch der Anorganischen Chemie*,

Walter de Gruyter, Berlin/New York **1985**.

[59] J.M. Thomas, W.J. Thomas, *Principles and Practice of Heterogeneous Catalysis*, VCH, Weinheim **1996**, 145.

[60] U. Onken, A. Behr *Chemische Prozeßkunde*, Georg Thime Verlag, Stuttgart **1996**.

[61] E. Drent, *Pure and Appl. Chem.* **1990**, *62*, 661.

[62] Hattori, H., Heterogenous Basic Catalysis. *Chem. Rev.* **1995**, 537.

[63] Lauron-Pernot, H., Luck, F., Popa, J. M., *Appl. Catal.* **1991**, *78*, 213.

[64] Pines, H., Pillai, C. N., *J. Am. Chem. Soc.* **1960**, *82*, 2401.

[65] H. Pines, J.A. Veseley, V.N. Ipatieff *J. Am Chem. Soc.* **1955**, *77*, 6314.

[66] T. Jashima, K. Sato, T. Hayasska, N. Hara *J. Catal.* **1972**, *26*, 303.

[67] K. Tanabe in: B. Imelik, C. Nacceche, G. Condurier, Y. BenTaari, J.C. Vedrine (Eds.) *Catalysis by Acids and Bases*, Elsevier, Amsterdam **1985**, 1.

[68] H.H. Kung, *Stud. Surf. Sci. Catal.*, *45*, Kodansha Tokyo **1989**.

[69] Hammett, L. P., Deyrup, A. J., *J. Am. Chem. Soc.* **1932**, *54*, 2721.

[70] H. Gorzawski, W.F. Hoelderich *J. Mol. Catal. A: Chem.* **1999**, *144*, 181.

[71] Aramendía, M. A., Boráu, V., García, I. M., Jiménez, C., Marinas, A., Marinas, J. M., Porras,A., Orbano, F. *J., Appl. Catal. A* **1999**, *184*, 115.

[72] Karge, H. G. *Stud. Surf. Sci. Catal.* **1991**, *65*, 133.

[73] Di Cosimo, J. I., Diez, V. K., Xu, M., Iglesia, E., Apesteguia, C. R., *J.Catal.* **1998**, *178*, 499.

[74] Fukuda, Y., Tanabe, K., *Bull. Chem. Soc. Jpn.* **1973**, *46*, 1616.

[75] Knötzinger, H., Huber, S., *J. Chem. Soc., Faraday Trans.* **1998**, *94*, 2047.

[76] K. Tanabe, W.F. Holderich, *Applied Catalysis* **1999**, *181*, 399.

[77] H. Hattori, H. Kumai, K. Tanaka, G. Zhang, K. Tanabe *Proc. 8th National Symposium on Catalysis Sindri*, India **1987** 243.

[78] K. Tanabe, M. Misono, Y. Ono, H. Hattori, *New Solid Acids and Bases*, Sud. Surf. Sci. Catal., *51*, Kadansha Tokyo **1989**.

[79] T. Yokoyama, T. Setoyama, M. Nakajiama, N. Fujita, T. Maki, K. Fukii *Appl. Catal. A* **1992**, *88*, 149.

[80] T. Tanabe, *Proceedings of the 8th International Congress on Catalysis*, Calgary, Canada **1988**, *5*, 85.

[81] J.B. Peri *J. Phys. Chem.* **1965**, *69 (1)*, 220.

[82] H. Knözinger, P. Ratnasamy, *Catal. Rev.-Sci. Eng.* **1978**, *17 (1)*, 31.

[83] H. Pines, C.N. Pillai, *J. Am. Chem. Soc.* **1960**, *82*, 2401.

[84] W.F. Hölderich, New reactions in various fields and production of specialty chemicals, Proceedings of the 10th International Congress on Catalysis, *Stud. Surf. Sci. Catal.* **1993**, *75,* 127±163.

[85] G. Suzukamo, M. Fukao, T. Hibi, K. Tanaka, K. Chikaishi, in: K. Tanabe, H. Hattori, T. Yamaguchi, T. Tanaka (Eds.), Acid-Base Catalysis, Proceedings of the Symposium Acid-Base Catalysis, Sapporo, Japan **1988**, Kodansha **1989**, 405.

[86] W.F. Hoelderich, *Catalysis Today* **2000**, *62*, 115.

[87] W.F. Hölderich, *Stud. Surf. Sci. Catal.* **1993**, *75* 127.

[88] H. Gorzawski, W.F. Hölderich, *Appl. Catal. A. General* **1999**, *179* 131.

[89] K.A. Bauer, A.K. Körber, *Old and new macrocyclic musk*, second international Haarmann & Reimer symposium on fragrance and flavor substances, Washington State University **1980**, 129.

[90] B.D. Mookherjee, R.A. Wilson, *Fragrance Chemistry*, E.T. Theimer Academic Press, New York **1982** 433.

[91] P.A. Wender, D.A. Holt, S.M. Sieburt, *J. Am. Chem. Soc.* **1983,** *105*, 3348.

[92] G. Wilke, *Angew. Chem.* **1957**, *69*, 397; **1963**, *75*, 10.

[93] W.S. Johnson, G.H. Daub *Org. Reactions* **1951**, *6*, 1.

[94] P.A. Plattner, G. Büchi Helv. Chem. Acta 1946, 29, 1068.

[95] G. Ohloff, J. Becker, K. Schulte-Elte, *Helv.* **1967**, *50*, 705.

[96] C. Fehr, G. Ohloff, *Helv. Chim. Acta* **1979**, *62*, 2655.

[97] D. Felix, J. Schreiber, G. Ohloff, A. Eschenmoser, *Helv. Chim. Acta* **1971**, *54*, 2895.

[98] P.Wieland, H. Kaufmann, A. Eschenmoser, *Helv.* **1967**, *50*, 2108.

[99] D. Felix, J. Schreiber, K. Piers, U. Horn, A. Eschenmoser, *Helv.* **1968**, *51*, 1461; R.K. Müller, D. Felix, J. Schreiber, A. Eschenmoser, *Helv.* **1970**, *53*, 1479.

[100] R.P. Lutz, *Chem. Rev.* **1984**, *84*, 205.

[101] M.Nishino, H. Kondo, A. Miyake, *Chem. Letters* **1973**, 667.

[102] N. Bluthe, N. Malacria, V. Gore *Tetrahedron Lett*ers **1983**, *24*, 1157.

[103] J. Nowicki, *Molecules* **2000**, *5*, 1033.

[104] H. Nosaki, T. Mori, R. Noyori *Tetrahedron Letters* **1967**, *9*, 779.

[105] C. Fehr, *Helv. Chem. Acta* **1983**, *66*, 2512.

[106] E.J. Corey,M. Chaykovsky, *J. Am.Chem. Soc.* **1964**, *86*,1639.

[107] D.A. Chass, D. Buddhasukh, P.D. Magnus, *J.Org.Chem.* **1978**, *43*, 1750.

[108] M. Julia, D. Uguen, *Bull. Soc. Chim. Fr.* **1976**, 513.

[109] H. Suginome, S. Yamada *Tetrahedron Letters* **1987**, *28*, 3963.

[110] V. Rautenstrauch, R.L. Snowden, S.M. Linder *Helv. Chim. Acta* **1990**, *73*, 896.

[111] M. Nagel, H.J. Hansen, G. Fra´ter *Synlett* **2002**, *2*, 275.

[112] H. Hundiecker *Ber.* **1942**, *75*, 1190.

[113] H. Hundiecker *Ber.* **1942**, *75*, 1197.

[114] A.T. Blomquist, R.D. Spencer *J. Am. Chem. Soc.* **1949**, *70*, 30.

[115] M. Stoll, A. Rouve, *Helv. Chim. Acta* **1947**, *30*, 1815.

[116] M. Stoll, A. Rouve, *Helv. Chim. Acta* **1947**, *30*, 1822.

[117] D.J. Hagena, K.A. Bauer, *Readily accessible internediates of macrocyclic musks*, second international Haarmann & Reimer symposium on fragrance and flavor substances, Washington State University **1980**, 145.

[118] A. Makita, *JP 05155802* **1993**, Nitsuko Kyoseki Kk, Japan.

[119] V. Prelog, L. Frenkiel, M. Kobelt, P. Barmann, *Helv. Chim. Acta* **1947**, *30*, 1741.

120 L.V. Hansley, *J. Am. Chem. Soc.* **1935**, *57*, 2303, U.S. Pat.2228268 **1941**.

121 M. Stoll, A. Commarmont, *Helv. Chim. Acta* **1948**, *31*, 1082 und 1435.

122 V.R. Mamdapur, P.P. Pai, K.K. Chakravarti, U.G. Nayak, S.C. Bhattacharyya, *Tetrahedron* **1964**, *20*, 2601.

123 A. Wartini, K. Ebel, G. Hieber, H. Weigel, *WO 2004/009524 A1* **2004**, BASF, Germany; *DE 102 32 750 A1* **2004**, BASF, Germany.

124 N.J. Leonard, C.W. Schimmelpfennig jr. **1958**, *23*, 1708.

125 C. Yuen et al. *J. Am. Oil Chem. Soc* **1994**, *71 (8)*, 911.

126 Y. Tanabe, A. Makita, EP 1270538 B1 **2005**, Japan Energy Corporation; WO 074752 **2001**.

127 A.T. Blomquist, R.D.Spencer, *J. Am. Cem. Soc.* **1948**, *70*, 30.

128 K.H. Ziegler, H. Eberle, H. Ohnlinger *Ann. Chemie* **1933**, *504*, 94.

129 K.H. Ziegler, R. Aurnhammer *Ann. Chemie* **1934**, *513*, 43.

130 S. Ställberg-Stenhagen, Ark. Kemi **1951**, *3*, 517.

131 D.Jr. Valentine, J.W. Scott, *Synthesis* **1978**, *5*, 329.

132 S. Fujimoto, K. Yoshikawa, M. Itoh, T. Kitahara *Biosci. Biotechnol. Biochem.* **2002**, *66*, 1389.

133 K.C. Nicolaou, S.P. Seitz, M.R. Pavia, N.A. Petasis *J. Org. Chem.* **1979**, *44*, 4011.

134 T. Takahashi, T. Nagashima, J. Tsuji *Tetrahedron Letters* **1981**, *22*, 1360.

135 Y. Tanabe, N. Matsumoto, T. Higashi, T. Misaki, T. Itoh, M. Yamamoto, K. Mitarai, Y. Nishi *Tetrahedron* **2002**, *58*, 8269.

136 J. Tsuji, T. Yamada, M. Kaito, T. Mandai *Tetrahedron Letters* **1979**, *22*, 2257.

137 J. Tsuji, T. Yamada, M. Kaito, T. Mandai *Bull. Chem. Soc. Jpn* **1980**, *53*, 1417.

138 T. Yamamoto, M. Ogura, T. Kanisawa *Tetrahedron* **2002**, *58*, 9209.

139 K.J. Ivin, *Olefin Metathesis*, Academic Press, London **1983**.

140 a) J.C. Mol, J.A. Moulijn, *Catalytic Metathesis of Alkenes*, Catalysis: Science and Technology; b) J.R. Anderson, M. Boudart, Springer Verlag: Berlin, Heidelberg **1987**, *8*, 69.

141 M. Siberijn, J.C. Mol, *Appl. Catal.* **1991**, *67*, 276.

142 M.F.C. Plugge, J.C. Mol, *Synlett Lett.* **1991**, 507.

143 J. Tsuji, S. Hashiguchi, *J. Organomet. Lett.* **1981**, *218*, 69.

144 A. Fürstner, *Synlett* **1999**, 1523.

145 A. Fürstner, G. Seidel, *J. Organomet. Chem.* **2000**, *606*, 75.

146 M.E. Maier *Angew. Chem.* **2000**, *112*, 2153.

147 R.H. Grubbs Handbook of Metathesis, *Wiley-VCH, Germany,* **2003**.

148 V.P. Kamat, H. Hagiwara, T. Suzuki, M. Ando *J. Chem. Soc., Perkin Trans. 1*, **1998**, 2253.

149 V.P. Kamat, H. Hagiwara, T. Katsumi, T. Hoshi, T. Suzuki, M. Ando *Tetrahedron* **2000** *56*, 4397.

150 E.J. Lenardao, G.V. Botteselle, F. de Azambuja, G. Perin, R.G. Jacob *Tetrahedron* **2007**,

63, 6677.

151 Y. Yoshida, N. Matsumoto, R. Hamasaki, Y. Tanabe *Tetrahedron Letters* **1999**, *40*, 4227.

152 J. Louie, C.W. Bielawski, R.H. Grubbs *J. Am. Chem. Soc.* **2001**, *123*, 11312.

153 Tanabe et al., US Patent 7268258 B2 **2007**.

154 M. Alas, M. Crochemore, *EP 626363* Appl. **1994**, Rhone-Poulenc Chimie SA. France.

155 C. Schommer, K. Ebel, T. Dockner, M. Irgang, W. Hölderich, H. Rast, *US Patent 49507663* **1990**, BASF, Germany; EP 0 352 674 B1 **1993**, BASF, Germany, DE 3920280 A1 **1991**, BASF, Germany.

156 L. Schuster, L. Arnold. *DE-21 11 722A* **1972**, BASF, Germany.

157 H. Froehlich, M. Schneider, W.Himmele, M. Strohmeyer, G. Sandrock, K. Baer, *DE--27 58 113 A1* **1979**.

158 C. Schommer, K. Ebel, T. Dockner, M. Irgang, W. Hölderich, H. Rast, DE 3825873 A1 **1990**, BASF, Germany.

159 www.corporate.basf.com .

160 A. Wartini, K. Ebel, G. Hieber, H. Weigel, *DE 10232750* **2004**, BASF, Germany.

161 www.seilnacht.com.

162 www.kronostio2.com.

163 Y.D. Dolmatov, A.I. Sheinkman, *Zhurnal Prikladnoi Khimii* **1970**, *43*, 249.

164 D. Heinz, W.F. Hoelderich, S. Krill, W. Boeck, K. Huthmacher, *J. Catal.* **2000**, *192*, 1.

165 M. Scheller, Dissertation, Deutsche Nationalbibliothek idn:961704055, **2001**, 14.

166 J. Clark, D. Macquarrie, *Chem. Soc. Rev.* **1996**, 303.

167 R.J. Farrauto, C.H. Bartholomew, *Fundamentals of Industrial Caralytic Processes*, Blackie Academic & Prof., London **1997**.

168 www.degussa.com/en/home.html.

169 www.sigmaaldrich.com.

170 D. Das, *internal report*, Nov. **2004**.

171 www.sachtleben.com.

172 D. Das, *internal report*, Feb. **2005**.

173 P. Kripylo, K.-P. Wendlandt, F. Vogt, *Heterogene Katalyse in der Chemischen Technik*, VEB Deutscher Verlag für Grundstoffindustrie, Leipzig **1993**.

174 C. Morterra, G. Cerrato *Langmuir* **1990**, *6*, 1810.

175 C. Morterra, G. Cerrato *Catal. Lett.* **1991**, *10*, 357.

176 Anatoliĭ Aleksandrovich Davydov, N. Sheppard, Molecular spectroscopy of oxide catalyst surfaces, Wiley **2003**. (ISBN-13: 978-0471987314)

177 J.M. Thomas, W.J. Thomas, *Principles and Practice of Heterogeneous Catalysis* VCH Verlagsgesellschaft Weinheim **1997**.

178 W. Yang C. Lee and R.G. Parr *Physical Review B* **1988**, *37*, 785.

179 Gaussian Basis Set Order Form; URL http://www.emsl.pnl.gov/forms/basisform.html; **2004**.

180 D.M. Antonelli, J.Y. Ying, *Angew. Chem. Int. Ed. Engl.* **1995** *34*, 2014.

181 D.M. Antonelli, *Microporous and Mesoporous Materials* **1999**, *30*, 315.

[182] www.telab.de.

[183] www.eurotherm-deutschland.de; www.eurotherm.com

~